UNIVERSIDADE DA BEIRA INTERIOR

Engenharia

Optimization of the Interoperability and Dynamic Spectrum Management in Mobile Communications Systems Beyond 3G

Orlando Manuel Brito Cabral

Thesis submitted in fulfilment of the degree of Doctor in
Electrical Engineering

Supervised by: Doctor Fernando José da Silva Velez
Co-supervised by: Doctor Neeli Rashmi Prasad

Covilhã, December 2010

To my Family and Friends.

Acknowledgements

The thesis was possible thanks to the contribution of many people. Foremost among these is Prof. Fernando J. Velez, my thesis mentor, whose technical excellence and unconditional support where the keystone to achieve the goals of this project. The discussions during our weekly meetings revealed to be essential in the conception of our formulations, and his vision on what future heterogeneous networks will be, was essential for this work to take form.

I am grateful to Prof. Neeli Prasad for her mentoring and for welcoming me for several months in her group at the CTIF of Aalborg University. It allowed me to work in an international group for mobile communications research, with different expertise and experience. It allowed me to acquire valuable work experience. The group and individual objectives changed my view over research work. Within this group, Albena Mihovska and Filippo Meucci were real motivators and mentors for one of the best contributions from my thesis. I also do not forget Dorthe Sparre who helped me on settling in Aalborg, Denmark.

To Instituto de Telecomunicações (IT) and Universidade da Beira Interior (UBI), I would like to acknowledge the excellent lodging and outstanding working conditions. IT and UBI supported my attendance to research meetings and conferences, essential for my research and to divulge this work. In particular, I would like to thank to Dr.ª Sara Correia and Eng.ª Conceição Camisão.

This work was done with a grant from FCT, grant SFRH/BD/28517/2006, to which I acknowledge. I also acknowledge several projects I was involved in: IST-UNITE, whose contributions were the basis for the initial work plan, to CROSSNET, our FCT project on the cross-layer design and cross-system aspects, COST 2100, COST IC0905 TERRA and COST 290 (and its very fruitful meetings).

I would like to thank to Alberto Segarra for being a good friend and helping in the construction of the IEEE 802.11e simulation tool. To the final year project and master students Jesus Juarez, Dany Santos, Rui Marcos, Francisco Merca, João Oliveira and Rui Costa, who were colleges in the work group and good friends. To the actual group of PhD students, João Ferro, Luís Borges, Norberto Barroca, Daniel Robalo and Rui Paulo for making the work group stable, with good environment, and a second family. To Helder Matos for being a good friend and good listener. To Paulo Machado for his precious help with the latex editor.

Finally, I am very grateful to my wife, Ana Luísa for all the support given and patience with my bad humor. To my mother and and sister Susana, for taking care of us in the most difficult moments.

Abstract

The future wireless ecosystem will heterogeneously integrate a number of overlapped Radio Access Technologies (RATs) through a common platform. A major challenge arising from the heterogeneous network is the Radio Resource Management (RRM) strategy. A Common RRM (CRRM) module is needed in order to provide a step toward network convergence. This work aims at implementing HSDPA and IEEE 802.11e CRRM evaluation tools.

Innovative enhancements to IEEE 802.11e have been pursued on the application of cross-layer signaling to improve Quality of Service (QoS) delivery, and provide more efficient usage of radio resources by adapting such parameters as arbitrary interframe spacing, a differentiated backoff procedure and transmission opportunities, as well as acknowledgment policies (where the most advised block size was found to be 12). Besides, the proposed cross-layer algorithm dynamically changes the size of the Arbitration Interframe Space (AIFS) and the Contention Window (CW) duration according to a periodically obtained fairness measure based on the Signal to Interference-plus-Noise Ratio (SINR) and transmission time, a delay constraint and the collision rate of a given machine. The throughput was increased in 2 Mb/s for all the values of the load that have been tested whilst satisfying more users than with the original standard. For the ad hoc mode an analytical model was proposed that allows for investigating collision free communications in a distributed environment.

The addition of extra frequency spectrum bands and an integrated CRRM that enables spectrum aggregation was also addressed. RAT selection algorithms allow for determining the gains obtained by using WiFi as a backup network for HSDPA. The proposed RAT selection algorithm is based on the load of each system, without the need for a complex management system. Simulation results show that, in such scenario, for high system loads, exploiting localization while applying load suitability optimization based algorithm, can provide a marginal gain of up to 450 kb/s in the goodput. HSDPA was also studied in the context of cognitive radio, by considering two co-located BSs operating at different frequencies (in the 2 and 5 GHz bands) in the same cell. The system automatically chooses the frequency to serve each user with an optimal General Multi-Band Scheduling (GMBS) algorithm. It was shown that enabling the access to a secondary band, by using the proposed Integrated CRRM (iCRRM), an almost constant gain near 30 % was obtained in the throughput with the proposed optimal solution, compared to a system where users are first allocated in one of the two bands and later not able to handover between the bands. In this context, future cognitive radio scenarios where IEEE 802.11e ad hoc modes will be essential for giving access to the mobile users have been proposed.

Keywords:

Common Radio Resource Management, Spectrum Aggregation, Beyond 3G, Cross-layer design, SINR, ad hoc network, event driven simulation, optimization.

Resumo

O futuro ecossistema sem fios vai integrar heterogeneamente um número de Tecnologias de Acesso Rádio (RAT) numa plataforma comum. O maior desafio nestas redes heterogéneas é a estratégia de Gestão de Recursos Rádio (RRM). É necessário um módulo da Gestão Comum de Recursos Rádio (CRRM) que estabeleça uma ponte para a convergência da rede. Este trabalho visa desenvolver ferramentas de avaliação de RRM entre redes HSDPA e IEEE 802.11e.

Pesquisaram-se melhorias inovadoras para a norma IEEE 802.11e utilizando-se optimização inter-camada para melhorar a qualidade de serviço (QoS) e utilizar eficientemente os recursos disponíveis, adaptando parâmetros como o espaçamento arbitrário entre tramas, diferentes procedimentos de backoff e as oportunidades de transmissão, bem como as políticas de acknowledgment (onde o tamanho de blocos recomendável alcançado é 12). Além disso, o algoritmo inter-camada proposto altera dinamicamente o tamanho da *Arbitration Interframe Space* (AIFS) e da janela de contenção (CW), de acordo com medidas obtidas a partir da qualidade de sinal recebido (SINR) e do tempo de transmissão, do atraso permitido e da taxa de colisões de cada máquina. O débito binário aumentou em cerca de 2 Mb/s para todos os valores de carga testados, satisfazendo-se mais utilizadores que com a norma original. Para o modo ad hoc, propôs-se um modelo analítico que permite investigar comunicações sem colisões num ambiente distribuído.

Também se considerou a adição de bandas de frequência extra e um CRRM integrado que permite agregação de espectro. Os algoritmos de selecção da RAT permitem determinar os ganhos obtidos usando a tecnologia WiFi como rede de apoio ao HSDPA. O algoritmo de selecção RAT proposto baseia-se na carga de cada rede, não sendo necessário um sistema de gestão complexo. Os resultados de simulação demonstram que, num cenário com carga elevada, obtém-se um ganho marginal de 450 kb/s no *goodput* explorando localização e aplicando o algoritmo de optimização baseado na adequabilidade da carga. Também se investigou o HSDPA no contexto dos rádios cognitivos, considerando duas estações de base operando em diferentes frequências (nas bandas do 2 GHz e 5 GHz) na mesma célula. O sistema escolhe automaticamente a frequência que vai servir cada utilizador através de um algoritmo Geral de Calendarização Multi-Banda (GMBS). Demonstrou-se que, permitindo o acesso a uma banda secundária e utilizando a proposta CRRM Integrado (iCRRM), obtém-se um ganho quase constante de 30 % para o débito binário utilizando a solução óptima, em comparação com um sistema em que os utilizadores são inicialmente atribuídos a uma das duas bandas, não podendo posteriormente migrar de banda. Neste contexto, propuseram-se cenários futuros para rádios cognitivos onde o modo ad hoc da norma IEEE 802.11e será essencial para utilizadores móveis.

Palavras-chave

Gestão Comum de Recursos Rádio, Agregação de Espectro, Pós-3G, optimização inter-camada, SINR, redes ad hoc, simulação baseada em acontecimentos, optimização

Table of Contents

List of Figures

List of Tables

List of Acronyms

3GPP	3rd Generation Partnership Project
AC	Access Category
ACK	Acknowledgement
ACt	Allocation Constraint
ACU	Admission Control Unit
ADDBA	Add Block ACK
AIFS	Arbitration Interframe Space
AMC	Adaptive Modulation and Coding
AoA	Angle of Arrival
AP	Access Point
ARF	Automatic Rate Fallback
ARQ	Automatic Repeat Request
AT	Aggregated Throughput
B3G	Beyond 3G
BA	Block Acknowledgement
BC	Bandwidth Constraint
BE	Best Effort
BER	Bit Error Rate
BFWA	Broadband Fixed Wireless Access
BK	Background
BRAN	Broadband Radio Access Networks
BS	Base Station
BSS	Basic Service Set
CA	Carrier Aggregation
CAP	Controlled Access Phase
CF	Contention Free
CFP	Contention Free Period
CP	Contention Period
CPC	Cognitive Pilot Channel
CPICH	Common Pilot Channel
CQI	Channel Quality Indicator
CR	Cognitive Radio
CRRM	Common Radio Resource Management
CS	Carrier Sense
CSI	Channel State Information
CSMA	Carrier Sense Multiple Access

CSMA-CA	Carrier Sense Multiple Access with Collision Avoidance
CTS	Clear to Send
CW	Contention Window
DCF	Distribute Coordination Function
DELBA	Delete Block Acknowledgement
DIFS	DCF Interframe Space
DIFS	Distributed Inter-Frame Space
DL	Downlink
DS	Distribution System
DSM	Distribution System Medium
DVB-H	Digital Video Broadcast - Handhelds
EDCA	Enhanced Distributed Channel Access
EDCAF	Enhanced Distributed Channel Access Function
EIFS	Extended Interframe Space
ETSI	European Telecommunications Standards Institute
FCC	Federal Communications Commission
FCS	Frame Check Sequence
FEC	Forward Error Correction
GAP	General Assignment Problem
GMBS	General Multi-Band Scheduling
H-ARQ	Hybrid Automatic Repeat Request
HC	Hybrid Coordinator
HCCA	HCF Controlled Channel Access
HCF	Hybrid Coordination Function
HSDPA	High Speed Downlink Packet Access
HS-DPCCS	High-Speed Dedicated Physical Control Channel
HS-PDSCH	High Speed Physical Downlink Shared Channel
HSUPA	High Speed Uplink Packet Access
iCRRM	Integrated CRRM
IFFT	Inverse Fast Fourier Transform
IFS	Interframe Space
IMT-A	International Mobile Telecommunications-Advanced
IP	Integer Programming
ISI	Inter-Symbol Interference
LAN	Local Area Network
LTE	Long Term Evolution
LTE-A	Long Term Evolution-Advanced

MAC	Medium Access Control
MBS	Multi-Band Scheduling
MCS	Modulation and Coding Scheme
MMPDU	MAC Management Protocol Data Unit
MO-GAP	Multiple Objectives GAP
MPDU	MAC Protocol Data Unit
MS	Mobile Station
MSDU	MAC Service Data Unit
NAV	Network Allocation Vector
nQSTA	non QoS station
NRTV	Near Real Time Video
OFDM	Orthogonal Frequency Division Multiplexing
OSI	Open Systems Interconnection
PC	Point Coordinator
PCF	Point Coordination Function
PER	Packet Error Rate
PF	Profit Function
PHY	Physical Layer
PIFS	Point Coordination Function (PCF) Interframe Space
PLCP	Physical Layer Convergence Procedure
PPDU	PLCP Protocol Data Unit
PSDU	Physical layer Service Data Unit
QAP	QoS AP
QBSS	QoS Network BSS
QLRC	QoS Long Retry Counter
QoE	Quality of Experience
QoS	Quality of Service
QSRC	QoS Short Retry Counter
QSTA	QoS STA
RA	Resource Allocation
RAN	Radio Access Network
RAT	Radio Access Technology
RNC	Radio Network Controller
RR	Round Robin
RRM	Radio Resource Management
RSS	Received Signal Strength
RTS	Request to Send

SA	Spectrum Aggregation
SDR	Software-defined Radio
SIFS	Short Interframe Space
SIFS	Short Inter-Frame Space
SINR	Signal to Interference-plus-Noise Ratio
SIR	Signal-to-Interference Ratio
SO-GAP	Single Objective General Assignment Problem
STA	Station
TC	Traffic Category
TDoA	Time Difference of Arrival
TID	Traffic Identifier
ToA	Time of Arrival
TS	Traffic Stream
TTI	Time Transmission Interval
TXOP	Transmission Opportunities
UMTS	Universal Mobile Telecommunication Systems
UP	User Priorities
VI	Video
VO	Voice
WCDMA	Wideband Code Division Multiple Access
WiMAX	World Wide Interoperability for Microwave Access
WLAN	Wireless Local Area Network
WM	Wireless Medium

Chapter 1

Introduction

1.1 Motivation

The fast development and deployment of multimedia wireless and mobile communication systems Beyond 3G (B3G) is mainly driven by the demand of multimedia traffic, and research on network design and multi-service traffic aspects is strategic. Furthermore, heterogeneous mobile and wireless networks are nowadays available in the market, with very different characteristics, and dimensioning approaches. The research community is now directing its interest towards new ways of optimising not only each system individually, through cross-layer design in the context of All-IP networks but also of achieving cross-system optimization, making the simultaneous use of systems with totally different access technologies transparent to the user. Innovative architectures and protocols are being proposed for this coexistence, and mechanisms to guarantee the Quality of Service (QoS) will be explored, including Medium Access Control (MAC) layer solutions. Since there are totally different protocols and requirements in each system, a harmonized solution is sought. Aspects of intersystem handover, dynamic resource allocation and dynamic spectrum use are going to be addressed. The QoS provision for each service (within different traffic classes), and, based on adequate characterisation parameters, the identification of suitable schemes and network planning methodologies to guarantee high capacity (in several scenarios) are of particular interest in this thesis. One of the main ideas to be explored is related with the need for cooperation among physical, MAC, network and transport layers; the way that this can be done and the new definitions of cross-layer protocols are therefore important areas for study and investigation.

FIGURE 1.1: Example of interoperability among WiMAX, WiFi and B3G.

The coexistence scenario across heterogeneous networks should be seen by the end user as the ability to attain a plethora of multimedia services under a single platform in a ubiquitous and transparent fashion, providing the impetus for system solutions addressing network discovery, selection, connection, and reselection as the terminal equipment migrates between collocated networks.

In the scope of this thesis, interoperability among B3G and IEEE 802.11 is investigated, since these technologies, together with IEEE 802.16 and Long Term Evolution, as shown in Figure 1.1, are widely seen as the enablers for converging the wireless and mobile worlds. By using the existing simulation platforms for different systems such as High Speed Downlink Packet Access (HSDPA) and WiFi, a common Radio Resource Management (RRM) module has been developed in order to provide a step toward network convergence to hide the heterogeneity between operators and technologies.

1.2 Objectives

This work aims at implementing HSDPA and IEEE 802.11e evaluation tools for evaluating RRM protocol performance. Furthermore, cross-layer scheduling and link adaptation provide key output to enhance the effective capacity and coverage in a more cost-effective way. The IEEE 802.11 (also known as WiFi) technology has seen high penetration in the Broadband Fixed Wireless Access (BFWA) market to provide data services to hotspot areas, mainly due to ease of network deployment and low cost. However, with the QoS constraints becoming evermore stringent, the IEEE opted to evolve the 802.11 standard to 802.11e, a WiFi technology

for QoS support. The key enhancement in this evolved standard can be found in the MAC layer, which now provides support for differentiated service classes and proposes techniques to enhance the ability of the Physical Layer (PHY) to deliver time-critical multimedia traffic. This work addresses innovative enhancement to IEEE 802.11e by pursuing research studies on the application of cross-layer signaling to improve QoS delivery, and provide more efficient usage of radio resources by adapting such parameters as arbitrary interframe spacing, a differentiated backoff procedure, and transmission opportunities, as well as acknowledgment policies. A key output from this work is also the development of an event-driven PHY/MAC layer simulator for IEEE 802.11e.

Radio Access Technology (RAT) selection algorithms have been studied in the literature, and nowadays equipment with several RATs incorporated is already common. One needs to determine the gains obtained by using WiFi as a backup network for HSDPA have been obtained. The coexistence of the two standards allows prevention of QoS deterioration when in a low mobility scenario. The proposed RAT selection algorithm is based on the load of each system, and the research seeks the gain on supported network load with the implementation of this QoS procedure over the HSDPA-alone system whilst considering positioning. As a consequence, when there is heavy load on the IEEE 802.11e network, acceptance of high-priority services will affect the delay in low-priority services like FTP.

Supporting additional system capacity and higher data rates through high speed RAT, such as the International Mobile Telecommunications-Advanced (IMT-A), users can be granted universal access to broadband services. One important enabling factor is the availability of bandwidth, which is also related to the assignment of frequency spectrum bands for IMT-A different technologies. This is impeded by the existing highly fragmented radio frequency spectrum that does not match the actual demand for transmission and network resources. Such fragmentation poses a challenge during dynamic spectrum use where multiple frequency bands can be assigned in support of the users and the mobile transmission system's ability to support a wide range of services across all elements of the network (i.e., core, distribution and access [1]).

The fragmented available spectrum can be virtually joined through the Spectrum Aggregation (SA) technique suggested by IMT-A and Long Term Evolution-Advanced (LTE-A) [3], [4], [5]. Information about how to aggregate contiguous and not contiguous parts of the highly fragmented spectrum to be used and how to allocate users over the dedicated and shared bands

of an operator, can improve the overall system capacity, through the integration of spectrum and network resource management functionalities.

1.3 Contributions

A substantial part of the work presented in this thesis followed the steps of the IST-UNITE European project in which scenarios were created, cross layer optimization for several RATs was proposed, protocols and mechanisms that allow for the interoperability of the same RATs were proposed.

This thesis has several original contributions on Optimization of the Interoperability and Dynamic Spectrum Management in Mobile Communications Systems Beyond 3G that have already been reflected in the work developed in the framework of the IST-UNITE project [6], [7] and CROSSNET project [8] and in papers published, accepted for publication or submitted to evaluation both in conferences and journals:

- After developing the IEEE 802.11e simulator, this work on event-driven simulation for IEEE 802.11e optimization was published in [9];
- The IEEE 802.11e standard specifies acknowledgement policies but it leaves the size of the buffer that implements this procedure open. The research of the impact of the buffer size on the implementation of IEEE 802.11e block acknowledgement policies was published in [10], [11];
- Two functions that provide the IEEE 802.11e Enhanced Distributed Channel Access (EDCA) Arbitration Interframe Space (AIFS) and the contention window limits in a dynamic manner are proposed in [12], trough a cross-layer design of a weighted scheduler algorithm;
- Research work was done on routing for ad hoc networks with the work colleague Joao Ferro [13], [14]. The channel conditions and link layer information of each station are used in determining the best possible path with the IEEE 802.11e cross-layer multi-hop simulator that incorporates network layer components;
- Cognitive radio in the scope of ad hoc networks was addressed in [15]. A network of wireless networks, consisting of a backbone infrastructure provided by HSDPA radio towers

hierarchically bonded with user access to a flexible wireless ad hoc IEEE 802.11e network is considered;

- Common Radio Resource Management (CRRM) interoperability between HSDPA and IEEE 802.11e was also addressed. A suitability function for the RAT selection was proposed and evaluated [16], [17]. In [18], the impact of positioning in the performance of RAT selection with the load suitability function was studied;

- In the scope of CRRM, besides managing several Radio Access Technologies, SA, a new new procedure proposed in Long Term Evolution (LTE), was also explored, in which several bunch of spectrum bands are managed. An Integrated CRRM (iCRRM) was proposed in [19] that facilitates the management of several spectrum bands.

1.4 Organization

The outline of this thesis is described in what follows.

Besides introduction, the thesis has more four Chapters, and six Appendices. Chapter 2 has two parts. The first part introduces the main aspects that characterize the IEEE 802.11e standard (Section 2.1 to 2.5). The second part presents the main aspects of the developed IEEE 802.11e simulator, as well as performance results (section 2.6 and 2.7). Finally conclusions are drawn in section 2.8, where proposal for future work are also discussed.

Chapter 3 presents the optimization of IEEE 802.11e. It is divided into three parts: Section 3.2 addresses the optimization of the BA procedure, while Section 3.3 addresses the optimization through cross-layer design. Section 3.4 presents an analytical formulation for a multi-hop ad hoc network. The first part starts by presenting the BA procedure followed by a review of the state of the art on BA. Then, the system scenario and assumptions in which tests were performed are addressed and finally a summary and conclusions regarding the BA studies are presented. The second part of the chapter starts by presenting the state of the art on optimization procedures for IEEE 802.11 and on the interoperability among wireless systems, then it are described the assumptions for system and scenarios, including details on traffic parameters, followed by the description of the developed cross-layer algorithm. Then, a comparison of simulation results between the presence and absence of the proposed weighted cross-layer design algorithm is performed. Very promising results are obtained by using the MAC plus PHY layers simulator.

Finally, conclusions are drawn as well as suggestions for future work. The third part of this Chapter presents the notation and formulation, followed by the network and model scope, then some numerical results and in the end, a summary and conclusions.

Chapter 4 is divided into three Sections that consider CRRMs in different perspectives. In the first Section, the CRRM has the capacity to schedule users in completely different RATs: one is centralized, HSDPA, whilst the other is distributed, WiFi. The interworking scenario is proposed, and the positioning based suitability policy is described, in terms of the RAT selection procedures and of the identification of suitable metrics for normalized load whilst WiFi and HSDPA. The numerical results accounting for localization in RAT selection are then addressed. Finally, the conclusions are drawn. In the second Section, one addresses a CRRM that is capable of scheduling users in different bands within the same RAT. First, the objective of the work and system model are presented, followed by the General Multi-Band Scheduling (GMBS) as a General Assignment Problem (GAP). Then, a formulation to obtain the average Signal to Interference-plus-Noise Ratio (SINR), with unitary reuse pattern is proposed and its dependence on the cell coverage distance is analyzed. Finally, the SA results with the proposed iCRRM are discussed, and conclusions are drawn. In this chapter it is also proposed a scenario for interoperability between HSDPA and WiFi in which the end-user is travelling in public transportation system and requesting multimedia services to the operator. It was sought the most efficient way to manage routing packets inside the WiFi ad hoc network. Finally, the challenges that need to be addressed in order to materialize the envisaged cognitive radio scenario in public transportation are discussed.

Finally Chapter 5 presents the conclusions, some final considerations and suggestions for future research.

Chapter 2

IEEE 802.11e Event Driven Simulation

In recent years, an amazingly rapid evolution in Wireless Local Area Network (WLAN) as occurred. Due to the low cost, and easiness of deployment, IEEE 802.11 WLANs have been used so widely that they become the dominant WLAN technology. This is mainly because the technology is reaching an unprecedented maturity in regard to providing higher bit rates as the time goes by; however, it could not fulfil the increasing demand for QoS support from the increasingly popular multimedia applications yet.

To overcome this limitation, the IEEE 802.11e standard [20] is specified aiming to support QoS by providing differentiated classes of service in the MAC layer and to enhance the ability of the physical layer so that they can deliver time-critical multimedia traffic, in addition to traditional data packets.

A C++ simulator was developed that enables simulations that analyse the performance and allows the improvement of IEEE 802.11e mechanisms, such as optimization of arbitrary inter frame spacing, differentiated backoff procedure, and the transmission opportunities for each service class, as well as experiments on acknowledgment policies.

This chapter is organized into two parts. The first part introduces the main aspects that characterize the IEEE 802.11e standard (Section 2.1 to 2.5). The second part presents the main aspects of the developed IEEE 802.11e simulator, as well as performance results (section 2.6 and 2.7). Finally conclusions are drawn in section 2.8, where proposal for future work are also discussed. Complete details on the Distributed Coordination Function are addressed in Appendix A, while Appendix B gives a detailed overview of the Hybrid Coordination Function.

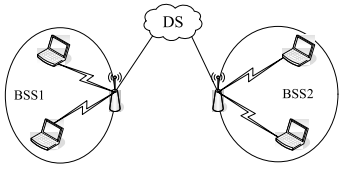

FIGURE 2.1: Architecture for IEEE 802.11e.

2.1 IEEE 802.11e general aspects

The IEEE 802.11 architecture consists of several components that interact to provide a WLAN that supports station mobility transparently to upper layers. The Basic Service Set (BSS) is the basic building block of an IEEE 802.11 Local Area Network (LAN). Figure 2.1 shows two BSSs, each of which have two stations that are members of the BSS. It is useful to think of the ovals used to depict a BSS as the coverage area within which the member stations of the BSS may remain in good quality communication. If a station moves out of its BSS it can no longer directly communicate with other members of the BSS. PHY limitations determine the direct station-to-station distance that may be supported. For some networks this distance is sufficient; for other networks, increased coverage is required. Instead of existing independently, a BSS may also form a component of an extended form of network that is built with multiple BSSs. The architectural component used to interconnect BSSs is the Distribution System (DS). IEEE 802.11 logically separates the Wireless Medium (WM) from the Distribution System Medium (DSM). Each logical medium is used for different purposes, by a different component of the architecture.

The DS enables mobile device support by providing the logical services necessary to handle address to destination mapping and seamless integration of multiple BSSs. An Access Point (AP) is a Station (STA) that provides access to the DS by providing DS services in addition to acting as a STA Data move between a BSS and the DS via an AP. All APs are also STAs; thus they are addressable entities. The addresses used by an AP for communication on the WM and on the DSM are not necessarily the same.

All data from non-IEEE 802.11 LANs enter the IEEE 802.11 architecture via a portal. The gateway provides logical integration between the IEEE 802.11 architecture and existing wired LANs. It is possible for one device to offer both the functions of an AP and a gateway.

For wireless PHYs, well-defined coverage areas simply do not exist. Propagation characteristics are dynamic and unpredictable, a small change in position or direction may result in dramatic

differences in signal strength. Whether a STA is stationary or mobile similar effects occur .

The IEEE 802.11e QoS facility provides MAC enhancements to support LAN applications with QoS requirements. The QoS enhancements are available to QoS STA (QSTA) associated with a QoS AP (QAP) in a QoS Network BSS (QBSS). This amendment provides two mechanisms for the support of applications with QoS requirements, the EDCA and the HCF Controlled Channel Access (HCCA) used to support applications with QoS requirements. To handle QoS traffic in a manner comparable to other IEEE 802.11 LANs, the IEEE 802.11 QoS facility requires the IEEE 802.11 MAC sublayers to incorporate functionalities that are not traditional.

The first mechanism, called the EDCA, delivers traffic based on differentiating User Prioritiess (UPs). This differentiation is achieved by varying the following for different UP values:

- amount of time a STA senses the channel to be idle before backoff or transmission;
- length of the contention window to be used for the backoff;
- duration a STA may transmit after it acquires the channel.

The second mechanism, called HCCA, allows for the reservation of Transmission Opportunitiess (TXOPs) with the HC. A non–AP QSTA based on its requirements requests o an entity called Hybrid Coordinator (HC) for a TXOPs, both for its own transmissions as well as for transmissions from the QAP to itself.

2.2 Main concepts MAC sublayer functions

The enhanced MAC architecture of WiFi with QoS support can be described as presented in Figure 2.2. PCF and Hybrid Coordination Function (HCF) are provided through the services of the Distribute Coordination Function (DCF). In a non QoS station (nQSTA) the HCF is not present, it is the basic model of a STA in the WM. In a QSTA implementation, both DCF and HCF are present. PCF is optional in all STAs.

2.2.1 Distribute Coordination Function

The fundamental access method of the IEEE 802.11 MAC is a DCF known as Carrier Sense Multiple Access with Collision Avoidance (CSMA-CA). The DCF shall be implemented in all

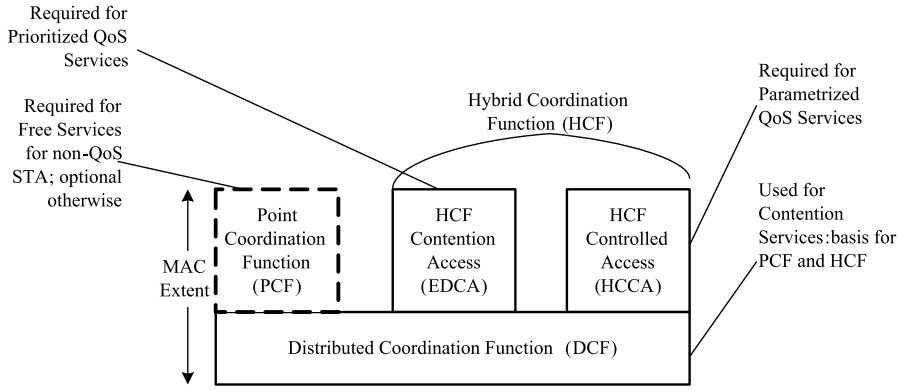

FIGURE 2.2: Medium access control architecture.

STAs, for use within both independent BSS and infrastructure network configurations. For a STA to transmit, it shall sense the medium to determine if another STA is transmitting. If the medium is not determined to be busy, the transmission may proceed. The CSMA-CA distributed algorithm mandates that a gap of a minimum specified duration exist between contiguous frame sequences. A transmitting STA shall ensure that the medium is idle for this required duration before attempting to transmit. If the medium is determined to be busy, the STA shall defer until the end of the current transmission. After deferral, or prior to attempting to transmit again immediately after a successful transmission, the STA shall select a random backoff interval and shall decrement the backoff interval counter while the medium is idle. A more complete overview of DCF is presented Appendix A, including the carrier sense mechanism, the interframe spacing, the random backoff timer and the backoff procedure, setting and resetting the network allocation vector, the usage of RTS/CTS with fragmentation.

2.2.2 Point Coordination Function

The IEEE 802.11 MAC layer may also incorporate an optional access method called a PCF, which is only usable on infrastructure network configurations. This access method uses a Point Coordinator (PC), which shall operate at the access point of the BSS, to determine which STA currently has the right to transmit. The operation is essentially that of polling, with the PC performing the role of the polling master. The operation of the PCF may require additional coordination, not specified in the IEEE 802.11 standard, to permit efficient operation in cases where multiple point-coordinated BSSs are operating on the same channel, in overlapping physical space.

The PCF uses a virtual Carrier Sense (CS) mechanism aided by an access priority mechanism. The PCF shall distribute information within beacon management frames to gain control of the medium by setting the Network Allocation Vector (NAV) in STAs. In addition, all frame transmissions under the PCF may use an Interframe Space (IFS) that is smaller than the Distributed Inter-Frame Space (DIFS) for frames transmitted via the DCF. The use of a smaller IFS implies that point-coordinated traffic shall have priority access to the medium over STAs in overlapping BSSs operating under the DCF access method. The access priority provided by a PCF may be utilized to create a Contention Free (CF) access method. The PC controls the frame transmissions of the STAs so as to eliminate contention for a limited period of time.

2.2.3 Hybrid Coordination Function

The QoS enhancement added by IEEE 802.11e amendment includes an additional coordination function called HCF that is only usable in a QoS network with QBSS configurations. The HCF shall be implemented in all QSTAs. The HCF combines functions from the DCF and PCF with some enhanced QoS-specific mechanisms and frame subtypes to allow a uniform set of frame exchange sequences to be used for QoS data transfers during both the Contention Period (CP) and Contention Free Period (CFP). The HCF uses both a contention-based channel access method, called the EDCA mechanism for contention-based transfer and a controlled channel access, referred to as the HCCA mechanism, for contention-free transfer. Appendix B provides a detailed overview of the Hybrid Coordination Function.

2.2.3.1 Enhanced Distributed Channel Access

The EDCA mechanism provides differentiated, distributed access to the WM for QSTAs using eight different UPs. The EDCA mechanism defines four Access Category (AC) that provide support for the delivery of traffic with UPs at the QSTAs. The AC is derived from the UPs as presented in Table 2.1. The mapping between UPs and ACs is described in Figure 2.3.

For each AC, an enhanced variant of the DCF, called an Enhanced Distributed Channel Access Function (EDCAF), contends for TXOPs using a set of EDCA parameters from the EDCA Parameter Set element or from the default values for the parameters when no EDCA Parameter Set element is received from the QAP of the QBSS with which the QSTA is associated, where:

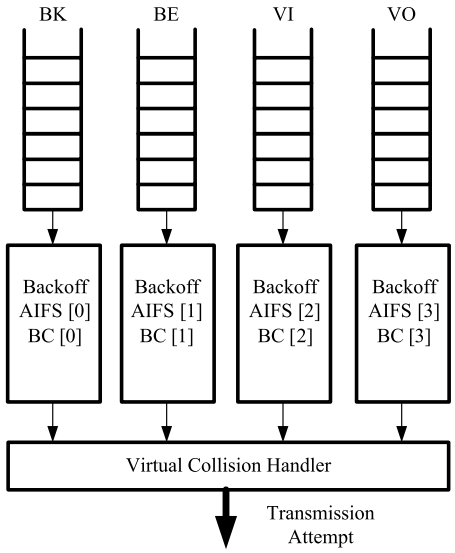

FIGURE 2.3: The access categories in EDCA.

TABLE 2.1: User priorities to access categories mappings

Priority	**UP (Same as 802.1D user priority)**	**802.1D Designation**	**AC**	**Designation**
Lowest	1	BK	AC_BK	Background
	2	—	AC_BK	Background
	0	BE	AC_BE	Best Effort
↓	3	EE	AC_BE	Best Effort
	4	CL	AC_VI	Video
	5	VI	AC_VI	Video
	6	VO	AC_VO	Voice
Highest	7	NC	AC_VO	Voice

1. The parameters used by the EDCAF to control its operation are defined by the MIB attribute table dot11QAPEDCATable [20] at the QAP and by MIB attribute table dot11-EDCATable [20] at the non-AP QSTA.

2. The minimum specified idle duration time is not the constant value DIFS as defined for DCF, but is a distinct value (contained in the MIB attribute table dot11QAPEDCATable-AIFSN [20] for a QAP and in the MIB table dot11EDCATableAIFSN [20] for a non-AP QSTA) assigned either by a management entity or by a QAP.

3. The contention window minimum and maximum limits, $aCWmin$ and $aCWmin$, respectively, from which the random backoff is computed, are not fixed per PHY, as with DCF, but are variable (contained in the MIB attribute tables dot11QAPEDCACWmin and

TABLE 2.2: EDCA default settings.

Access Category	CWmin	CWmax	AIFS
AC_BK	*aCWmin* (7)	*aCWmax* (255)	SIFS + 7*TS
AC_BE	*aCWmin* (7)	*aCWmax* (255)	SIFS + 3*TS
AC_VI	(*aCWmin*+1)/2-1	*aCWmin* (7)	SIFS + 2*TS
AC_VO	(*aCWmin*+1)/4-1	(*aCWmin*+1)/2-1	SIFS + 2*TS

dot11QAPEDCACWmax for a QAP and in the MIB attribute tables dot11EDCATableCWmin and dot11EDCATableCWmax for a non-AP QSTA) and assigned by a management entity or by a QAP, as presented in Table 2.2.

4. Collisions between contending EDCAFs within a QSTA are resolved within the QSTA so that the data frames from the higher priority AC receives the TXOP and the data frames from the lower priority colliding ACs behave as if there were an external collision on the WM. However, this collision behavior does not include setting retry bits in the MAC headers of MAC Protocol Data Units (MPDUs) at the head of the lower priority ACs, as would be done after a transmission attempt that was unsuccessful due to an actual external collision on the WM.

5. During an EDCA TXOP won by an EDCAF, a QSTA may initiate multiple frame exchange sequences to transmit MAC Management Protocol Data Units (MMPDUs) and/or MAC Service Data Units (MSDUs) within the same AC. The duration of this EDCA TXOP is bounded, for an AC, by the value in dot11QAPEDCATXOPLimit MIB variable for a QAP and in dot11EDCATableTXOPLimit MIB table for a non-AP QSTA.

The management frames shall be sent using the access category AC_VO without being restricted by admission control procedures. A QSTA shall also send management frames using the access category AC_VO before associating with any BSS, even if there is no QoS facility available in that BSS.

A more complete overview of HCF is given in Appendix B, which includes details on EDCA TXOP, obtaining an EDCA TXOP, multiple frame transmission in an EDCA TXOP, and the EDCA backoff procedure.

2.2.3.2 HCF Controlled Channel Access

The HCCA mechanism uses a QoS-aware centralized coordinator, called a HC, and operates under rules that are different from the PC of the PCF. The HC is collocated with the QAP of the QBSS and uses the HC's higher priority of access to the WM to initiate frame exchange sequences and to allocate TXOPs to itself and other QSTAs in order to provide limited-duration Controlled Access Phase (CAP) for CF transfer of QoS data.

The HC traffic delivery and TXOP allocation may be scheduled during the CP and any locally generated CFP (generated optionally by the HC) to meet the QoS requirements of a particular Traffic Category (TC) or Traffic Stream (TS). TXOP allocations and contention-free transfers of QoS traffic can be based on the HC's QBSS-wide knowledge of the amounts of pending traffic belonging to different TS and/or TCs and are subject to QBSS-specific QoS policies. The HCF protects the transmissions during each CAP using the virtual CS mechanism.

2.2.4 Coexistence of DCF, PCF, and HCF

The DCF and the centralized coordination function (either PCF or HCF) shall coexist in a manner that permits both to operate concurrently within the same BSS. When a PC is operating in a BSS, the PCF and DCF access methods alternate, with a CFP followed by a CP.

When an HC is operating in a QBSS, it may generate an alternation of CFP and CP in the same way as a PC, using the DCF access method only during the CP. The HCF access methods (controlled and contention-based) operate sequentially when the channel is in CP. Sequential operation allows the polled and contention-based access methods to alternate, within intervals as short as the time to transmit a frame exchange sequence.

2.2.5 Overview of fragmentation/defragmentation

The process of partitioning a MAC Service Data Unit (MSDU) or a MAC Management Protocol Data Unit (MMPDU) into smaller MAC level frames, MPDUs, is called fragmentation. Fragmentation creates MPDUs smaller than the original MSDU or MMPDU length to increase reliability, by increasing the probability of successful transmission of the MSDU or MMPDU in cases where channel characteristics limit reception reliability for longer frames, as shown in Figure 2.4. QSTAs may use fragmentation to use the medium efficiently in consideration of

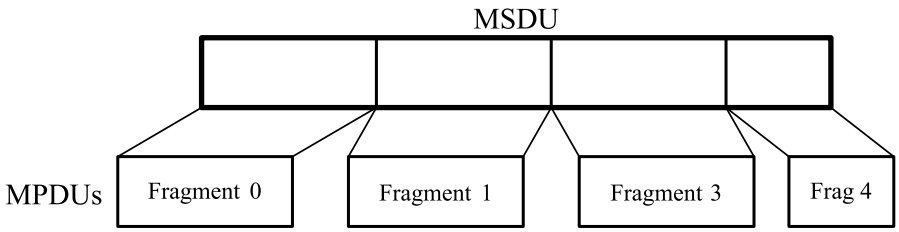

FIGURE 2.4: Fragmentation.

the duration available in granted TXOPs. Fragmentation is accomplished at each immediate transmitter. The process of recombining MPDUs into a single MSDU or MMPDU is defined as defragmentation. Defragmentation is accomplished at each immediate recipient.

Only MPDUs with a unicast receiver address shall be fragmented. Broadcast/multicast frames shall not be fragmented even if their length exceeds adot11FragmentationThreshold.

The MPDUs resulting from the fragmentation of an MSDU or MMPDU are sent as independent transmissions, each of which is separately acknowledged. This permits transmission retries to occur per fragment, rather than per MSDU or MMPDU. Unless interrupted due to medium occupancy limitations for a given PHY or TXOP limitations for QSTA, the fragments of a single MSDU or MMPDU are sent as a burst during the CP, using a single invocation of the DCF or EDCA medium access procedure. The fragments of a single MSDU or MMPDU are either:

- Sent during a CFP as individual frames obeying the rules of the PC medium access procedure or
- Sent as a burst in an EDCA or HCCA TXOP.

2.3 Block Acknowledgment

The Block Acknowledgement (BA) mechanism improves channel efficiency by aggregating several acknowledgments into one frame. There are two types of Block ACK mechanisms: immediate and delayed. Immediate Block ACK is suitable for high-bandwidth, low-latency traffic while the delayed Block ACK is suitable for applications that tolerate moderate latency. The QSTA with data to send using the Block ACK mechanism is referred to as the originator, and the receiver of that data as the recipient.

The Block ACK mechanism is initialized by an exchange of Add Block ACK (ADDBA) Request/Response frames. After initialization, blocks of QoS data frames can be transmitted from

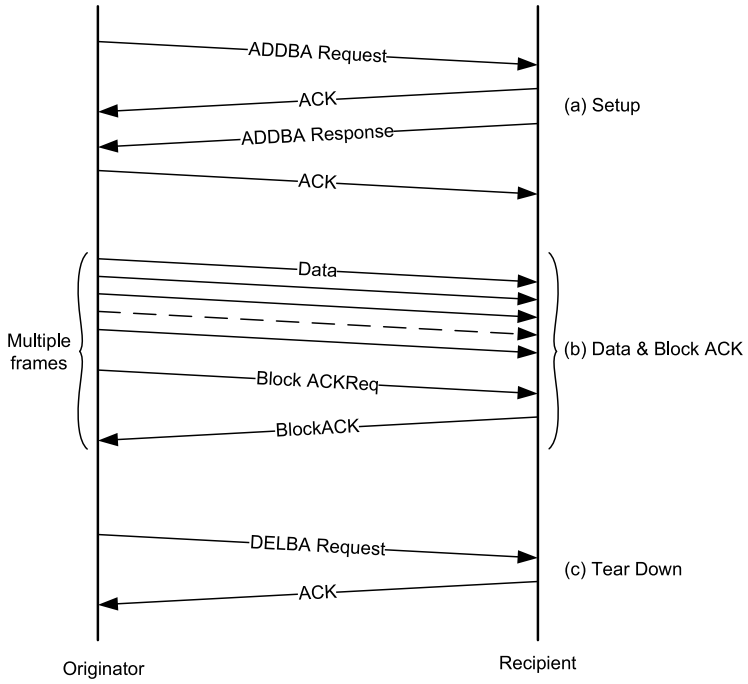

FIGURE 2.5: Block ACK sequence.

the originator to the recipient. A block may be started within a polled TXOP or by winning EDCA contention. The number of frames in the block is limited, and the amount of state that is to be kept by the recipient is bounded. The MPDUs within the block of frames are acknowledged by a BlockAck control frame, which is requested by a BlockAckReq control frame.

Figure 2.5 illustrates the message sequence chart for the setup, data and Block ACK transfer, and the teardown of the Block ACK mechanism.

2.3.1 Setup and modification of the Block ACK parameters

A QSTA that intends to use the Block ACK mechanism for the transmission of QoS data frames to a peer should first check whether the intended peer QSTA is capable of participating in Block ACK mechanism by discovering and examining its buffer of Block ACK. If the intended peer QSTA is capable of participating, the originator sends an ADDBA Request frame indicating the Traffic Identifier (TID) for which the Block ACK is being set up. The Block ACK Policy and Buffer Size fields in the ADDBA Request frame are advisory and may be changed by the recipient. The receiving QSTA responds by an ADDBA Response frame. The receiving QSTA, which is the intended peer, has the option of accepting or rejecting the request. When the QSTA accepts, then a Block ACK agreement exists between the originator and recipient. When the

QSTA accepts, it indicates the type of Block ACK and the number of buffers that it allocates for the support of this block. If the receiving QSTA rejects the request, then the originator shall not use the Block ACK mechanism.

Once the Block ACK exchange has been set up, data and ACK frames are transferred using the procedure described in the next section.

2.3.2 Data and ACK transfer

After setting up for the Block exchange following the procedure in previous section, the originator may transmit a block of QoS data frames separated by SIFS period, with the total number of frames not exceeding the Buffer Size subfield value in the associated ADDBA Response frame. Each of the frames have the ACK Policy subfield in the QoS Control field set to Block ACK. The RA field of the frames is be the recipient's unicast address. The originator requests acknowledgment of outstanding QoS data frames by sending a BlockAckReq frame. The recipient has to maintain a Block ACK record for the block.

Subject to any constraints in this subclause about permitted use of TXOP according to the channel access mechanism used, the originator may:

- Separate the Block and BlockAckReq frames into separate TXOPs;
- Split a Block frame across multiple TXOPs;
- Sequence or interleave MPDUs for different RAs within a TXOP.

A protective mechanism (such as transmitting using Request to Send (RTS)/Clear to Send (CTS)) should be used to reduce the probability of other STAs transmitting during the TXOP. If no protective mechanism is used, then the first frame that is sent as a block has a response frame and has the Duration field set so that the NAVs are set to appropriate values at all STAs in the QBSS.

The originator uses the Block ACK starting sequence control to signal the first MPDU in the block for which an acknowledgment is expected. MPDUs in the recipient's buffer with a sequence control value that any complete MSDUs from buffered preceding MPDUs and indicate these to its higher layer. The recipient then releases any buffers held by preceding MPDUs.

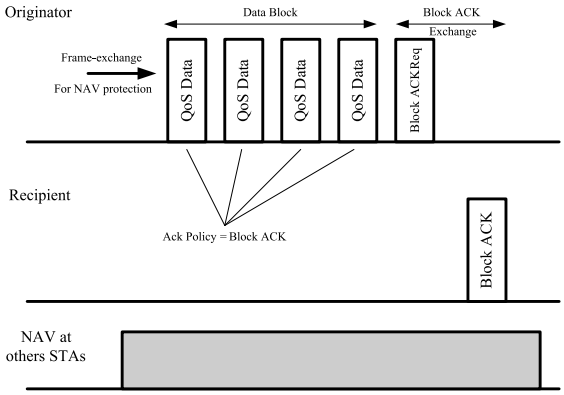

FIGURE 2.6: Immediate Block ACK.

The range of the outstanding MPDUs (i.e., the reorder buffer) begins on an MSDU boundary. The total number of frames that can be sent depends on the total number of MPDUs in all the outstanding MSDUs. The total number of MPDUs in these MSDUs may not exceed the reorder buffer size in the receiver.

The recipient maintains a Block ACK record consisting of originator address, TID, and a record of reordering buffer size indexed by the received MPDU sequence control value. This record holds the acknowledgment state of the data frames received from the originator.

If the immediate Block ACK policy is used, the recipient responds to a BlockAckReq frame with a Block ACK frame. If the recipient sends the Block ACK frame, the originator updates its own record and retries any frames that are not acknowledged in the Block ACK frame, either in another block or individually. If the delayed Block ACK policy is used, the recipient responds to a BlockAckReq frame with an ACK frame. The recipient then sends its Block ACK response in a subsequently obtained TXOP. Once the contents of the Block ACK frame have been prepared, the recipient sends this frame in the earliest possible TXOP using the highest priority AC. The originator responds with an ACK frame upon receipt of the Block ACK frame.

The Block ACK frame contains acknowledgments for the previous MPDUs. In the Block-ACK frame, the QSTA acknowledges only the MPDUs starting from the starting sequence MPDU until the last MPDU that has been received, and the QSTA sets bits in the Block ACK bitmap corresponding to all other MPDUs to 0. If the BlockAck frame indicates that an MPDU was not received correctly, the originator retries that MPDU subject to that MPDU's appropriate lifetime limit. A typical Block ACK frame exchange sequence using the immediate Block ACK is presented in Figure 2.6. A typical Block ACK sequence using the delayed Block ACK is presented

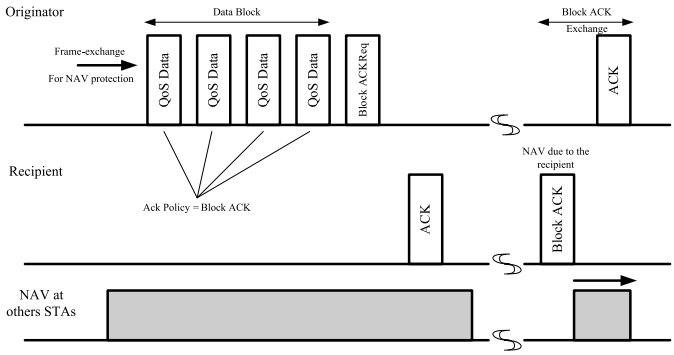

FIGURE 2.7: Delayed Block ACK.

in Figure 2.7. The subsequent Block ACK request starting sequence number is higher than or equal to the starting sequence number of the immediately preceding BlockAckReq frame.

The originator may continue to transmit MPDUs to the recipient after transmitting the BlockAckReq frame, but before receiving the Block ACK frame (applicable only to delayed Block ACK). The bitmap in the Block ACK frame includes the status of frames received between the start sequence number and the transmission of the BlockAckReq frame. A recipient sending a delayed Block ACK frame may update the bitmap with information on QoS data frames received between the receipt of the BlockAckReq frame and the transmission of the Block ACK frame.

If there is no response (i.e., neither a Block ACK nor an ACK frame) to the BlockAckReq frame, the originator may retransmit the BlockAckReq frame within the current TXOP (if time permits) or within a subsequent TXOP. MSDUs that are sent using the Block ACK mechanism are not subject to retry limits but only to MSDU lifetime. The originator need not set the retry bit for any possible retransmissions of the MPDUs.

The BlockAckReq frame is discarded if all MSDUs referenced by this BlockAckReq frame have been discarded from the transmit buffer due to expiry of their lifetime limit. In order to improve efficiency, originators using the Block ACK facility may send MPDU frames with the ACK Policy subfield in QoS control frames set to Normal ACK if only a few MPDUs are available for transmission. The Block ACK record is updated irrespective of the ACK Policy subfield in the QoS data frame for the TID with an active Block ACK. When there is sufficient number of MPDUs, the originator may switch back to the use of Block ACK. The reception of QoS data frames using Normal ACK policy are not used by the recipient to reset the timer to detect Block ACK timeout. This allows the recipient to delete the Block ACK if the originator does not switch back to using Block ACK.

2.3.3 Receive buffer operation

Upon the reception of a QoS data frame from the originator for which the Block ACK agreement exists, the recipient shall buffer the MSDU regardless of the value of the ACK Policy subfield within the QoS Control field of the QoS data frame. The recipient always indicates the reception of MSDU to its MAC client in order of increasing sequence number.

2.3.4 Teardown of the Block ACK mechanism

When the originator has no data to send and the final Block ACK exchange has completed, it signals the end of its use of the Block ACK mechanism by sending the Delete Block Acknowledgement (DELBA) frame to its recipient. There is no management response frame from the recipient. The recipient of the DELBA frame releases all resources allocated for the Block ACK transfer.

The Block ACK agreement may be torn down if there are no Block ACK, BlockAckReq, or QoS data frames (sent under Block ACK policy) for the Block ACK's TID received from the peer within a duration of Block ACK timeout value.

2.4 IEEE 802.11a Physical and Link Layer

The IEEE 802.11a standard [2] [21] defines an Orthogonal Frequency Division Multiplexing (OFDM)-based PHY that operates in the 5 GHz frequency bands, being able to achieve bit-rates as high as 54 Mb/s. It defines 8 non-overlapping channels of 20 MHz each across the low and middle 5 GHz bands (5.15-5.35 GHz) and 4 more channels across the high 5 GHz band (5.725-5.825 GHz). Each of these channels is divided into 52 subcarriers, with each subcarrier being approximately 300 kHz wide. In each channel 48 subcarriers are used for data transmission, while the remaining four subcarriers are used as pilots for coherent detection. A high data rate is achieved by combining 48 lower bit-rate data streams transmitted in parallel, each modulating a different subcarrier. The parallel transmission of 52 modulation symbols, one in each subcarrier, forms an OFDM symbol. These OFDM symbols are created by an Inverse Fast Fourier Transform (IFFT), which combines the subcarriers before transmission.

TABLE 2.3: IEEE 802.11a PHY modes.

Mode	Modulation	Code Rate	Bit-rate	BpS
1	BPSK	1/2	6 Mb/s	3
2	BPSK	3/4	9 Mb/s	4.5
3	QPSK	1/2	12 Mb/s	6
4	QPSK	3/4	18 Mb/s	9
5	16-QAM	1/2	24 Mb/s	12
6	16-QAM	3/4	36 Mb/s	18
7	64-QAM	2/3	48 Mb/s	24
8	64-QAM	3/4	54 Mb/s	27

TABLE 2.4: IEEE 802.11a OFDM PHY characteristics.

Characteristics	Value	Comments
aSlotTime	9 μs	slot time
aSIFSTime	16 μs	SIFS time
aDIFSTime	34 μs	$aDIFSTime = aSIFSTime + 2aSlotTime$
aCWmin	15	min contention window size in unit of *aSlotTime*
aCWmax	1023	max contention window size in unit of *aSlotTime*

IEEE 802.11a specifies 8 different transmission modes, obtained with different combinations of modulation and convolutional code rate. Each transmission mode corresponds to a different bit-rate. Within an OFDM symbol the same transmission mode is used in all data subcarriers. The IEEE 802.11a transmission modes are listed in Table 2.3, together with the respective number of bytes transmitted in one OFDM symbol (Bytes-per-Symbol, BpS), and the IEEE 802.11a OFDM PHY characteristics in Table 2.4. The convolutional encoder always encodes data with code rate 1/2. The 3/4 and 2/3 codes are derived from the original 1/2 code by a technique called puncturing. Puncturing is a procedure for omitting some of the encoded bits in the transmitter, and inserting a dummy "zero" metric into the convolutional decoder at the receiver, in place of the omitted bits. This technique is a simpler and more efficient way of generating a higher code rate.

Within indoor radio environments, signals coming from multiple indirect paths added to the direct path induce delay spread. This may be large enough to cause Inter-Symbol Interference (ISI) if high rates are used. In OFDM counters this effectis opposed within each subcarrier by transmitting data in parallel using lower-rate subcarriers. However, ISI can be further reduced with the introduction of a guard interval in the beginning of each OFDM symbol. A guard interval longer than the maximum channel excess delay ensures that ISI is eliminated. With a guard interval of length T_g, a new block duration is obtained as $T_b' = T_g + T_b$. In IEEE 802.11a, T_g=T_b/4=800 ns, which means that T'_b=4 ns.

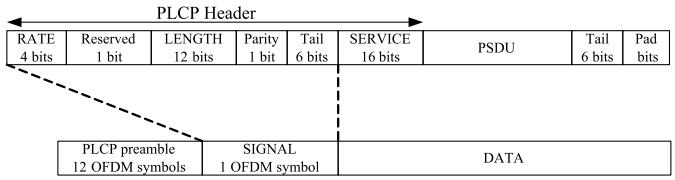

FIGURE 2.8: Format of the IEEE 802.11a PPDU.

The cyclic prefix has two drawbacks worth to be mentioned. One of them is the overhead transmitted over the radio channel, which reduces the maximum data rate achievable on top of OFDM. The other one is that the cyclic prefix of duration T_g leads to a power loss, as the receiver only uses the energy received during time T_b, discarding the energy that corresponds to T_g. A power loss α_g must thus be taken into account:

$$\alpha_g = \frac{T_b}{T_b'} \tag{2.1}$$

Consequently, the ratio between the effective average symbol energy and the noise power spectral density, E_{av}/N_o, is related to the SINR in the following way:

$$\frac{E_{av}}{N_o} = \alpha_g \cdot \frac{E_s}{N_o} = \alpha_g \cdot SINR \tag{2.2}$$

where E_s/N_0 is the ratio between the raw average symbol energy (i.e., including the energy of the cyclic prefix) and the noise power spectral density (see Annex F).

The PLCP Protocol Data Unit (PPDU) frame format is depicted in Figure 2.8. It consists of a Physical Layer Convergence Procedure (PLCP) preamble of 12 OFDM symbols, followed by the PLCP SIGNAL field and a variable size DATA field.

The preamble field is composed of 10 repetitions of a “short training sequence” (used for automatic gain control, diversity selection, timing acquisition, and coarse frequency acquisition in the receiver) and two repetitions of a “long training sequence” (used for channel estimation and fine frequency acquisition in the receiver), preceded by a guard interval. The PLCP header is composed of the SIGNAL field and the SERVICE field. The former constitutes an OFDM symbol, and is transmitted with the lowest rate (BPSK-1/2), being composed of the payload RATE indicator, a reserved bit, the payload LENGTH, an even parity bit and six “zero” tail bits. The SERVICE field belongs to the DATA part and comprises seven “zero bits” used to synchronise the descrambler, followed by 9 bits reserved for future use. The DATA field also comprises the

Physical layer Service Data Unit (PSDU) followed by 6 “zero” tail bits and a number of pad bits so that the total length of the DATA part corresponds to an integer number of OFDM symbols. The DATA part is encoded with the RATE specified in the SIGNAL field.

Link adaptation

Link-adaptation can be based on several techniques:

1. Adaptation of frame size;
2. Automatic Repeat Request (ARQ);
3. Forward Error Correction (FEC);
4. Selection of coded modulation schemes with different bandwidth efficiency (bits/symbol) and thus different physical bit-rate (this technique is usually called as rate-adaptation).

All these techniques incur on an overhead penalty, which must be weighted against the overall goodput and energy efficiency that can be achieved. There are several proposals of link-adaptation schemes presented in [22], [23], [24], [25].

Another rate-adaptation mechanism for IEEE 802.11a is proposed in [26] and further developed in [27]. In this algorithm, the sender chooses the bit-rate that achieves the highest goodput taking into account a Channel State Information (CSI) estimate and the number of transmission attempts. A PHY mode threshold table is calculated based on a conditional probability density function that models channel status variation. This rate-adaptation mechanism is compared with Automatic Rate Fallback (ARF) by means of computer simulation, demonstrating its better performance. The algorithm considers no CSI feedback protocol. Instead the sender estimates the path loss at the receiver based on the received power of frames that come from the receiver (e.g., ACK and CTS frames) and on the transmission power indication in the PPDU. Thus, it is assumed that the path loss is the same in both directions, which may not be true due to multipath effects. The sender also estimates the noise at the receiver based on local noise power, which does not take into account the differences in terms of the experienced interference.

A requirement for the effectiveness of link-adaptation is to have a good estimate of the channel status. This can be accomplished with different techniques. In [22] and [28] the estimation of the packet error probability is obtained from the ratio between the number of failed transmissions and the total number of transmission attempts. The disadvantage of such approach is that

it usually takes a significant number of transmission attempts to infer a good packet error probability estimate. When the channel is subject to fading effects, the reception quality may change faster than link-adaptation.

The ARF algorithm presented in [29] also bases its decisions on the number of missing acknowledgements. However, it is simpler as it does not seek to obtain an accurate packet error probability estimate. Instead, it lowers or raises the bit-rate based on a small number of losses or successful transmissions (2 or 10 respectively).

Another technique is based on the estimation of the received power and SINR experienced at the receiver. Techniques to estimate the received power and the SINR are presented in [30] and [31]. Such approaches are assumed in the link-adaptation techniques presented in [25], [26], [32] and [27]. The simulations presented in these studies show that link-adaptation based on SINR estimates is more efficient than ARF. However, they assume perfect estimates, which are usually difficult to obtain. In fact, the tolerance on the received power estimate considered in [33] ranges from ± 5 dB to ± 8 dB. In the techniques proposed by [26] and [27], the error could even be magnified by the fact that the estimates assume that the path loss is symmetric and the noise experienced by the receiver is the same as that experienced by the sender.

In our simulations we implement a procedure very similar with the one of [26]. We estimate the received power and SINR experienced at the receiver, based on the last reception of that machine. In this algorithm, the sender chooses the bit-rate that achieves the highest goodput taking into account the SINR estimate. A PHY mode threshold table is calculated based on simulations carried out. This values are presented next.

2.5 Simulator description

This Section describes the simulator used and addresses the tests that enabled to verify its validity.

2.5.1 State transition diagram and actions description

The state transition diagram used to build the simulator is presented in Figure 2.9. Table 2.5 presents the actions related with each event.

TABLE 2.5: Actions of the events in the simulator

	ACTIONS
1	**Save:** Time creation packet Length packet Fragmentation (if it is required) Know destination Know type of packet Buffer [AC] !=NULL **Schedule:** STOP_LTN_DIFS (clock + AIFS) State = LISTEN_DIFS
2	**Schedule:** STOP_TX (clock + packet_length). See the TXOPLimit to check if it is possible to send another frame Backoff_condition=0 for STA in LISTEN_DIFS State = TX
3	**Schedule:** STOP_RX_ACK (clock + ACK) State = LISTEN_SIFS
4	State = WAIT_ACK
5	Erase the packet **Save:** Increment number of packets transmitted Delay of the transmission State = IDLE
6	Increase the number of collisions Backoff_condition = 1; State = WAIT
7	**Schedule:**

	STOP_LTN_DIFS (clock + AIFS) State = LISTEN_DIFS
8	Refresh NAV **Deschedule:** STOP_LTN_D **Schedule**: STOP_RX (clock + NAV) State = WAIT
9	**If (backoff_condition == 1)** Generate backoff Decrement backoff_value each time slot **Else** Decrement backoff_value each time slot State = BACKOFF_TIMER
10	Suspend backoff procedure Refresh NAV **Schedule:** STOP_RX (clock + NAV) State = WAIT
11	**Schedule:** STOP_RX (clock + RX) State = RX
12	**Schedule:** START_TX (clock + SIFS) State = LISTEN_SIFS
13	**Save:** Time creation packet Length packet Fragmentation (if it is required) Know destination

	Know type of packet Buffer [AC] !=NULL Backoff_condition = 1 State = WAIT
14	**Schedule:** STOP_TX (clock + packet_length) See the TXOPLimit to check if it is possible to send another frame Backoff_condition=1 for STA in LISTEN_DIFS State = TX
15	State = IDLE
16	**Schedule:** STOP_LTN_DIFS (clock + AIFS) State = LISTEN_DIFS
17	**Schedule:** STOP_LTN_DIFS (clock + AIFS) State = LISTEN_DIFS
18	State = IDLE
19	**Schedule:** STOP_LTN_DIFS (clock + AIFS) State = LISTEN DIFS
20	**Schedule:** STOP_RX (clock + packet_length) State = RX
21	**Schedule:** STOP_RX (clock + packet_length) State = RX
22	**Schedule:** START_TX (clock + SIFS) State = LISTEN_SIFS
23	State = TX

	Schedule: STOP_TX (clock + packet_length)
24	State = RX **Schedule:** STOP_RX (clock + packet_length)
25	Decrement backoff_value **If (backoff_value == 0)** **Schedule:** START_TX (clock) **Else** **Schedule:** Time_Slot (clock + SIFS) State= Backoff_Timer

The following events cause transition/change of the machine state:

NEW_PCK	a new packet is generated;
STOP_LTN_D	end of the AIFS period for sensing the medium;
STOP_LTN_S	end of the Short Inter-Frame Space (SIFS) period for sensing the medium;
TIME_SLOT	the STA decrements the backoff_value;
START_TX	the station starts to transmit;
STOP_TX	stop of the transmission;
START_RX	start of the reception;
STOP_RX	stop of the reception;
STOP_TX_RES	stop the transmission of an acknowledgement;
ACK_OK	the acknowledgement was received;
ACK_NOK	the acknowledgement was not received.

A detailed description of possible states for the Machines, Medium and Packe, the simulation Entities, the simulation Variables, and the functions for events is given next.

Machine states

States

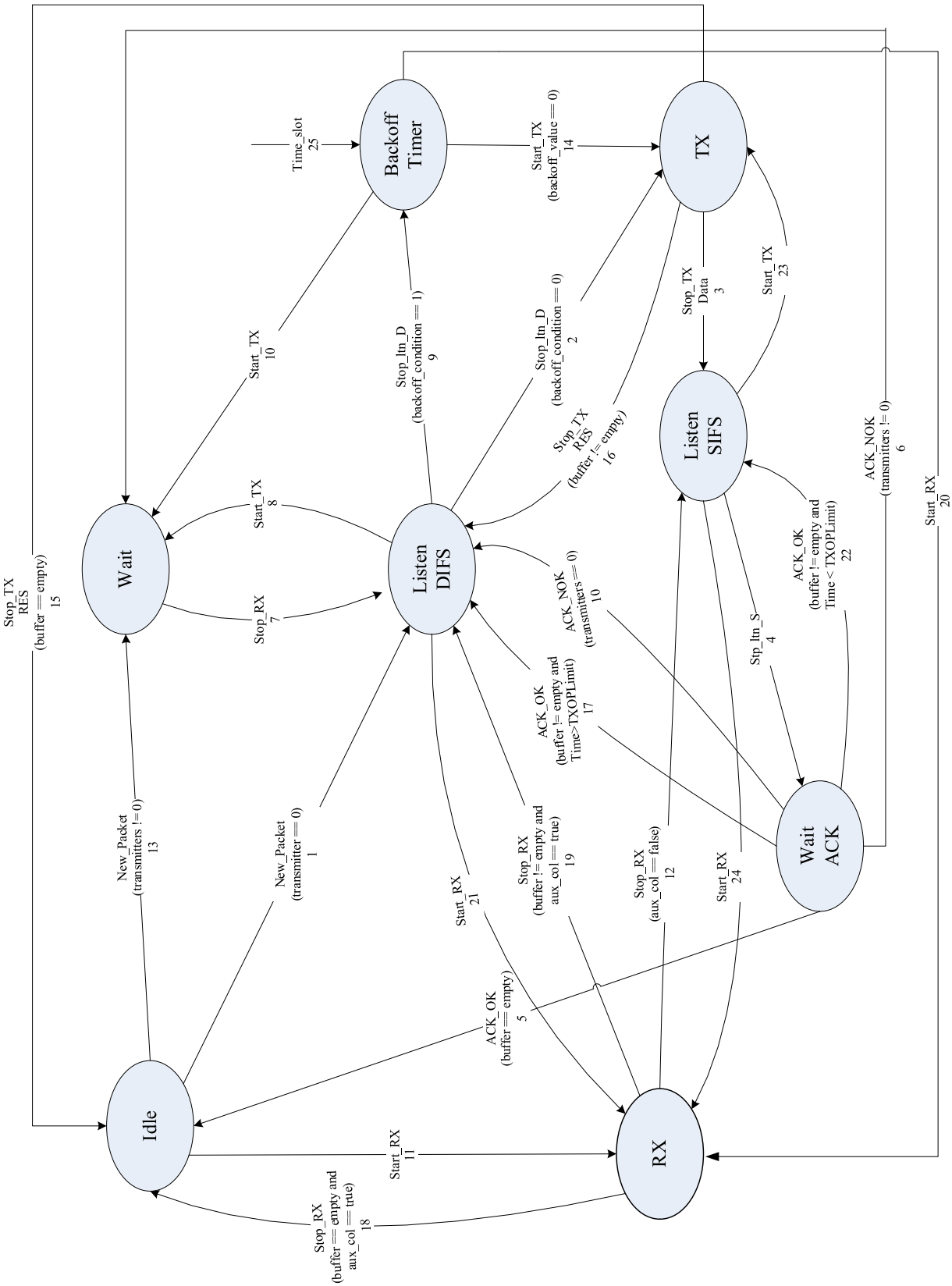

FIGURE 2.9: State transition diagram (the incoming arrow for the *Backoff_Timer* state means a transition from and to the same state).

Idle: buffer is empty;

Wait: backoff counter is frozen;

Listen DIFS: waiting AIFS;

Backoff Timer: decreasing the backoff timer;

TX: transmitting packet;

Listen SIFS: waiting SIFS;

RX: receiving a packet;

Wait ACK: waiting an acknowledgement;

TX ACK: transmitting an acknowledgement.

Queues

Empty: buffer is empty;

Not empty: can have p packets waiting to be transmitted.

Medium states

Free: medium is free, no one is transmitting;

Not free: medium not free, there is someone transmitting and someone receiving.

Packet states

Payload;

time of generation;

backoff condition: can be either 0, 1 or 2, for never generated, to be generated, already generated, respectively;

origin;

destination;

backoff value;

Ncollision: number of collisions the packet has suffered;

packet_type: type of packet, can be of BK, BE, VI and VO;

frag: it is a list that takes several fragments;

rts_first: serves to know if it is the first fragment to be sent or not.

There are the following entities in the simulations:

Entities:

Machine: the objects of this class are the AP and the STAs

- attributes
  - buffer[4]: contains the packets for each access category;
  - colisions[4]: contains the collisions of each access category;
  - location: contains the 2D position;
  - tx_power: indicates the power when the machine is transmitting;
  - tx_node: indicates if the machine is transmitting or not;
  - state[4]: contains the state of each access category;
  - delay[4]: contains the delays for each access category;
  - num_packets[4]: contains the number of packets transmitted of each access category:
  - TXOP_limit: the time that the machine shall not pass before listen an AIFS;
  - SBlock_ACK: if the machine has the Block Ack policy with another machine;
  - VBlock_ACK: the value of the Block ACK's buffer;
  - RBlock_ACK: the receiver Block ACK's buffer;
  - packet_loss[4]: contains the packets lost for each AC;
  - retransmissions[4]: contains the number of retransmissions for each AC.
- methods
  - AddFragment(Possible_packets p, fragment f): adds a fragment to a packet in one of the queues;
  - AddPacket(PacketWiFi p): adds a packet to one of the queues;
  - AddPacketADDBAReq(PacketWiFi p): adds a ADDBA Request packet to one of the queues;

* AddPacketADDBARes(PacketWiFi p): adds a ADDBA Response packet to one of the queues;
* AddPacketRES(PacketWiFi p): adds a Response packet to one of the queues;
* ChangeSBlock(Possible_packets p, int d, StateBlock s): changes the state of SBlock_ACK buffer with a destination;
* ChangeVBlock(Possible_packets p, int d, double v): changes the value of VBlock_ACK buffer with a destination;
* DecVBlock(Possible_packets p, int d): decrements the value of VBlock_ACK buffer with a destination;
* Del_Frags(Possible_packets p, int d, int o, vector<Machine> *m): erases all the fragments sent by Block ACL policy to a destination;
* RemoveFirstPacketLost(Possible_packets p): removes a packet when the L_COL is reached from the queue p;
* RemovePacket(Possible_packets p): removes the packet from the queue p;
* RemovePacketsBlockSent(Possible_packets p, int d): removes the packets sent by Block ACK policy to a destination;
* RemovesPacketsEmpty(Possible_packets p, int d, double c, bool a): removes empty packets to a destination and update the delays;
* ResetTXOP_limit(): changes the value of the TXOP_limit to 0;
* SetState(Possible_packets p, State s): sets the state of the buffer p to state s;
* SetTXOP_limit(double x, Possible_ packets p): changes the TXOP_limit to a value ;
* Buffers_size(Possible_packets p): returns the size of the buffer p;
* Buffers_size(): returns the number of packets in all buffers;
* DataPackets_to_i(Possible_packets p, int o, int d): counts the data packets to a destination;
* Packets_to_i(Possible_packets p, int o,int d): counts the total packets to a destination;
* GetTXOP_limit(): returns the value of the TXOP_limit;
* GetVBlock(Possible_packets p, int d): returns the value of the VBlock_ACK buffer to a destination;

    - GetFirstPacketLost(Possible_packets p): gets a packet which has waited the response during the ACK Time_out from the queue p;
    - GetLastPacket(Possible_packets p): returns the last packet sent from the queue p;
    - GetNextPacket(Possible_packets p): returns the next packet to send from the queue p;
    - ADDBAReqPackets_to_i(Possible_packets p, int o, int d): returns a boolean if there is a ADDBA Request packet in the buffer p;
    - CheckPacketEmpty(Possible_packets p, int d): returns a boolean if there is a empty packet in the buffer p;
    - PacketsNotSent(Possible_packets p): returns a boolean if there are packets not sent in the buffer p;
    - GetState(Possible_packets p): returns the state of the buffer p;
    - GetSBlock(Possible_packets p, int d): returns the state of the buffer p to the destination d.

Packet: the objects of this class are the packets that fill in the buffer

- attributes
    - payload;
    - time_gen: when it was created;
    - backoff_condition: 0 do not generate backoff, 1 generate backoff, 2 decrement backoff down to 0;
    - origin: the originator of the traffic;
    - destination: to whom it is to be transmitted;
    - backoff_value: number of slots to be decremented;
    - Ncolision: number of collisions the packet has suffered;
    - packet_type: it can be of VO (voice), VI (video), BE (best effort) and BK(background);
    - frag: queue of fragments of the packet;
    - rts_first: used to check if the fragment is the first or not.
- methods

* AddFrag(Possible_packets p, fragment f): adds a fragment to the packet;
* ChSentFalse(bool x): changes the variable send of the last fragment sent to false;
* ChangeSend(): changes the variable send of the first fragment not sent to true;
* DelFrag(): erases the last fragment sent of the packet;
* IncNcollisions(): increments the number of collisions the packet suffered;
* SetBackoffcondition(int x): changes the variable backoff_condition of the packet;
* FragsNotSent(): returns the number of the fragments not sent in the packet;
* GetBackoffcondition(): returns the variable backoff_condition of the packet;
* GetBackoffvalue(): returns the variable backoff_value of the packet;
* GetDestination(): returns the variable destination of the packet;
* GetPayloadNextFrag(): returns the variable payload of the first fragment to send;
* GetPayloadLastFrag(): returns the variable payload of the last fragment sent;
* GetPayloadSecFrag(): returns the variable payload of the second fragment to send;
* GetNcolision(): returns the number of collisions of the packet;
* GetModulationLastFrag(): returns the variable modulation of the last fragment sent;
* SetModulationNextFrag(double x): changes the variable modulation of the fragment x;
* SetrxDataNextFrag(double x): changes the variable rxData_Pr_db of the fragment to x;
* SetSNRNextFrag(double x): changes the variable SINR_db of the fragment to x;
* GetSNRLastFrag(): returns the variable SINR_db of the last fragment sent;
* GetTimeGen(): returns the variable time_gen of the packet;
* GetBlockLastFrag(): returns the variable Block of the last fragment sent;
* GetRTSPacket(): returns the variable rts_first of the packet;

    - GetTypeLastFrag(): returns the variable type of the last fragment sent;
    - GetTypeNextFrag(): returns the variable type of the first fragment to send;
    - GetTypePacket(): returns the variable send of the fragment to false;
    - ChSentFalse(bool x): changes the variable packet_type of the packet.

Event: the objects of this class are the events, they are stored in a list

- attributes
    - event_time: period at which the period is going to take place;
    - t_event: type of event already presented before;
    - origin: the originator of the event;
    - destination: the destination of the event.
- methods
    - set_event: sets the event attributes to the new ones.

Channel: only one object of this class is created. It stores the data that has to be passed trough events

- attributes
    - transmitters: number of transmitters at that moment;
    - aux_col: when a collision occurs this variable is set to true;
    - n_collisions: total collisions suffered;
    - clock.

Output: one object of this class is created per simulation. It stores the main outputs of the simulation. As a simulation runs for some time, these outputs are stored in a vector. At the end the simulations the averages are calculated

- attributes
    - delay_total_BK;
    - delay_total_BE;
    - delay_total_VI;

    - delay_total_VO;
    - delay_average_BK;
    - delay_average_BE;
    - delay_average_VI;
    - delay_average_VO;
    - colisions_total;
    - colisions_rate;
    - packets_total_BK;
    - packets_total_BE;
    - packets_total_VI;
    - packets_total_VO;
    - chann_utilization;
    - thr_total;
    - thr_per_sec.

Lista: a object of this class (one list) is created to store the events.

- attributes
    - lis: contains al the events;
    - inter: iterator of the list.
- methods
    - del_event_after: erases all the events after some time;
    - Get_next_event(): returns the first event in the list;
    - see_event_machine(): checks if a given event is in the list.

Random_generator: the objects of this class generate a random number with uniform distribution

Distributions: the objects of this class generate random numbers with a given distribution.

There are the following simulation variables:

Simulation variables

event_list: is the list in which all the events are sorted by time;

stations: a vector which contains all the stations;

output: where the main outputs are saved.

There are the following input variables:

Input variables

MT: total number of stations;

SIMULATION_TIME 100000: simulation lifetime in ms;

DATA_RATE 20000000.0: data rate in bits;

PAYLOAD_BK 12000: payload of the BK packets;

PAYLOAD_VO 1280: payload of the VO packets;

PAYLOAD_VI 10240: payload of the VI packets;

PAYLOAD_BE 12000: payload of the BE packets;

DIFS 0.034: DIFS size in ms;

SIFS 0.016: SIFS in ms;

INTER_ARRIVAL_BK 12.5: interarrival time for BK packets in ms;

INTER_ARRIVAL_VO 20: interarrival time for VO packets in ms;

INTER_ARRIVAL_VI 10: interarrival time for VI packets in ms;

INTER_ARRIVAL_BE 2: interarrival time for BE packets in ms;

SLOT 0.009: SLOT time in ms;

ACK_SIZE 112: acknowledgement size in bits;

DEGREES_FREEDOM 2: number of simulations that will be taken with different random seeds;

RTS_TH 3000: RTS threshold, to use a RTS procedure;

RTS_SIZE 160: RTS size in bits;

CTS_SIZE 112: CTS size in bits;

CW_MIN 31: CWmin;

L_COL 8: collisions limit;

TXOP_BK 0: TXOP size for the BK traffic, being 0 means that only one MSDU can be transmitted in a TXOP;

TXOP_BE 0: TXOP size for the BK traffic;

TXOP_VI 3.008: TXOP size for the VI traffic in ms;

TXOP_VO 1.05: TXOP size for the VO traffic in ms.

The simulator was build in standard C++. The definition of the functions used to initialize the traffic, to generate the backoff, the AIFS, and of the functions that deal with the events (that change the state of the machines as well) is the following::

2.5.2 Functions for the events

The functions that deal with the events are the following:

- Initialize(list_events, ed, stations, fs): this function adds machines to the scenario and schedules the traffic for them(ed is an event and fs is an object for writing);
- AIFS(Possible_packets p): generates the AIFS for a given AC;
- Generate_backoff(int colisoes): generates the backoff for a given AC, it depends on the number of collisions;
- New_pck_bk(list_events, ed, stations, chan, fs): this function adds packets to a given buffer (BK). The fragmentation of the MSDU into several MPDU (if required) is performed here. Also a new arrival is scheduled here;

- Stop_ltn_d(list_events, ed, stations, chan, fs): the packet in a given buffer of a given machine is made available and the payload compared with the RTSLimit to answer if the packet will be sent with RTS/CTS method or not. With this function the simulator verifies the backoff_condition, and determines if the machine has to send the packet normally, to generate a backoff, or to continue decreasing the backoff_value;

- Time_slot(list_events, ed, stations, chan, fs): this function will be applied to machines that are in the Backoff_Timer state. When the machine invokes the backoff procedure, all the machines that are in Backoff_Timer state are going to schedule an event time_slot to decrease the backoff_value by one unit. When the backoff_value reaches zero then the machine will start the transmission;

- Start_TX(list_events, ed, stations, chan, fs): first of all, it is checked if there is an internal collision, if there is none, the machine will obtain a TXOP. Then, if there is enough time to send the packet, the transmission will start. The other machines will update their NAVs, for this MPDU plus another, if there is one, and if it is possible to send (according to the TXOP limit policy);

- Start_RX(list_events, ed, stations, chan, fs): the buffer of the machine which is going to receive is set to RX state;

- Stop_TX(list_events, ed, stations, chan, fs): the buffer of the machine which is transmitting is set to LISTEN_SIFS state;

- Stop_RX(list_events, ed, stations, chan, fs): this function detects if there is a collision. If the transmission is successful then the receiver will send an ACK to confirm the data. If a collision is detected then the receiver will not send the ACK. Then, after an ACKTimeout time, the sender will invoke the backoff procedure;

- Stop_ltn_S(list_events, ed, stations, chan, fs): it sets the state of the transmitter machine to WAIT_ACK;

- RES_ok(list_events, ed, stations, chan, fs): if the machine receives an ACK then checks if there are more MPDUs or MSDUs to transmit, and if the TXOP will allow sending them;

- RES_nok(list_events, ed, stations, chan, fs): it will perform the procedures inherent to a retransmission.

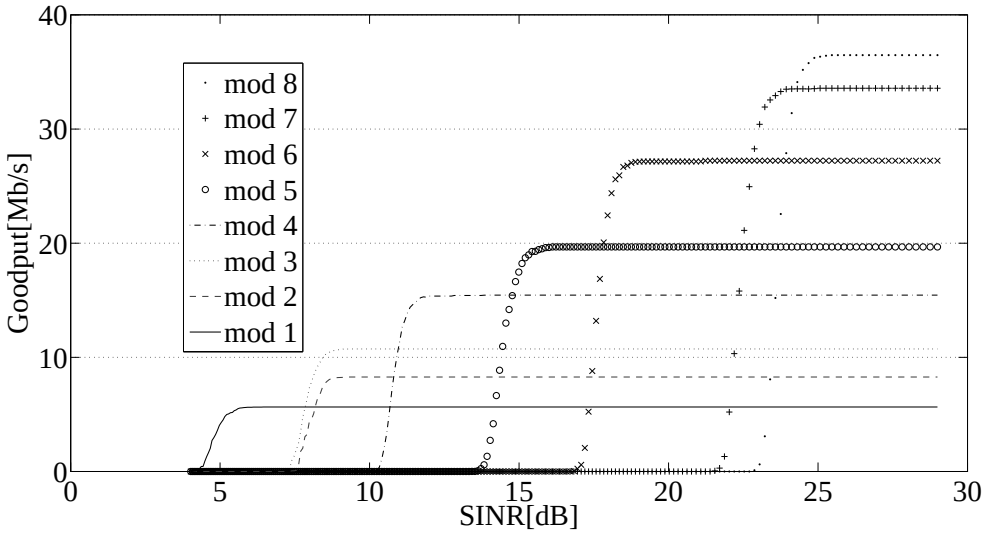

FIGURE 2.10: Goodput vs SNR for the 8 different transmission modes without fragmentation.

2.5.3 Validation of the simulator

According to the IEEE 802.11 standard, the length of an MSDU must be less than or equal to 2304 octets. The length of a fragment MPDU shall be an equal even number of octets for all fragments except the last one of a fragment burst, which may be smaller.

In this section, the validity of the developed simulator is verified. It is assumed that the MSDUs to be transmitted are all of 2304-octet long, and each MSDU might be either not fragmented or fragmented up to 10 equal-size MPDUs.

The results of goodput performance for different PHY modes are presented in Figure 2.10 (without fragmentation), and in Figure 2.11 (with fragmentation). As expected, the higher rate PHY modes show better goodput performance in the high SINR range, while the lower rate PHY modes have better goodput performance in the low SINR range.

One interesting observation is that the goodput performance of PHY mode 3 (QPSK modulation with rate coding) is always better than of PHY mode 2 (BPSK modulation with rate coding) under all SINR conditions. The rationale behind is that, although QPSK has worse error performance than BSPK, the worst performance of the rate convolutional code compared to the rate convolutional code has more dominating effect. Therefore, without the appropriate power control schemes, PHY mode 2 may not be a good choice at the presence of PHY mode 3. Another observation from the figures is that, for the same PHY mode, fragmentation decreases the maximum goodput due to the overheads, however, improves the goodput performance at certain SINR range.

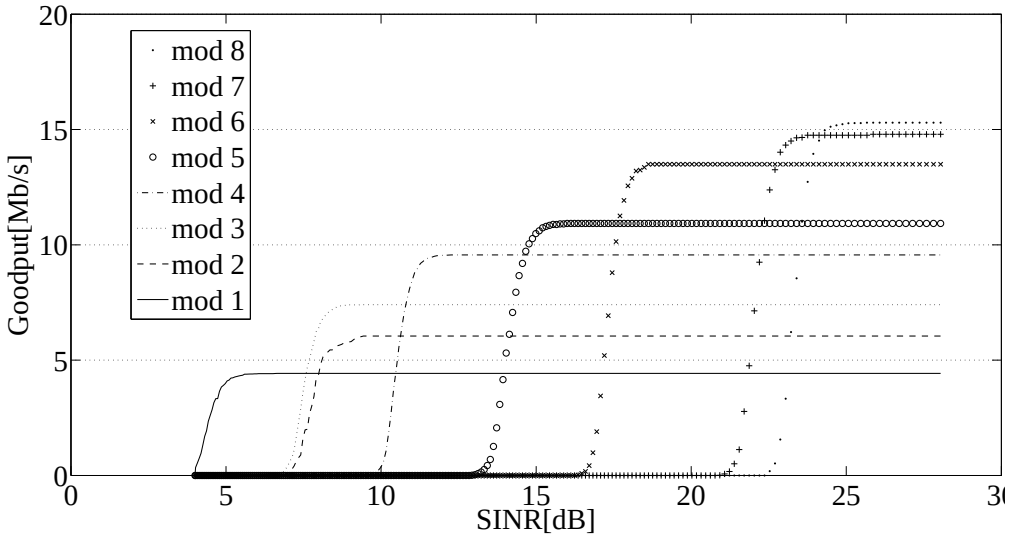

FIGURE 2.11: Goodput vs SNR for the 8 different transmission modes with fragmentation.

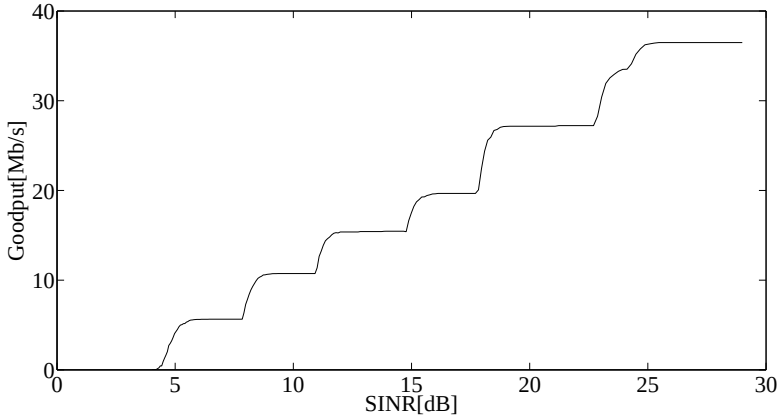

FIGURE 2.12: Goodput vs SINR without fragmentation when an optimal transmission mode selection is used.

The optimal combination of the PHY mode to achieve the best goodput for different SNR conditions without and with fragmentation is presented in Figure 2.12 and Figure 2.13, respectively.

The values used for transmission mode selection are extracted from Figure 2.12. If we call to the SINR threshold for mode k (SMT_k), the transmission mode m is selected as follows:

- m=8 if $SMT_8 \leq SINR\_max$;
- m=7 if $SMT_7 \leq SINR\_max < SMT_8$;
- m=6 if $SMT_6 \leq SINR\_max < SMT_7$;
- m=5 if $SMT_5 \leq SINR\_max < SMT_6$;
- m=4 if $SMT_4 \leq SINR\_max < SMT_5$;

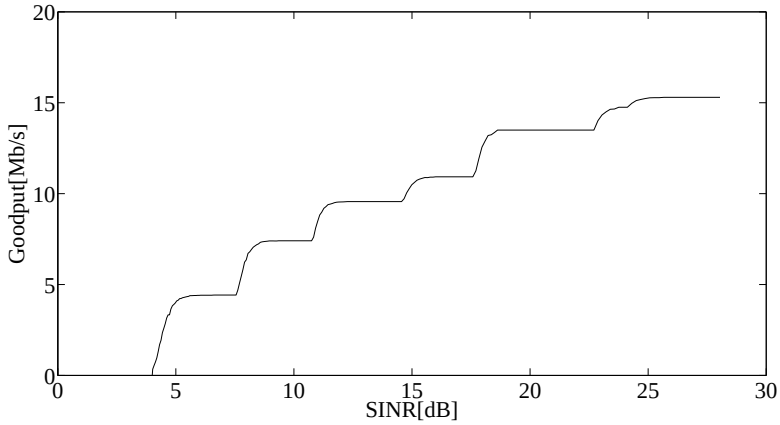

FIGURE 2.13: Goodput vs SINR with fragmentation when an optimal transmission mode selection is used.

TABLE 2.6: IEEE 802.11a PHY modes.

Mode	**Bit-rate**	**%**	**Radius**
1	6 Mb/s	0.4	The rest
2	9 Mb/s		
3	12 Mb/s	8.4	33.82
4	18 Mb/s	26.0	28.30
5	24 Mb/s	19.2	22.78
6	36 Mb/s	20.1	19.13
7	48 Mb/s	3.8	14.35
8	54 Mb/s	22.0	13.24

- m=3 if $SMT_3 \leq SINR\_max < SMT_4$;
- m=1 otherwise.

After selecting the transmission mode, the sender uses always the maximum transmission power. The PHY mode distribution in the square is presented in Table 2.6.

The bird's-eye view of cell area is presented in Figure 2.14.

2.5.4 Performance results

System, scenario and assumptions

It was considered a cellular WiFi system where each cell has a set N+1 IEEE 802.11e stations communicating through the same wireless channel. While station 0 is the AP or QAP, the other N are wireless STA or QSTA. The propagation time is assumed to be absorbed by some mechanisms of the IEEE 802.11. Each station has four buffers as IEEE 802.11e standard commands. It

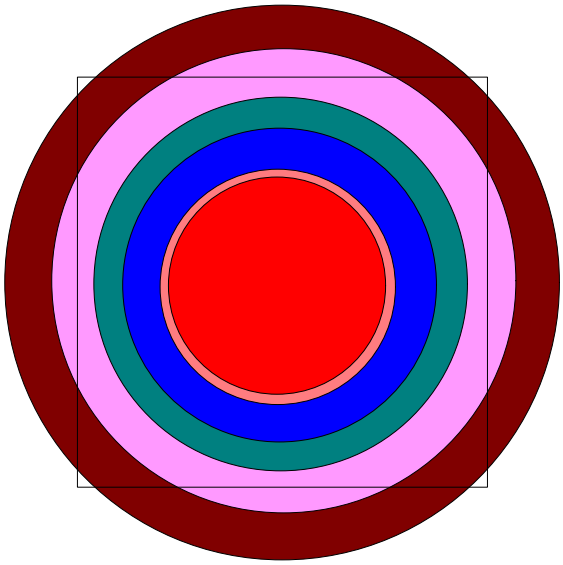

FIGURE 2.14: Bird's view of cell area.

TABLE 2.7: Traffic parameters [2]

AC	**Voice (VO)**	**Video (VI)**	**Background (BK)**
Packet size	1280 bit	10240 bit	18430 bit
Packet interval	20 ms	10 ms	12.5 ms
symmetry	symmetric	asymmetric	asymmetric

was assumed an infinite buffer size. This buffer will be filled with a MSDU generator that characterises the service being dealt in the given buffer. If the MSDU is bigger than a fragmentation threshold, it will be fragmented. In order to cope with service quality, the packet transmission follows the EDCA IEEE 802.11e MAC procedure. Due to collisions or interference a packet may not be correctly received.

The users are assumed to be static, and are distributed uniformly in a square area of 2500 square meter, Figure 2.14.

The topology to be implemented consists of several wireless stations and an AP. Three types of traffic sources were chosen, namely high priority voice, medium priority video and low priority FTP data. The traffic sources parameters are shown in Table 2.7.

Simulation results

Results include packet delay, goodput in bit per second, and channel utilization. It consider MAC and PHY layers. It are the average of 20 simulations (each with different random seeds). Results with MAC layer alone are presented in [34].

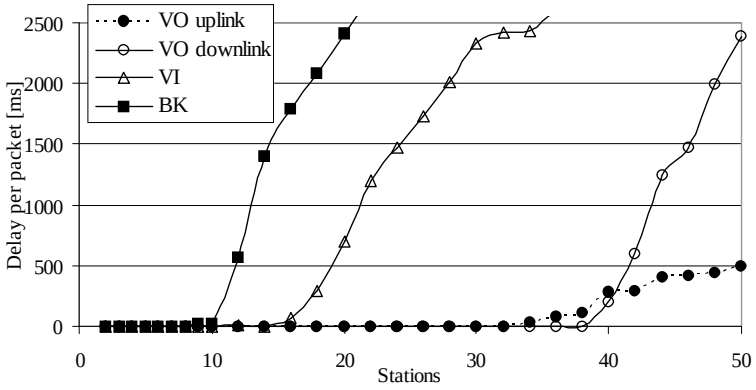

FIGURE 2.15: Delay as a function of the number of nodes for VO, VI, and BK applications.

Packet delay is the period of time between the moment at which the packet arrives to the buffer and the moment at which the packet is successfully transmitted. The results for stand alone VO (uplink and downlink traffic), BK (downlink traffic only) and VI (downlink traffic only) are presented in Figure 2.15.

In terms of grade of service, from [35] the voice application supports delays up to 30 ms, the video application supports delays up to 300 ms, while the delay for the background applications can be up to 500 ms. Hence, our QAP supports up to 40 voice users, 18 video users, and 11 background users with an appropriate degree of QoS. The system is limited by the downlink connection.

Another performance measure is the maximum goodput achievable for a given channel capacity. It is certain that a fraction of the channel capacity is used up in form of overhead, acknowledgments, retransmission, token delay, etc.

Channel capacity is the maximum possible data rate, i.e., the signalling rate on the physical channel. It is assumed that the data rate or transmission rate vary between 6 and 54 Mb/s. Goodput is the amount of user data that is carried by the wireless network. The results for goodput as function of the number of stations are presented in Figures 2.16 and 2.17. The maximum achieved goodput is 16 Mb/s.

Figure 2.17 presents the goodput for VO applications in both directions. When the number of stations is higher than 40 the goodput decreases; this is due to small CW size. The goodput in the downlink is equal to 64kb/s up to 38 stations. For more than 38 stations, the collisions start to occur very often and the goodput of each station decreases.

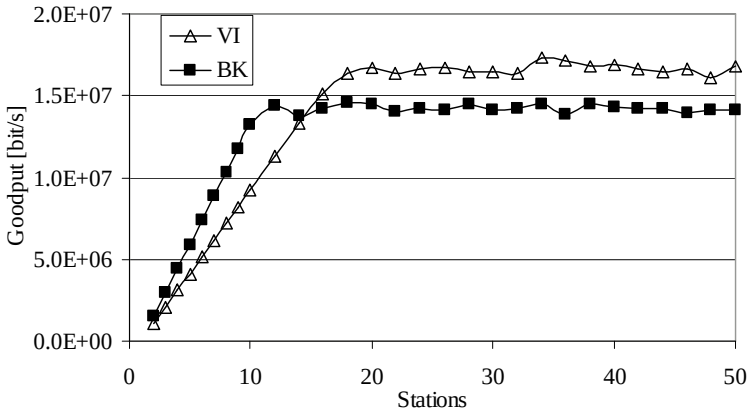

FIGURE 2.16: Goodput as a function of the number of nodes for VI, and BK applications.

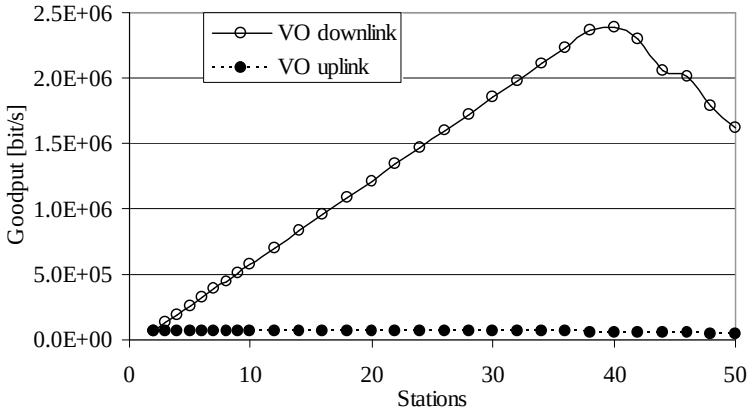

FIGURE 2.17: Goodput as a function of the number of nodes for VO, downlink and uplink directions.

Due to the scarcity of wireless bandwidth, we also studied the medium utilization, and we computed the average data rate for the client stations. Since the distribution of users in the square is uniform, it is easy to compute the probability of a given transmission mode, being easy to compute the average data rate.

The channel utilization is the ratio of goodput over the average data rate, and is presented in Figure 2.18 (as a function of the number of stations). The highest obtained value for utilization is around 80 %, and is obtained for VI. The lowest one is obtained for VO traffic. This occurs because the packet size is much higher for VI than for VO.

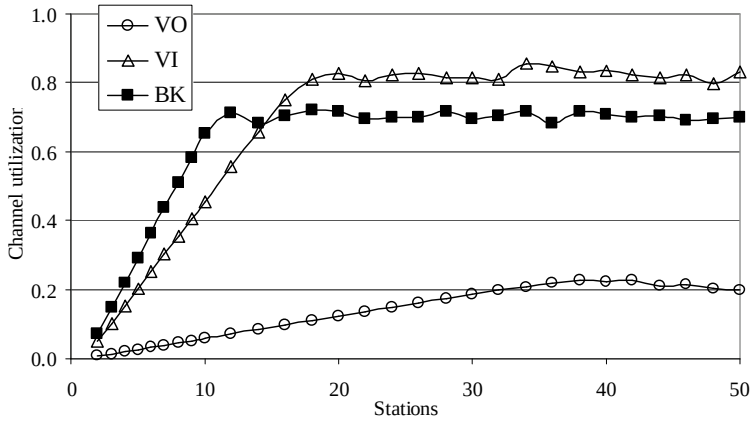

FIGURE 2.18: Channel utilization, as a function of the number of nodes, for VO, VI, and BK applications.

2.6 Summary and conclusions

The developed IEEE 802.11e event driven simulator is a tool that allows for tuning-up several parameters like the ones dealing with the use block acknowledgement, normal acknowledgement, and no acknowledgement policies. Policies have been tested that provide access to the medium, that ensure a given grade of service, based on the channel SINR, delays, and a given bit error rate. This C++ simulator was developed for many practical reasons since it allows avoiding interactions with the higher levels of the protocol stack and fully controlling and tracing the MAC protocol operations and performance figures. Its development allowed for creating a simulation framework which fully supports fragmentation [36]. Besides, our simulator also supports the ad-hoc mode [37], which is not the case of the OMNet++ simulator [38]. This MAC layer simulator also facilitates to evaluate the service quality in IEEE 802.11e in order to enable simulations accounting for inter-working with Worldwide Interoperability for Microwave Access (WiMAX) and High Speed Downlink Packet Access (HSDPA) with QoS support. This interoperability is supported in the context of the IT-MOTION tool [39] whilst improving scheduling algorithms performance and Common Radio Resource Management (CRRM) techniques [18].

In the simulations, higher values of goodput are found for the VI and BK applications, mainly because the frames transmitted in these services are longer than the ones for the voice application but also the application data rate is higher. As a consequence, the number of supported stations of VI and BK is lower than the number of supported VO stations.

It should be noticed that the use of small CW for the VO access category may not be a very good idea since when the number of stations is higher than 38 the goodput starts to decrease due to

a small CW size. By suffering successive collisions the retransmission threshold is overcome causing the increase of packet losses. As CW is longer for the BK traffic, there is a longer period for the random backoff generator to generate a backoff. The collisions do not exist in BK and VI applications because the data traffic is only present for downlink direction (from access point to stations). As the VO traffic is bidirectonal, collisions occur very frequently because, apart of the access point, all the stations are contending to access to the medium.

For further work, we suggest to address handover policies between APs where a scenario supporting more than one cell can be used.

Chapter 3

Optimization of IEEE 802.11e

Optimization of IEEE 802.11e MAC protocol performance can be addressed by modifying several parameters left open in the standard, like block size and acknowledgement policies in order to improve the channel efficiency. The use of small block sizes leads to a high overhead caused by the negotiation, on the other hand the use of large block sizes causes long delays, which can affect negatively real-time applications (or delay sensitive applications).

Other optimization problems can focus on closed procedures and parameters presented in the standard. It was studied in this work a dynamic Contention Window (CW) limits generator and Enhanced AIFS procedure which generates AIFS in a dynamic manner taking into account the network conditions like normalized load, PHY layer conditions like average SINR experienced in past receptions, stream conditions, like average Bit Error Rate (BER) and packet delay suffered.

This Chapter is organized into three parts, a first part, Section 3.2 dedicated to the optimization of the Block Acknowledgement (BA) procedure, a second part, Section 3.3 dedicated to the optimization through cross-layer design and a third part, Section 3.4 dedicated to an ad hoc analytical model

The first part starts by presenting the BA procedure followed by the state of the art on BA, then the system, scenario and assumptions in which tests were performed and finally a summary and conclusions regarding the BA studies. The second part of the chapter starts by presenting the state of the art on optimization procedures for IEEE 802.11 and on the interoperability among wireless systems, then the assumptions for system and scenarios are described , including details on traffic parameters, followed by the description of the developed cross-layer algorithm, by the

simulation results with and without the proposed weighted cross-layer design algorithm, and, finally, conclusions are presented as well as suggestions for future work. The third part presents the notation and formulation for the analytical model, followed by the network and model scope, then some numerical results and in the end conclusions.

3.1 Motivation

Recent years have seen an immense growth in the popularity of wireless applications that require high throughput. To support such growth, standardization bodies such as the IEEE 802.11 have formed task groups to investigate and standardize features providing increased QoS and higher throughputs. One of these extensions is the Acknowledgement (ACK) policy feature included in the ratified IEEE 802.11e amendment for QoS support [20], which is the focus of the first part of this Chapter. The block size is a parameter left open in the standard for vendors to use the one that better fit their needs. In particular, we investigate the policy regarding the block size for a video application. The BA procedure improves system throughput results by reducing the amount of overhead required by a station to acknowledge a burst of received traffic [40], [41]. It acknowledges a block of packets by a single ACK, instead of using several ACKs, (one for each packet), saving the AIFS period, the backoff counter time, and the acknowledgement time. The number of frames that can be transmitted within a block is called block size. It is limited and is not specified in the standard. To find the most suitable block size, several one have been tried on different loaded scenarios with and without mixture of services.

Under the paradigm of wireless systems coexistence, recent theoretical developments have targeted cross-layer design as the key to efficiently exploit the available spectral resources. Strong interactions exist between the channel environment conditions with the networking issues of resource allocation. This suggests that several problems that are traditionally considered as networking issues, and are typically designed independently of the transmission techniques, need to be re-examined and therefore cross-layer design and optimization will be the way forward. The possibility of opportunistic communications in wireless link and the modalities of communication offered by the wireless medium motivate designers to infringe the layered architecture whilst overcoming the unique problems created by the wireless communications. Time-varying link quality allows for opportunistic usage of the channel, whereby the parameters can be dynamically adapted according to the variation of the channel quality. If the application layer information or the channel state indicator is made available to layers that are not immediate

neighbours, we may refer the new technique as cross-layer design [42], [43]. Although some authors advocate a cautionary use of cross-layer design [44], namely due to the unintended adverse interactions, if adequate care is put in the totality of the design an adoption from the manufacturers alliances (and even standardisation bodies) is viable, and long-term architectural value of cross-layer design may be enabled [43]. One of the aims of this Chapter is to propose and explore an optimization algorithm for IEEE 802.11e that enhances capacity of the system while increasing the traffic with QoS support. Also, in the presence of heterogeneous systems, this concept can be further exploited to include cross-system parameters, making the simultaneous use of systems with totally different access technologies transparent to the user. Besides intensive computations, Genetic Algorithms (GAs) [45], [46] may be used to optimize the weights for the proposed algorithm functions.

3.2 The Block Acknowledgment procedure

The BA mechanism (see Figure 2.5) improves channel efficiency by aggregating several acknowledgments into one frame [40], [41]. There are two types of BA mechanisms: immediate and delayed. Immediate BA is suitable for high-bandwidth, low-latency traffic while the delayed BA is suitable for applications that tolerate moderate latency. The QSTA with data to send using the BA mechanism is referred to as the originator, and the receiver of that data as the recipient. The BA mechanism is initialized by an exchange of ADDBA Request/Response frames. After initialization, blocks of QoS data frames can be transmitted from the originator to the recipient. A block may be started within a polled TXOP or by winning EDCA contention. The number of frames in the block is limited, and the amount of state that is to be kept by the recipient is bounded. The MPDUs within the block of frames are acknowledged by a BA control frame, which is requested by a BlockACKReq control frame. The response to the BlockACKReq will acknowledge all the correctly received frames and request the badly received to be transmitted again.

3.2.1 Related work

Analytical frameworks to model BA have been published [47], [48], [49] but the results are not based on a realistic approach to the problem nor account for the achievable QoS, because the use of several service classes with different priorities (the base for EDCA) is not considered

at all. The existing theoretical approaches [47], [48], [49], assume that the buffer is always full, do not consider the hidden terminal problem, nor assume a multi-rate scenario. In [47], [48] an analytical framework was presented to model an ad-hoc network under the standard IEEE 802.11e with the BA procedure for a completely simplified scenario. The hidden/exposed terminal problem is one fundamental issue in WLANs but most of the existing analytical models either assume it does not exist, or do not consider the EDCA features of IEEE 802.11e (or do not account for the delay or any other QoS metric) [47], [48]. Results presented in [47], [48] express the block size as a function of the goodput in saturation conditions. Results show that the block size should be as high as possible, which can be misleading when we consider QoS. In [49] an analytical approach to model the BA in IEEE 802.11e was proposed without accounting for the hidden terminal problem. The multi-rate feature in the same environment was also not considered. Further, the packet loss due to errors in the channel was not taken in consideration. Finally, the use of EDCA procedures, like several virtual queues, for the several classes of service are also not considered, i.e., this work does not consider the IEEE 802.11e standard at all.

From the simulation approaches presented in the literature the one that is most similar to the work proposed here was proposed in [50]. In [50], several combinations for the block size are presented, and a scheduler based on the delay and amount of data in the buffer is proposed. The work presented here is an improvement of this approach and provides a more extensive study on the block size while considering use-perceived QoS.

3.2.2 System, scenario and assumptions

A cellular WiFi system was considered where each cell has a set of N+1 IEEE 802.11e stations communicating through the same wireless channel. While station 0 is the QoS Access Points (QAP), the other N are QoS stations (QSTA).

The propagation time is assumed to be absorbed by some mechanisms of the IEEE 802.11. Each station has four buffers whose size depends on the kind of service being dealt in order to guarantee a given value for the goodput (payload of the packet at MAC level).

These buffers will be filled with MSDU generated that characterises the service being dealt in the given buffer. If the MSDU is bigger than a fragmentation threshold, it will be fragmented. In order to cope with service quality the packet transmission follows the EDCA IEEE 802.11e

TABLE 3.1: MAC and PHY parameters.

Slot time	0.009 ms
ACK size	112 bit
SIFS	0.016 ms
DIFS	0.034 ms
RTS threshold	4000 bit
RTS size	160 bit
CTS size	112 bit
CWmin	31 slots
CWmax	1280
Collisions threshold	7
Fragmentation threshold	8192
Simulation time	100 s

MAC procedure. Due to collisions or interference a packet may not be correctly received. The interference issues are addressed by using a radio propagation model presented in Appendix C. Each packet is deleted from the buffer only after the reception of an acknowledgement, or if it has suffered more than a given number of collisions, overcoming the collision threshold limit.

The users are assumed to be static, and are distributed uniformly in a square area of 2500 square meter. The physical layer used is the IEEE 802.11a, presented in Chapter 2. The physical and MAC parameters are presented in Table 3.1. The proposed simulations estimate the received power and SINR experienced at the receiver, based on the last reception of that machine, a procedure very similar to the one applied in [26]. The use of the Request/Clear-to-send (RTS/CTS) procedure is implemented only if the packet size is larger than a given threshold, RTS threshold in Table 3.1.

In the algorithm proposed in [26] the sender chooses the bit-rate that achieves the highest throughput taking into account the SINR estimate. More details on physical layer implementation used in the simulator can be found in [51].

Three types of traffic sources were chosen, namely high priority VO, medium priority VI, and low priority FTP data as BK traffic. The traffic sources parameters are presented in Table 3.2, as well as the AC of each type of traffic.

We implemented the BA procedure with minor modification to the existing features like TXOP and RTS/CTS as already explained and without disturbing the overall TXOP and RTS/CTS procedure. When a TXOP is gained, the transmission starts and the origin will know if a BA

TABLE 3.2: Traffic parameters [2], and usage.

AC	**Voice (VO)**	**Video (VI)**	**Background (BK)**
Packet size	1280 bit	10240 bit	18430 bit
Packet interval	20 ms	10 ms	12.5 ms
Usage	50 %	30 %	20 %
symmetry	symmetric	asymmetric (downlink)	asymmetric (downlink)

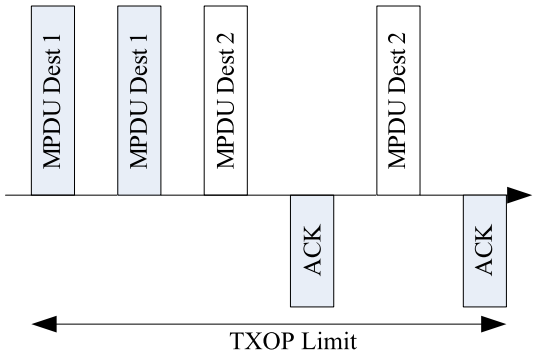

FIGURE 3.1: Illustration of the BA procedure within a TXOP.

procedure is implemented with this destination. If this is true, it will not wait for an acknowledgement, but just a SIFS and start the next transmission for the same destination or not depending on which is the next packet in the buffer. Figure 3.1 presents this procedure for destination 1 that has the BA procedure implemented and for destination 2 without the BA. At the beginning of a transmission for a user with active BA procedure, if the block size threshold is reached, a block ACK request packet is added to the buffer to the top-1 place in the queue to be transmitted as the next in line packet.

At the beginning of a transmission for a user with BA procedure active, if the block size threshold is reached, a block ACK request packet is added to the buffer to the top-1 place in the queue to be transmitted after the packet now being transmitted.

3.2.3 Simulation results

The objective of the simulations was to investigate the gain of the BA procedure for a single service and for a mixture of services. In terms of grade of service, the voice application supports delays up to 30 ms, the video application supports delays up to 300 ms, while the delay for background applications can be up to 1000 ms [35].

Standalone services

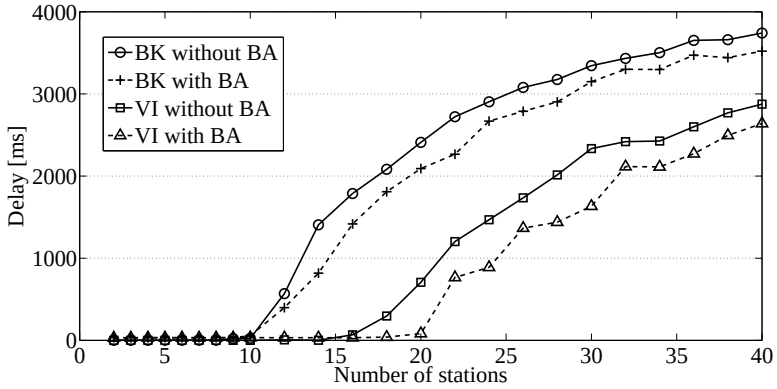

FIGURE 3.2: Delay for BK and VI with and without Block ACK.

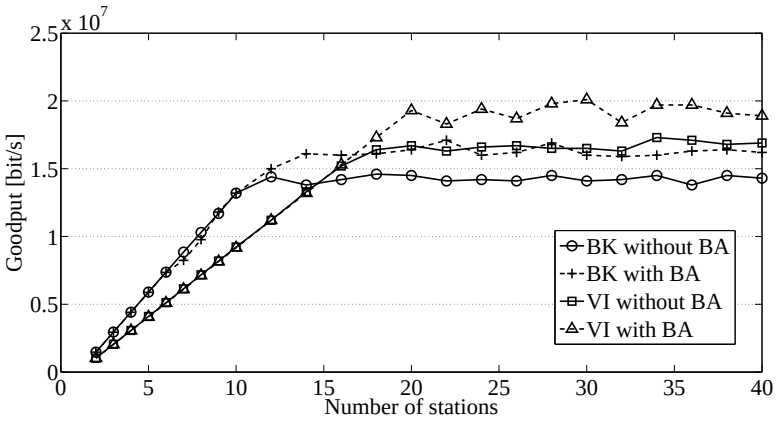

FIGURE 3.3: Goodput for BK and VI with and without Block ACK.

As previously mentioned, the BA mechanism improves the channel efficiency by aggregating several acknowledgments into one frame. To investigate the proposed BA procedure for the stand-alone service a BA procedure with a block size of 16 fragments was adopted. This procedure is simulated only for BK and VI traffic. For VO application it is certain that BA is not a solution because of the large delays that occur when the buffer is filled with 16 packets (i.e., the delay of the first one would be 320 ms). Figure 3.2 presents the delay for BK and VI traffic. It starts to increase around 12 stations for BK and at 16 stations for VI and increases more for a higher number of stations. As expected, the delay is lower when the BA procedure is used. The improvement (reduction) for BK traffic is 300 ms on the average after 12 stations, while for VI traffic it is 420 ms on the average after 16 stations. The goodput is presented in Figure 3.3 for BK and VI for simulations lasting 10 s. The improvement is of 2 Mb/s and 2.2 Mb/s in average, after 12 stations, for BK traffic and after 16 stations for VI, respectively.

Block Acknowledgement with mixtures of applications

This part of the work explores which should be the policy regarding the block size with mixtures

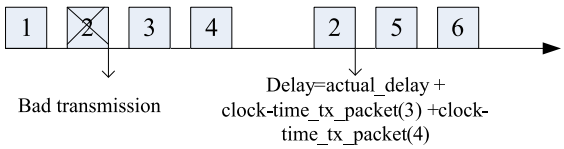

FIGURE 3.4: Procedure to count delay.

of applications. For the purpose we have investigated the BA policy for a video service, an application that is delay-sensitive. Additionally, we have investigated the BA block size for background service that is not delay sensitive. Simulations were performed for 100 s and around 40 times for each number of stations, {15, 20, 25, 30, 35, 40, 45} and each block size, {4, 8, 12, 16}. The users started the negotiation to initiate BA procedure in the beginning of the simulation so all the packets of video and background traffic were transmitted within the BA procedure.

The use of the BA procedure in a scenario with a mixture of applications running at the same time was further studied. On the one hand, the overhead caused by the negotiation to establish the BA procedure, and to maintain the BA causes bad performance when a small block size is used. On the other hand, the packet losses caused by the voice users with higher priority in the system, influences the overall QoS on the system and mainly on the video service since we considered in this simulations, that if a packet is not correctly received at a given time the following packets sent within this block will have the delay of the badly sent packet after transmitted added to their delay, Figure 3.4.

The impact of packet retransmissions in the delay is therefore increased. Figure 3.5 presents the delay for each access category. For BK traffic the delay starts to increase considerably with more than 20 stations (12 in the standard procedure). This service class will transmit very rarely since the voice and video traffic will always be scheduled first. For video traffic the delay starts to increase in the 35 stations. In contrast with BK and VI, VO applications present a negligible delay.

The delay impacts mostly the video application. Figure 3.6 shows the results for various block sizes for transmitted video application. Regardless on the number of stations, the BA procedure reduces the delay. Certain sensitivity is observed for a block size of 16, which is the size that gives the highest delay for a total of 1-25 stations. For a larger number of stations the best block size is 16. Smaller block sizes are not that efficient in decreasing the delay.

When 30 stations are being served in the system the results for the delay with BA is near 5 ms for all block sizes, while without BA the delay goes up to 80 ms. For 35 stations the difference

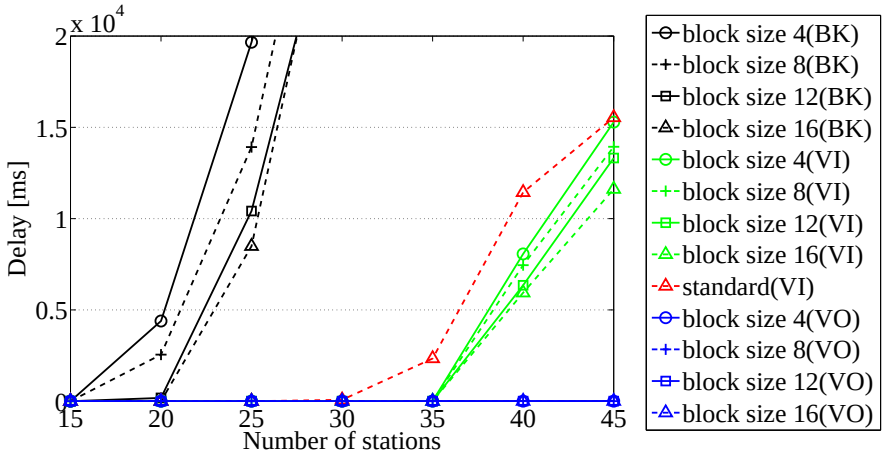

FIGURE 3.5: Delay for all services with Block ACK implemented for VI and BK traffic.

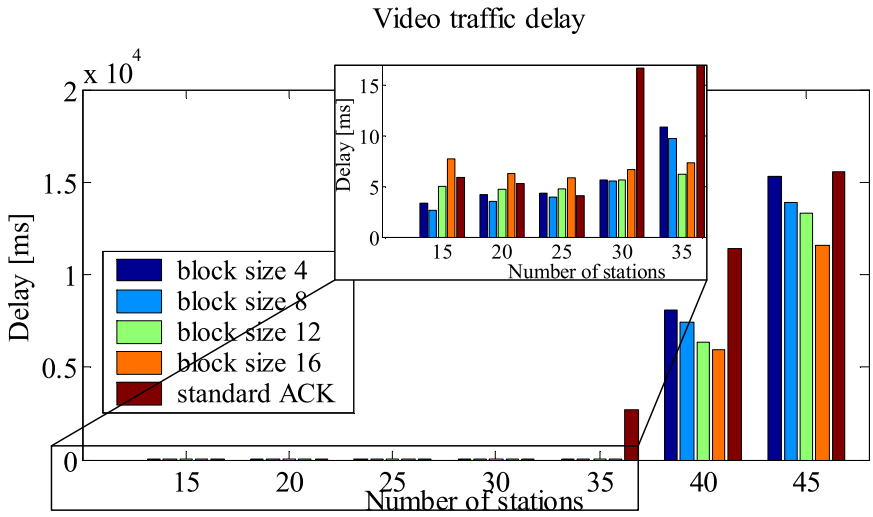

FIGURE 3.6: Delay for video traffic.

is even higher: a minimum near 5 ms is obtained for block size 12, while the delay without BA is near 2.3 s. Results for 40 and 45 advise the use of block size 16, although the network is already overloaded (and the delay will just keep growing up to infinity). Figure 3.7 illustrates this fact. When less then 40 stations are present the confidence intervals are very small for all the buffers. When there are 40 or more stations the confidence intervals increase. One can therefore extrapolate that there are stations that manage to transmit and have a small delay while others transmit from time to time, causing very high delays. The behaviour observed in Figure 3.6 occurs due to the overhead caused by the blockACK request, and the delays caused by bad receptions affected mostly the block size 16, but providing lower delays for higher loaded scenarios. The solution is neither to use a large block size (as large as 16) nor a small block size (as low as 4). The former increases the delay causing problems to the application using these

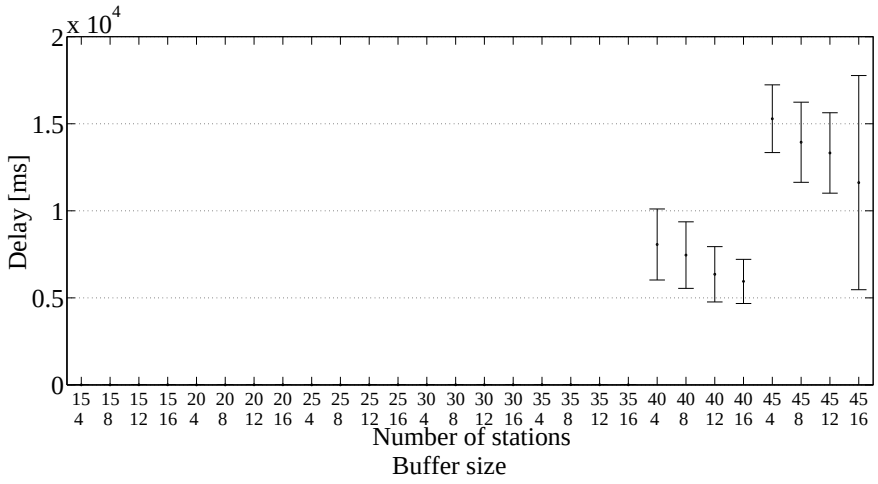

FIGURE 3.7: Confidence intervals for the delay of video traffic.

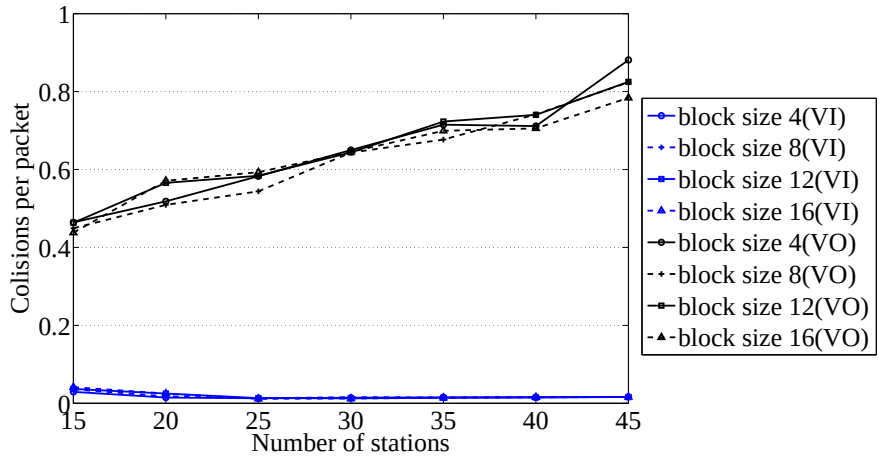

FIGURE 3.8: Collisions for video and voice traffic.

packets, while the latter causes some unnecessary overhead by requesting very often block ACK requests.

The advised block size shall be 12 since it is the one that provides lower delay in a scenario where the load is still manageable, at least for the case where BA is used.

Figure 3.8 and 3.9 present the average number of collision per packet and packet loss rate, respectively. It can be extracted from these results that the number of collisions per packet and the packet loss rate do not significantly depend on the block size.

Figure 3.10 presents the results of the goodput in the system in the downlink. Without the BA the maximum goodput achieved is near 11 Mb/s, while with BA is near 14 Mb/s for block size 12 and 16. The decreasing behaviour after 25 stations occurs due to the high number of collisions,

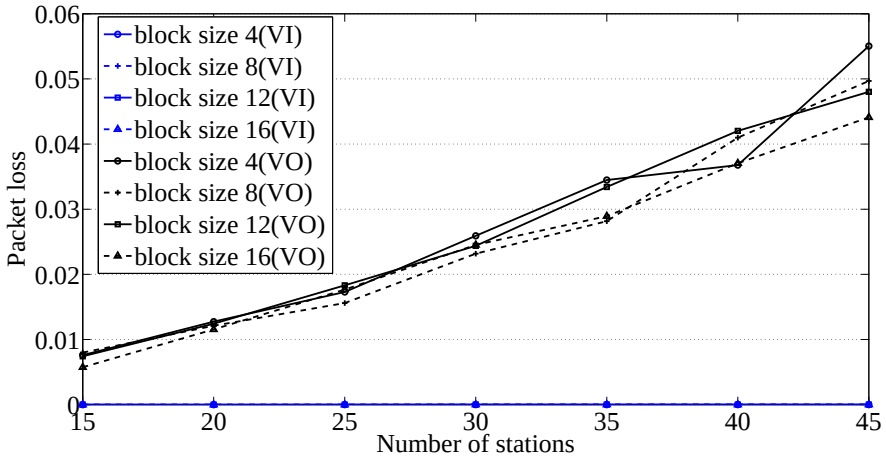

FIGURE 3.9: Packet loss for voice and video traffic.

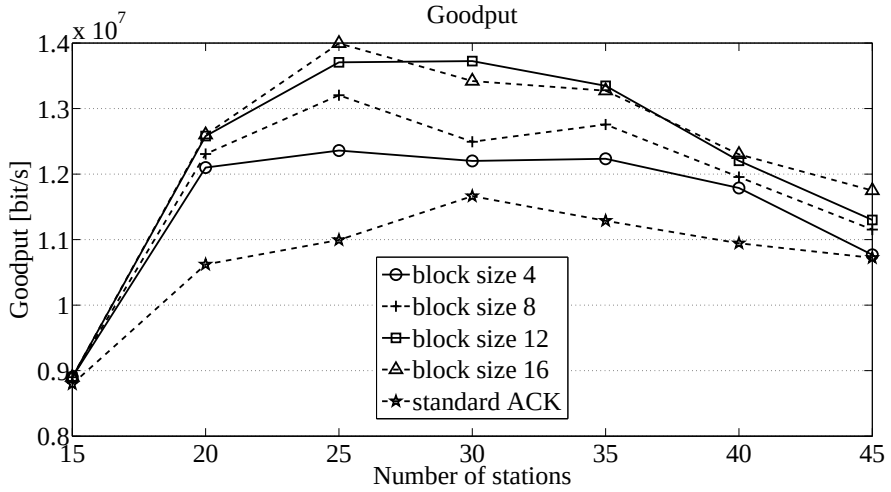

FIGURE 3.10: Total goodput with BA implemented for video and background traffic.

and as the BK traffic has low priority, ends up not being transmitted giving its turn to voice and video users. As voice traffic provides higher overhead, the resulting goodput is lower.

Figure 3.11 presents the goodput only for the video service class. Only after 30 stations the achieved throughput is different when using and not using BA. The highest goodput is found for block size 16, and is more than 10 % higher relatively to the case of standard ACK. The increasing behaviour of the goodput is verified up to 40 stations.

3.2.4 Summary and conclusions

This work investigated the BA size as a policy to decrease delays and ensure a stable system. The investigation was based on tuning several parameters and investigated the effect of a procedure with and without BA. Several policies were investigated. Although for lower values of the

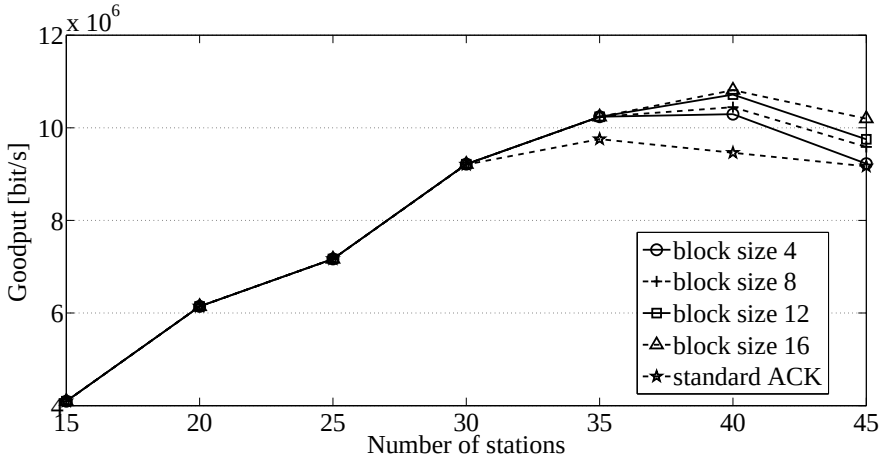

FIGURE 3.11: Video goodput with Block ACK implemented for video traffic.

number of stations the use of BA leads to a slightly worst system performance, the BA procedure provides an improvement in highly loaded scenarios. The improvement is of 2 Mb/s and 2.2 Mb/s in average, for BK traffic and VI traffic, respectively.

In a scenario with mixture of services the most advised block size is 12 since it is the one that provides lower delays in a highly loaded scenario, while the users are still within the capacity of the AP. The number of supported user increases from 30 to 35. Note that 35 stations is the total number of VO plus VI and BK users.

3.3 Cross-layer design

In IEEE 802.11e wireless local area networks, rate allocation depends on access categories and user priorities. The strategies for its improvement use physical (PHY) and application layer information to optimize the Medium Access and Control (MAC) protocol. In this chapter, we propose a distributed cross-layer algorithm that dynamically resizes the arbitrary inter-frame space and the contention window. This algorithm simultaneously accounts for PHY, MAC and application layer information. A scheduler that uses some of the algorithm metrics is proposed as well. The results for a stand-alone service and the multi-service case are very promising, as they provide augmented system capacity whilst supporting more QoS users (an increase of around 30 % for 15 stations and of around 24 % for 20 stations). Besides supporting extra users, the weighted scheduling algorithm behaves as a call admission control algorithm since it de-prioritises the stations that jeopardise the system, not giving them access to the shared channel.

3.3.1 Related work

Recently, there have been great efforts to analyze and improve the performance of the IEEE 802.11 MAC protocol. Several theoretical models were proposed, e.g., the one from [52], and simulators were developed, e.g., the one from [53], in order to analyse, optimize and improve IEEE 802.11 DCF performance. Models for scheduling were proposed in several papers. In [54], a packet scheduling model has been developed to improve IEEE 802.11 capacity. Besides, the distributed fair scheduling proposed in [55], applies the ideas behind fair queuing in the wireless domain. The capacity of IEEE 802.11 was improved by modifying the backoff mechanism or tuning various parameters like the inter-frame spacing time [56], [57], [58], [59]. Other works propose to dynamically altering the value of the CW [60], [61], [62]. The authors from [63] address the enhancement for HCF to improve its Admission Control Unit (ACU). It basically sets the TXOPs in order to avoid starvation for resources from lower priority AC like BE and BK. Another work that improves the performance of IEEE 802.11e networks by setting the values of the limit for the TXOP is presented in [64]. It proposes a new MAC protocol based on the reservation of the wireless channel through the use of the TXOP limit parameter. Each traffic class monitors the MAC queue and computes the TXOP limit value at runtime. Thus based on the class priority and flow data rate, both intra and inter QoS differentiation are ensured. In [65], an Adaptive Enhanced Distributed Coordination Function is derived from the EDCF if the IEEE 802.11e amendment. Relative priorities are provisioned by adjusting the size of the CW of each traffic class accounting for both applications requirements and network conditions. In [66] the best configuration for $CWmin$ and $CWmax$ are found for each AC, as well as TXOP limits.

In order to support accurate optimization of B3G radio and network planning, there is a need for a flexible and open evaluation tool that provides a framework to support cross-system simulations in a cost-effective manner. By its nature, simulation evaluation tool design is a challenging task, in an effort to provide a trade-off between accurate system modelling, and complexity, which will adversely affect the simulation time. To facilitate the use of our simulator in the context of a C++ simulator for the interoperability between IEEE 802.11e and different radio access technologies, we developed our own IEEE 802.11e simulator in C++ from scratch. The knowledge and flexibility gained in this process allowed us to easily include new algorithms in our C++ code (which is frequently a limitation when third-party programming code is used) whilst enabling the inclusion of this simulator in the IT-MOTION HSDPA simulation tool [18],

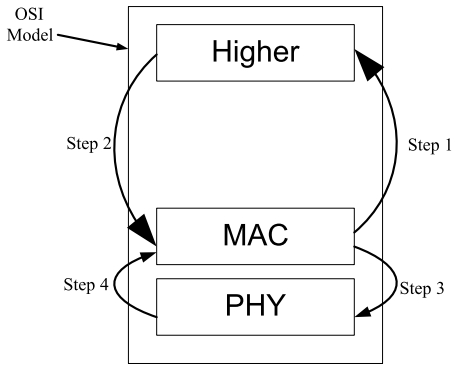

FIGURE 3.12: Downward and upward information flows within cross-layer design.

[39], allowing for performing research on CRRM and the support of interoperability between HSDPA and WiFi.

The support of high network throughputs can benefit from cross-layer design techniques. Although layering is today the driving methodology, strict layering principles may result in inefficient implementations of B3G wireless networks. Moreover, specific issues in wireless networks (e.g., radio resource shortage, power restriction consumption, etc.) call for further optimizations in network performance. From the cross-layer design perspective, significant attention is given to the interfacing methodology among PHY, MAC, network and transport layers. An example of the application of these interactions to solve our problem is shown in Figure 3.12.

Typically, protocol evaluation platforms are not managed by the same task manager/processor, otherwise computation time would be prohibitive. Hence, the interface is usually managed by look-up tables, which are computed off-line. The traditional problem is how to reflect the physical layer assumptions, implications, and scenarios on the system level when independent simulation platforms are employed with different time granularities. References [67], [68], [69] have addressed these issues, while [70] is targeting the link level interface, given Multiple Transmit Multiple Receive (MTMR) techniques for Multiple-Input-Multiple-Output (MIMO) MC-CDMA. In [35] a list of characterisation parameters was identified in the context of cross-layer design whilst suggesting values for their range of variation.

3.3.2 System, scenario and assumptions

Lets consider a cellular WiFi system where each cell has a set $N+1$ IEEE 802.11e stations communicating through the same wireless channel. While station 0 is the Access Point or QoS Access Point (QAP), the other N wireless terminals or QoS stations (QSTAs). The propagation

TABLE 3.3: Traffic Parameters [2].

AC	**Voice (VO)**	**Video (VI)**	**Background (BK)**
Packet size	1280 bit	10240 bit	18430 bit
Packet interval	20 ms	10 ms	12.5 ms
Usage	50 %	30 %	20 %

time is assumed to be absorbed by the different mechanisms of the IEEE 802.11. Each station has four buffers whose size depends on the kind of service being dealt in order to guarantee a given value for the goodput (payload of the packet). For simulation purposes, one considers buffers with infinite size. These buffers will be filled with a MAC Service Data Unit (MSDU) generator that characterises the service being dealt in the given buffer. If the MSDU is bigger than a fragmentation threshold, it will be fragmented. In order to cope with service quality the packet transmission follows the Enhanced Distributed Channel Access (EDCA) IEEE 802.11e MAC procedure. Due to collisions or interference a packet may not be correctly received. The interference issues are addressed and the radio propagation model from [71] is considered. The hidden and exposed terminal problems are addressed as in the standard, e.g., for a given payload threshold the RTS/CTS procedure is implemented. Each packet exits the buffer only after the reception of an acknowledgement, or if it has suffered more than a collision threshold. In this first phase the users are assumed to be static, and are distributed uniformly in a square area of 2500 square meter. The implemented topology consists of several wireless stations and an Access Point (AP). Three types of traffic sources were chosen, namely high priority voice, medium priority video and low priority background (FTP data). The parameters for the traffic sources characterization are shown in Table 3.3, where the constitutive ACs of each type of traffic are also presented.

3.3.3 Cross-layer algorithm

The use of optimized procedures for link adaptation rather than static link layer parameters may enable improved opportunistic use of the WLAN radio channel. Downward information application flow is proposed in this work together with channel state indicator information, both made available to the MAC layer, in a cross-layer design approach. The IEEE 802.11e basic access procedure allows for machines which are far from the Access Point to monopolise the channel, and does not allow for prioritising any packets from any machine. Besides, the use of four buffers for each service class is not enough to guarantee a certain grade of service (GoS) when the communication medium is very loaded. In this work, we propose to enhance the impact

of the AIFS and CW MAC parameters, by generating their values as a function of not only the service class but also the current delay, channel conditions, and the channel utilization of each wireless machine. In several papers available in the literature the use of these mechanisms were always presented as independent enhancements, and not considering the channel conditions [66], [64], [63], [65]. Here, we analyse the system performance when this two enhancements are simultaneously implemented, and always considering channel conditions and current delay. Hence, it is not a mere rate allocation strategy, the proposed techniques actually implements cross-layer design. The algorithm was developed for voice, video and background applications since voice and video are delay sensitive services. One also considers a service that was not delay sensitive, like the background traffic. The objective is to support the highest number of users, with service quality support and enhanced system capacity.

Enhanced AIFS

The proposed optimization algorithm prioritises users with highest delay. The intention is to give them the highest priority after a given threshold. One proposes to use the following potential function for the delay weight:

$$DelayWeight_{AC}(CurrentDelay) = C_{AC}^{\frac{CurrentDelay}{K_{AC}}}, \tag{3.1}$$

where *CurrentDelay* is the current delay of the first packet in the queue of the AC, while C_{AC} and K_{AC} are constants whose values need to be found.

For voice packets, the GoS threshold (acceptable delay) is 30 ms, meaning that delays higher than 30 ms are not acceptable. In turn, for video packets, the GoS delay threshold is 300 ms, while for background packets it is 1000 ms [35]. The metric satisfied users is used ahead and it is based on satisfying these three thresholds.

For each access category, a prioritization procedure can be implemented that prevents the delay to overcome the threshold. This procedure involves the use of a potential function since one is seeking a function that grows very fast after a given limit. For voice, the delay weight was obtained by using $C_{AC} = 5$ and $K_{AC} = 15$ while, for video one considered $C_{AC} = 5$ and $K_{AC} = 62$. For background traffic one considered $C_{AC} = 5$ and $K_{AC} = 520$. This set of parameters lead to three different functions for the delay weight, one for each access category.

These functions are only applied if the $DelayWeight_{AC}(CurrentDelay)$ is lower than a given threshold for the respective AC, $threshold_{AC}$. Otherwise, the $threshold_{AC}$ value is used, i.e., $DelayWeight_{AC}(CurrentDelay) = threshold_{AC}$. In our example, one considers $threshold_{AC} = 15$ for all applications.

Besides the delay, it is also essential to differentiate the users by their channel utilization. In WiFi systems, a station with low SINR can monopolize the channel if it is far away from the AP, since it takes more time to transmit; owing to this either the lowest supported data rates, or higher error or collisions. In order to provide this differentiation, an update of the channel usage is performed every 100 ms. This channel usage parameter proposed by us, *ChannelUsageParameter*, is a parameter that takes values between 1 and 10, and is used to prioritise packets in the internal queues of the AP. This decision is based on the next selection metric, where the highest value gives the highest *ChannelUsageParameter*,

$$M_j = \frac{PhyDataRate_j}{AverageThroughput_j(p)}. \tag{3.2}$$

The $AverageThroughput_j(p)$ is the average throughput in the last time period p for user j, while $PhyDataRate_j$ is the instantaneous data rate supported for user j that depends on the actual value of the SINR of user j. This is a common metric used to provide fairness in schedulers for systems like HSDPA. The Enhanced AIFS (EAIFS) is computed dynamically, and depends on the delay weight, the channel usage parameter, and on the value of AIFSN, i.e., $EAIFS_{AC}(DelayWeight_{AC}, ChannelUsageParameter(i))$. In our simulations, we found that an appropriate function is the following

$$EAIFS_{AC} = 26 - DelayWeight - CannelUsageParameter. \tag{3.3}$$

Although this procedure might add some delay to stations not delayed, it increases fairness in channel utilization, and will allow for extra stations to be served with the appropriate service quality.

Enhanced contention window

A dynamic procedure to get the contention window value after each successful transmission or collision was also implemented. We believe that this adaptation will increase the total traffic goodput, which becomes limited when using the basic EDCA, mainly for high traffic load.

In the basic EDCA the values of *CWmin* and *CWmax* are statically set for each access category. After each successful transmission, the *CW* values are reset to *CWmin*. We propose to reset the *CW* to values which are based on the collision rate of a given machine, on the delay, and also on the channel usage, by considering the type of access category. This procedure is a trade-off between wasting some backoff time or risking a collision (and the subsequent retransmission of the whole packet). After each unsuccessful transmission, the source has to wait for a timeout to know that the packet is lost. Then, it doubles its *CW* and tries to retransmit reducing, this way, the probability of a collision. After each successful transmission, the basic EDCA mechanism simply sets the contention window of the corresponding category to its minimum value regardless the network conditions. Here, we propose to change this mechanism, and differentiate among access categories by using different factors to get the value of the *CW*. Motivated by the fact that when a collision occurs a new one is likely to occur in the near future, we propose to get the contention window value by dynamically making it depend on the delay weight, on the channel usage parameter, and on a collision rate component, i.e., $CW_{new}(DelayWeight_{AC}, ChannelUsageParameter(i), ColRate_{AC})$.

In our tests we used the following function to find the contention window:

$$CW_{new} = \alpha_{AC}(16 - DelayWeight + 10 - CannelUsageParameter + 16 \cdot ColRate), \qquad (3.4)$$

where the constant α_{ac} is used to prioritise each class of service. One considered α_{ac} = 1 for the voice class, α_{ac} = 2 for video and α_{ac} = 3 for the background class. The *ColRate* is computed by using

$$ColRate = \frac{collisions_j(p)}{packets_j(p)}, \qquad (3.5)$$

where $collisions_j(p)$ is the number of collisions of station j which occurred in the period p, while $packets_j(p)$ is the total number of packets that have been sent or received in period p. A value of the weight of *ColRate* of 16 was found to be the value which provided better results after several simulations.

We denoted this approach as the Enhanced Contention Window (ECW) procedure. The ECW procedure also considers the channel conditions. For video, it can be seen from (3.5) that the

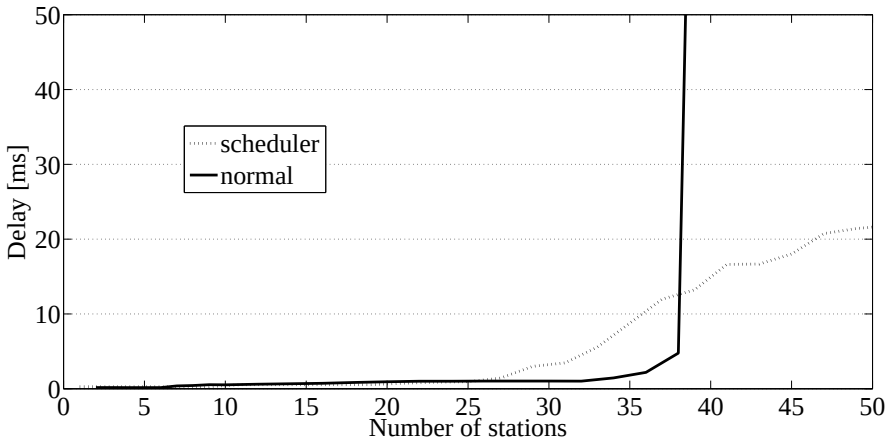

FIGURE 3.13: Delay for VO in the access point with and without scheduler.

contention window doubles its value, since it has lower priority than voice, while the background traffic who has even lower priority, it is three time higher than for voice.

This is the basis of the proposed scheduler, where we use the *ChannelUsageParameter* to reorder packets in the access point. We started by extracting initial results for standalone services, which were very optimistic. For VO, as the limitation occurs in the access point, its higher priority is provided to VO in the AP (by reducing the contention window and the inter-frame spacing) the number of supported users increase significatively, as it can be seen in Figure 3.13. Without the use of the scheduler, the supported number of user is around 37 while, with the use of the scheduler, it goes up to 50 users. Regarding VI and BK traffic, just by reducing the inter-frame spacing, a gain in the delay and goodput was obtained. However with the approach from (3.4), when we extracted results for a multi-service scenario, the performance was poor for background and video traffic, because, depending on the values given to C_{ac}, K_{ac} and α_{ac}, voice traffic is being prioritised over the other ACs.

As a result of this initial analysis, to optimize our base algorithm for a multi-service scenario, for each AC, the decision was to give different weights to the variables *DelayWeight*, *ChannelUsageParameter* and the *ColRate*. For a given number of stations n, we have considered a set of 9 weights, W=(W_{VO1}, $W_{VO2,}W_{VO3}$, W_{VI1}, $W_{VI2,}W_{VI3,}W_{BK1}$, $W_{BK2,}W_{BK3}$) whose values needed to be sought. In order to find these variables, 10000 simulations have been performed by randomly varying each weight in the set {1, 2, 3, 4, 5, 6}. These weights are applied in the following way to obtain the new values for the CW:

$$CW_{new} = \alpha_{AC} \left[\begin{array}{l} W_{AC0}(16 - DelayWeight) + \\ W_{AC2}(10 - ChannelUsageParameter) + W_{AC3} ColRate \cdot 16 \end{array} \right]. \quad (3.6)$$

where W_{ACi} is the i^{th} weight for the AC, with $AC \in \{VO, VI, BK\}$ and $i \in \{1,2,3\}$. From these 10000 results, we have chosen the optimum combinations, i.e., the ones that provide higher number of satisfied user for the cases of 15, 20, 25, 30 and 35 stations. Note that each of these stochastic simulations were run 10 times to achieve statistical relevance. The respective achieved weights are the following:

W_{15}=(3,1,2,1,2,2,1,1,2);

W_{20}=(5,1,3,3,2,4,1,1,6);

W_{25}=(2,1,2,1,5,1,6,6,1);

W_{30}=(2,1,2,1,5,1,6,6,1);

W_{35}=(2,4,1,3,2,1,5,6,1).

We were not able to apply any of the analytical models sought in the literature to get the optimised weights, since analytical models available for IEEE 802.11e do not account for collisions due to the hidden terminal problem. Besides, most of these models only consider saturation conditions, which does not match our approach. The authors from [72] present a model for EDCA procedure in saturation conditions, but in the end it only accounts for two service classes and even with only two service classes, it is not a convex problem. In [73], several physical data rates are considered but, again, saturation conditions are assumed. In [74], several arrival rates are considered to also account for the EDCA procedure, turning this model into a non-convex problem. Besides brute force, an empirical approach to find the weights that suit the system may be to use GA. This topic is left for future study.

3.3.4 Cross-layer design simulation results

The initial results are presented to demonstrate that the scheduler works properly for a standalone service scenario. However, our aim was always to achieve improvements for the multiservice case. Figure 3.14 presents a comparison of the results for the goodput with all applications in the AP between the standard case and the case when the scheduler is used.

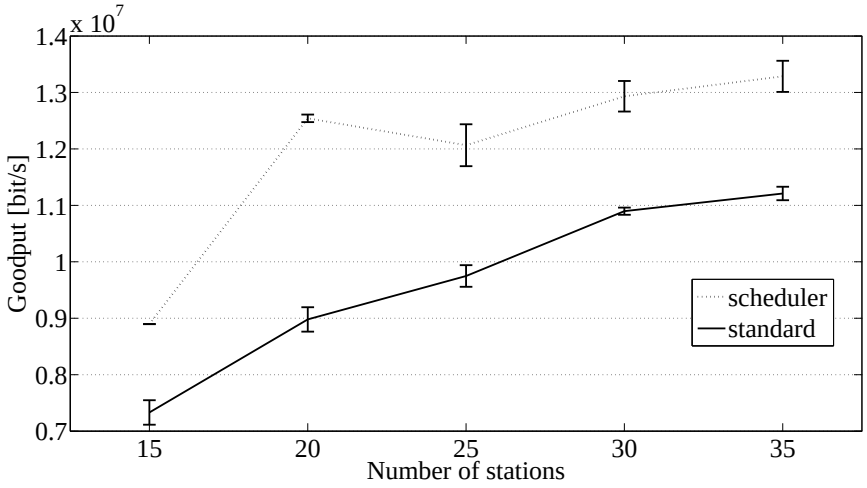

FIGURE 3.14: Goodput in the Access point with and without scheduler.

A gain around 2 Mb/s can be observed when compared with the results for the standard scheduler. Regarding the scheduler curve behaviour, there is an increase on the goodput from 15 to 20 because more users are added to the system. As the system has enough capacity to support them, the goodput increase accordingly. When the number of user increases from 20 to 25 stations, the system starts to have more users than the ones it can actually support, at least with our algorithm.

Hence, in order to support the highest number of user, it ends up by not serving video and background users that are far from the AP, since it is much easier to support a user at 64 kb/s than one at 1024 kb/s.

Nevertheless, this is not the major enhancement of the algorithm. This gain could be easily obtained by prioritising VI or BK traffic. The major feature consists of prioritising different traffic types, i.e, access categories, while satisfying more users, Figure 3.15. It can be observed that our algorithm satisfies almost 100 % of the users for 15 and 20 stations in the scenario, serving with QoS more 30 % for 15 stations, 24 % for 20 stations, and 13 % for 25 stations. For higher number of stations, there is still a slight gain in user satisfaction relatively to the standard IEEE 802.11e scheduler. For the standard scheduler, in the case of 15 users, there is less satisfaction in comparison with the case of 20 stations. Since the users are more spread, the hidden terminal occurs more often. As a consequence, collisions are more likely to occur. However, with our scheduler, this limitation has been solved as it provides higher variation in the backoff procedure, since the CW length accounts for the collision rate.

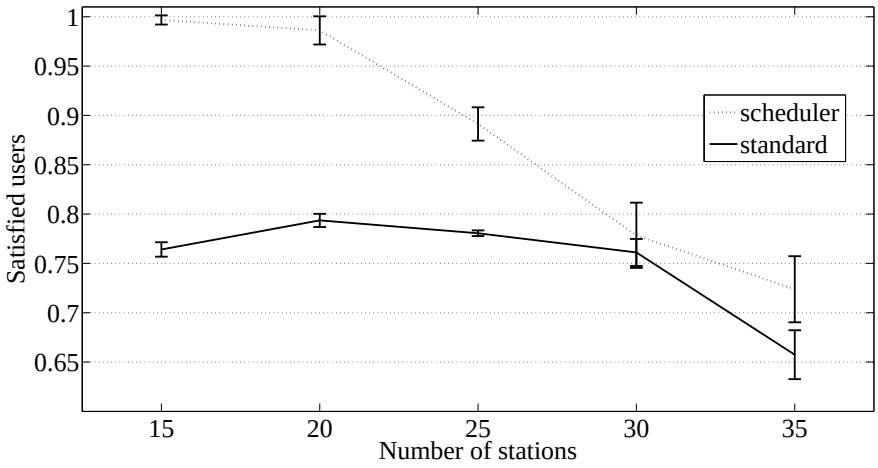

FIGURE 3.15: Satisfied users with and without scheduler.

In Figure 3.16 one can observe that the application of the scheduler ends up working as a call admission control algorithm, as it de-prioritises packets from the users far from the access point, which will cause the all system to have a bad performance when the scenario is overloaded. Now, users with the highest transmission mode, TM, i.e., TM7 and TM8, from Table 2.6 , become the ones with the highest satisfaction. The rationale behind this result is the following: to try and support all users is not recommendable since it is actually impossible to achieve an appropriate system performance for users badly covered. The best approach is to keep satisfied the highest number of users. This is performed by de-prioritising the users that are far away from the AP, which tend to suffer more collisions and occupy the channel for longer time.

The proposed algorithm might seem to cause some unfairness as it prioritises the users closer to the AP. However, this is not a reality, as it is shown in Figure 3.17. Actually, our scheduler provides a value for the fairness among stations always higher than the standard one, except for around 15 users. The fairness was measured by using the following Jain's fairness index [75] for evaluating how fair a particular allocation:

$$F = \left(\sum_{i=1}^{n} y_i\right)^2 / \left(n \sum_{i=1}^{n} y_i^2\right) \tag{3.7}$$

where n is the total number of station and y_i are the individual station throughputs. The averages for the delays were also extracted. However, by de-prioritising the users far from the AP we get some wide confidence intervals, because the averages are influenced by the points that have a high deviation from the average. Even though, the obtained results allow for understanding what the behaviour of the average delay is.

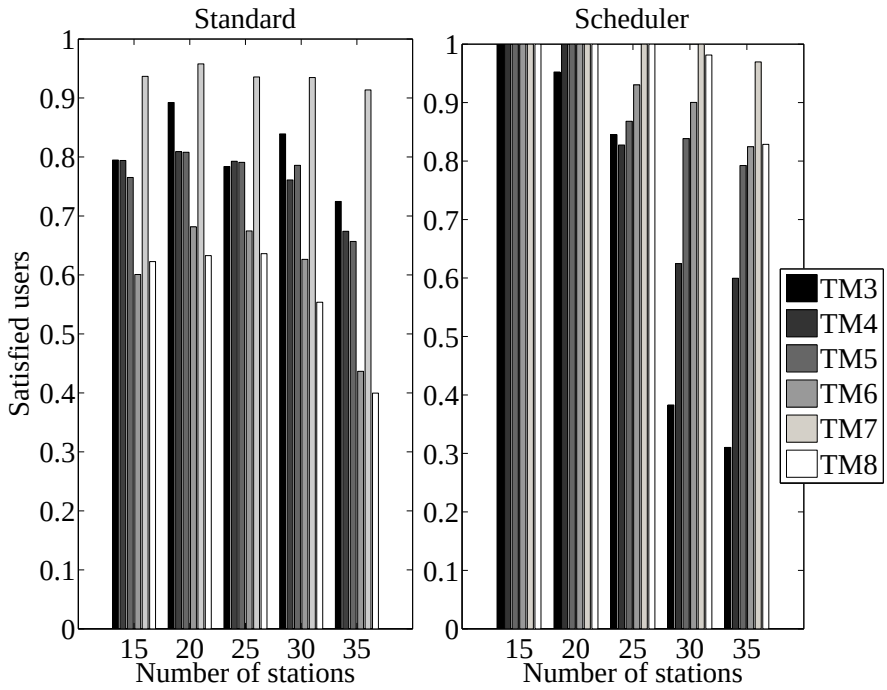

FIGURE 3.16: Satisfied users with and without scheduler dependent of the TM.

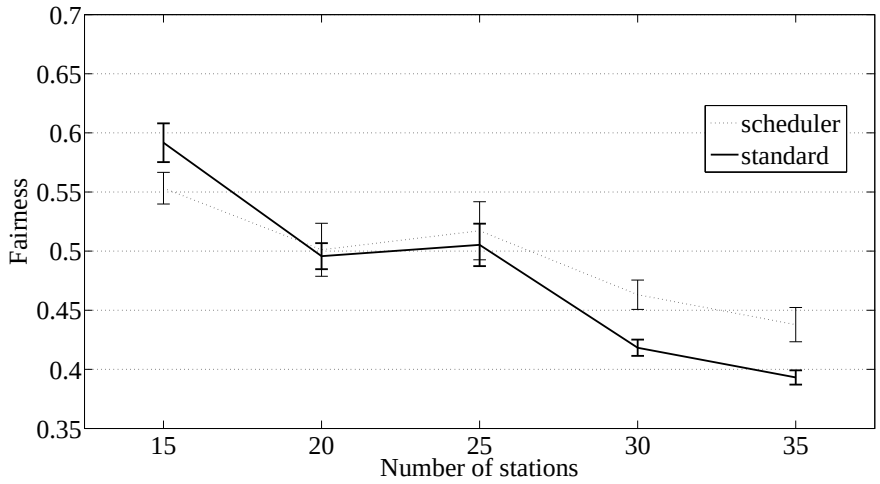

FIGURE 3.17: Fairness among stations with and without scheduler.

For voice and video traffic, the delays are higher when the scheduler is considered, but still below the threshold. We have de-prioritise these service classes, up to the GoS threshold, which is still acceptable. By acting this way, we are now able to provide access to the background traffic class that with 15 users, with the standard scheduler, almost never had the chance to transmit, maintaining an acceptable service quality, as the delays keep bellow the GoS threshold, Figure 3.18.

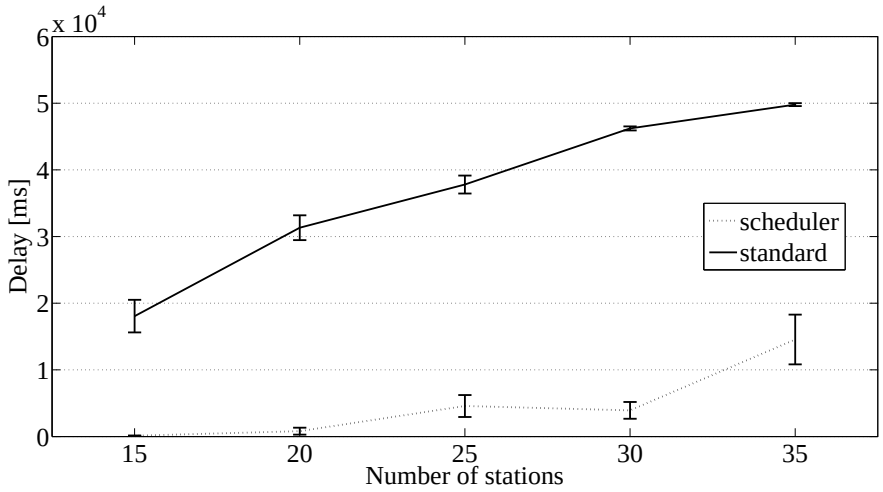

FIGURE 3.18: Delay for the background traffic.

3.3.5 Summary and conclusions

This Chapter proposed a distributed scheduling algorithm that changes the size of the AIFS and the CW length dynamically according to a periodically obtained fairness measure based on the SINR and transmission time, a delay constraint and the collision rate of machine j. Depending on the load in the system, these metrics have different influence in the system performance. The need to change the weight these metrics have on the computation of the AIFS and the CW was identified. The weights were found for several loads for a case scenario with given traffic parameters, but they can be found for any other case scenario with different traffic parameters.

The proposed algorithm has showed improvements providing the highest goodput, lowest delays, supporting more users than the standard with higher QoS. It increases the throughput in 2 Mb/s for all the loads tested. It satisfies more users than the standard (30 % more for 15 stations, 24 % for 20 stations and 13 % for 25 stations), while ensuring the appropriate grade of service. The delay for background traffic is never manageable in the standard for the loads tested while in our algorithm the background traffic only starts having problems when more than 20 stations are in the scenario.

Besides supporting more users, our algorithm can work as a call admission control algorithm as it de-prioritises stations that jeopardise the system in such a way that they do not gain access to the channel. It increases the goodput maximizing the number of supported users. When the load is not manageable it starts to de-prioritising users far from the AP with lowest modulation and coding scheme so that it can support more users closer to the BS with QoS.

In future work, handover policies between APs will also be an objective to be fulfilled, where a scenario using more than one cell can be supported. As the parameters found best suit this case scenario, at the moment we are implementing a dynamic procedure based on genetic algorithms to perform weights optimization online so that this procedure will always be optimized in a given scenario. Our simulator was also integrated into the IT-MOTION simulator for HSDPA. Chapter 4 adresses the work performed to optimise inter-working among different systems (e.g. WiFi, HSDPA, and WiMAX) in the context of CRRM.

3.4 Analytical model for an IEEE 802.11e ad hoc network

In this Section, an analytical model is proposed for IEEE 802.11e ad hoc networks generating packets to a random neighbour. The conceived model is validated by using the IEEE 802.11e simulator presented in Chapter 2.

In the literature there are mostly analytical works on the performance evaluation of IEEE 802.11 networks, confined either to the infrastructure mode or to single-hop ad hoc networks, or networks with very few hidden terminals. To the best of our knowledge, we present the first analytical model to derive the throughput in non-saturation conditions in multi-hop ad hoc IEEE 802.11e networks with nodes randomly placed according to a multi-dimensional Poisson distribution. The model is useful to investigate the hidden terminal problem and propose collision free communications, one of the major issues within decentralized networks. Simulations of the IEEE 802.11e MAC protocol enables to verify the proposed model. Improvements and fine tuning of the model are left for future work.

3.4.1 Related work

The authors from [52] addresses modeling of the behaviour of IEEE 802.11 by using Carrier Sense Multiple Access (CSMA) in saturation conditions. This analytical work is the foundation for other works on the capacity of IEEE 802.11 networks.

Reference [74] presents a model for IEEE 802.11e using the CSMA mechanism in non-saturated conditions. It is a single hop model where the hidden terminal problem is not considered. It is able to account for several traffic models with specific distributions in the same same scenario. References [76], [77] present a model for IEEE 802.11 for multi-hop multi-radio networks with

finite load. It considers a specific topology with multi-radios able to listen in several channels, which is not common in ad hoc networks. These works do not describe the IEEE 802.11 standard since it proposes a single-radio protocol. Besides, it does not account the hidden terminals.

The authors from [78] present an analytical model that computes the IEEE 802.11 throughput and average delay in the presence of both unicast and broadcast traffic, several realistic issues are addressed, as pre- and post-transmission backoffs, variable frame length and finite MAC buffers.

References [79], [80] present a model to derive the saturation throughput for a single channel in a multi-hop wireless network. It accounts for hidden terminals using the CSMA protocol.

Our proposal considers a multi-hop scenario, whilst accounting for hidden terminals and real traffic sources in a IEEE 802.11e network.

3.4.2 Notation and formulation

An analytical model for IEEE 802.11 networks was developed in [74] for non-saturated conditions and single-hop scenarios. Several sources of traffic were simultaneously implemented in this model. Here, we upgrade this work to model an ad hoc network.

The model presented in [74] characterises the behaviour for each station. The following probabilities were considered in our model:

q - the probability that at least one packet is waiting for a transmission at the start of a counter decrement;

p - the collision probability given that the station is attempting transmission;

b - Markov chain's stationary distribution;

τ - the stationary distribution's probability that the station transmits in a slot;

P_{idle} - the probability that the next slot is sensed idle.

P_{idle}, τ, and b depend on p and q as follows:

$$\tau(p,q) = \frac{1}{b(p,q)} \left(\frac{q^2 W_0}{(1-p)(1-q)(1-(1-q)^{W_0})} - \frac{q^2 P_{idle}}{1-q} \right) \tag{3.8}$$

$$
\begin{aligned}
b(p,q) &= (1-q)+\frac{q^2W_0(W_0+1)}{2(1-(1-q)^{W_0})}+\frac{q(W_0+1)}{2(1-q)} \\
&\cdot \left(\frac{q^2W_0}{1-(1-q)^{W_0}}+(1-P_{idle})(1-q)-qP_{idle}(1-p)\right) \\
&+ \frac{pq^2}{2(1-q)(1-p)}\cdot\left(\frac{W_0}{1-(1-q)^{W_0}}-(1-p)P_{idle}\right) \\
&\cdot \left(2W_0\frac{1-p-p(2p)^{m-1}}{1-2p}+1\right)
\end{aligned} \tag{3.9}
$$

where W_0 is the minimum contention window, and P_{idle} will be explained ahead.

Equations (3.8) and (3.9) model the behaviour of a terminal in a single hop WiFi network. To model a multi-hop ad hoc network, more concepts and assumptions have to be introduced. We assume that stations are distributed using a two-dimensional Poisson point process with density ρ, which means that the probability of finding i terminals in a given area A is given by:

$$P(i|A) = \frac{(\rho A)^i e^{-\rho A}}{i!}. \tag{3.10}$$

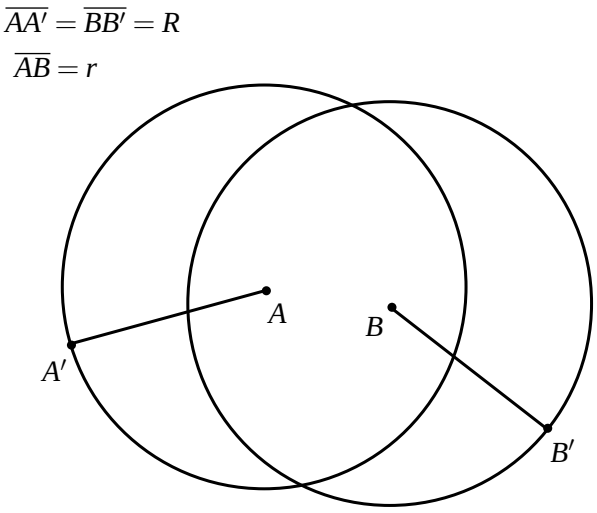

FIGURE 3.19: One hop transmission example.

Figure 3.19 presents an example of a transmission between station A and B. By considering the same transmitted power for each station, and assuming the same scenario regarding propagation, the hearing/transmission range of each station is the same; therefore $\overline{AA'} = \overline{BB'} = R$, where R is the hearing/transmission range. The nomenclature that will be needed ahead is the following :

- $N(A)$ is the hearing area of station A;

- $N = \rho\pi R^2$ is the number of stations within the hearing zone of a given transmiting station;
- r is the distance between A and B;
- $U(r) = N(B) - N(A)$ is the non-overlapping area, which is the hearing area for one station but not to the other, i.e., B can listen but A cannot, which is equal to the hearing area where A can listen but not B (which is easily proven since the areas are the same);
- $C(r) = N(B) \cap N(A)$ is the common area where A and B can listen.

3.4.3 Network model

It is assumed that the entire network shares the same communication channel. Therefore, the actions of the neighbouring terminals depend on their neighbours. We assume that there are n terminals in the scenario with a wide area, and each station has N neighbours. Then, the probability of no collision in a given area is defined by:

$$1 - p = (1 - \tau)^{N-1}, \tag{3.11}$$

where $N = \rho\pi R^2$. It means that there are no collisions since, at the most, there is only one station transmitting. To calculate the throughput, we need to know how much time is spent on each of the states. After the average time spent in a successful transmission is determined, it is possible to obtain the throughput. The medium in a given area, as our Markov chain, can be in an idle state, a successful transmission, or a collision. The average time spent in these three states is given as follows:

$$E_s = (1 - P_{TX})\sigma + \sum_{i=1}^{N} P_{s_i} T_s + \sum_{j=2}^{n} C_j^n P_{c_j} T_c, \tag{3.12}$$

where P_{s_i} is the probability for station i to successfully transmit:

$$P_{s_i} = \tau \cdot (1 - \tau)^{|C(r)|} \cdot (1 - \tau)^{|U(r)|}. \tag{3.13}$$

T_s is the expected time taken for a successful transmission, and T_c is the expected time taken for a collision. Besides, P_{c_j} gives the probability for all the r stations within a given area to have a collision:

$$P_{c_j} = \prod_{i=2}^{j} \tau^i (1 - \tau)^{j-i} \cdot \frac{(\rho\pi R^2)^i e^{-\rho\pi R^2}}{i!}. \tag{3.14}$$

σ is the slot time, and $|X|$ is the number of elements of X. The probability that at least one station attempts to transmit is given by:

$$P_{TX} = 1 - \prod_{i=1}^{N}(1-\tau). \tag{3.15}$$

After the average duration of each state is found, the throughput can be found by estimating the amount of time a station is successfully transmitting data

$$S_i = \frac{P_{s_i} L_i}{E_s}, \tag{3.16}$$

where L_i is the expected time spent transmitting data from source i. The normalised throughput of the system is then given by

$$S = \sum_{i=1}^{N} S_i. \tag{3.17}$$

P_{idle} is the probability for the channel to be idle, when no station is transmitting, and is given by:

$$P_{idle} = (1-\tau)^{N-1} = 1 - p. \tag{3.18}$$

The offered load is represented by the probability of a packet becoming ready to be transmitted, λ. According to [2], as the traffic for WiFi has a constant interarrival, we consider that packet arrivals are uniformly distributed across slots and $\lambda = min(E_s/interarrivaltime, 1)$.

3.4.4 Scope of the model

The proposed model assumes a fixed packet size. It was also assumed that channel errors are only caused by collisions and a simple queue model was considered. It is possible to add complex models based on Gaussian or Pareto distributions, commonly used in the communications field, without adding further states into the Markov chain. For example, the q values could be calculated by using more elaborated queueing models.

As it is assumed that stations are distributed using a two-dimensional Poisson point process with density ρ stations per square meter, the expected value of the distribution is ρ. After a large number of simulations, the Mobile Stations (MSs) will in average occupy an area $1/\rho$, assuming that each MS will occupy a square.

TABLE 3.4: Mapping of ρ, *N*, *#C*, *#U*.

ρ	*N*	*#C*	*#U*
$9.580 \cdot 10^{-3}$	37	30	7
$8.622 \cdot 10^{-3}$	29	22	7
$7.665 \cdot 10^{-3}$	25	20	5
$4.790 \cdot 10^{-3}$	21	16	5
$3.832 \cdot 10^{-3}$	13	8	5
$1.916 \cdot 10^{-3}$	9	6	3
$9.580 \cdot 10^{-4}$	5	2	3

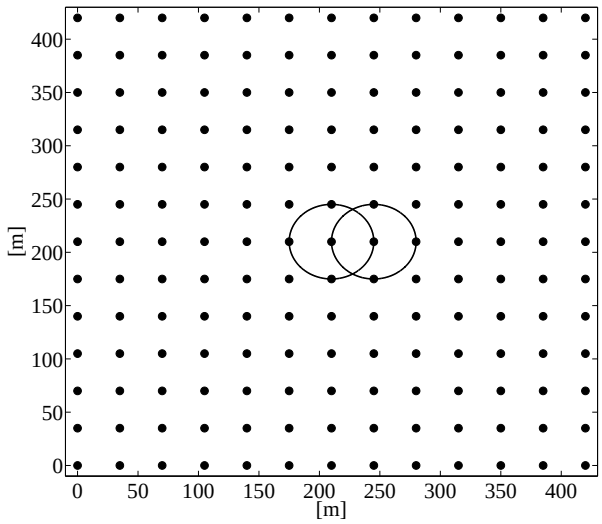

FIGURE 3.20: Topology for $N = 5$.

By assuming that all MSs are distributed like in Figure 3.20, the following set of densities $\rho = \{9.580 \cdot 10^{-3}, 8.622 \cdot 10^{-3}, 7.665 \cdot 10^{-3}, 4.790 \cdot 10^{-3}, 3.832 \cdot 10^{-3}, 1.916 \cdot 10^{-3}, 9.580 \cdot 10^{-4}\}$ were considered. All the considered topologies are presented in Appendix D. These topologies consider 169 stations in 13 lines per 13 columns. Each of the values for the densities corresponds to a given set of neighbours, as presented in Table 3.4. The corresponding sizes of the considered areas vary accordingly.

This topology was assumed because an infinite size is not viable due to computational limitations. The extracted statistics consider the station in the position (7, 7), i.e., 7^{th} line from botom, 7^{th} column from the left. This size is appropriate because, besides simulations that were performed for the case of 15x15 grid where statistics for the station in the position (8, 8) were analysed and are similar to the results with a grid 13 per 13 for the station in the position (7, 7).

Finally, it is worthwhile to mention that the number of machines that are on the non-overlapping area and overlapping areas, are given by *#U* and *#C*, respectively.

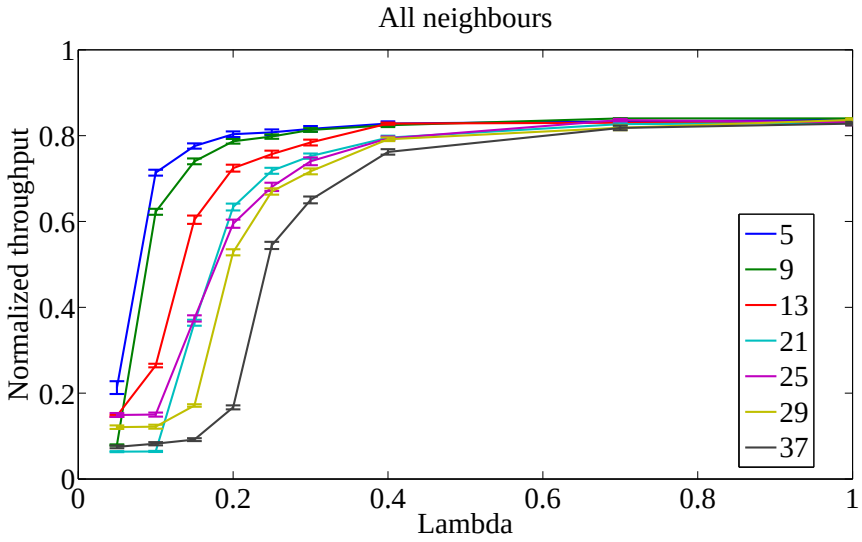

FIGURE 3.21: Normalized throughput for all neighbours

.

3.4.5 Numerical results

By varying the arrival rate, densities and corresponding number of neighbours theoretical and simulation results may be obtained. The simulated Aggregated Throughput (AT) is obtained by considering

$$S = \sum_{i=1}^{N} S_i. \tag{3.19}$$

P_s can be found in the simulations by using the classical definition of probability (by Laplace). L is considered to be the time that 8000 bits using the lowest modulation available in IEEE 802.11a takes to be transmitted. The duration of the slots in IEEE 802.11a is E_s=9 μs, while the value of N depends on the topology. The usual 95% confidence interval is represented in the curves for the simulation results by the vertical bars.

Figure 3.21 presents the simulations AT for all neighbours, as a function of the load. The maximum achievable AT is 0.7. The higher the density is, the less load it supports, as it is more difficult to get to the maximum achievable value of AT (0.8) . Figures 3.22 - 3.25 present the variation of AT as a function of λ for all the considered topologies.

For an arrival rate $\lambda = 0.05$ s^{-1}, for N=5 and N=9, the simulation results are not close to the theoretical results. But for all the other values of $\lambda = \{0.1, 0.15, 0.20, 0.25, 0.30, 0.40, 0.70\}$, the theoretical and simulated values are very close. As the density increases, the number of neighbours increases. For higher values of the load, $\lambda <$ 0.2, the theoretical results are a little bit far from the simulated results.

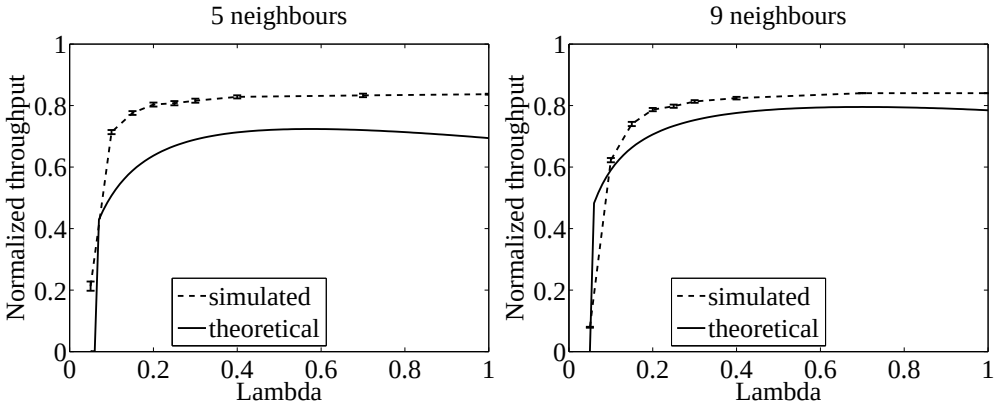

FIGURE 3.22: Normalized throughput as a function of λ for N=5 and N=9.

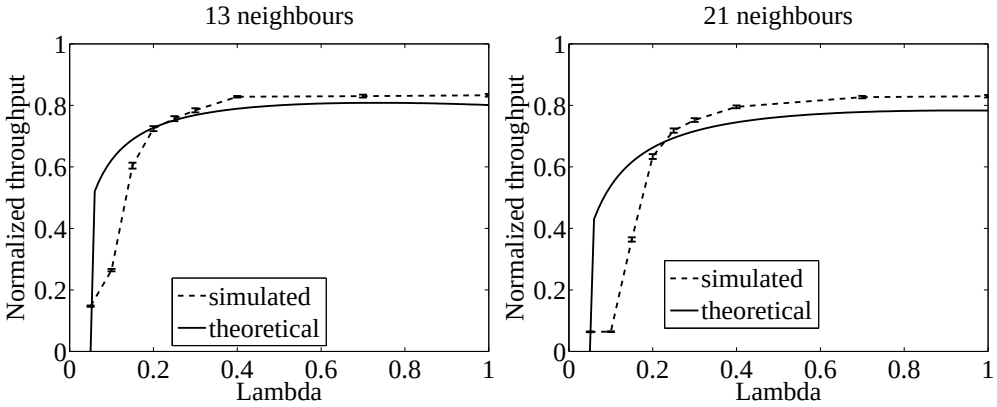

FIGURE 3.23: Normalized throughput as a function of λ for N=13 and N=21.

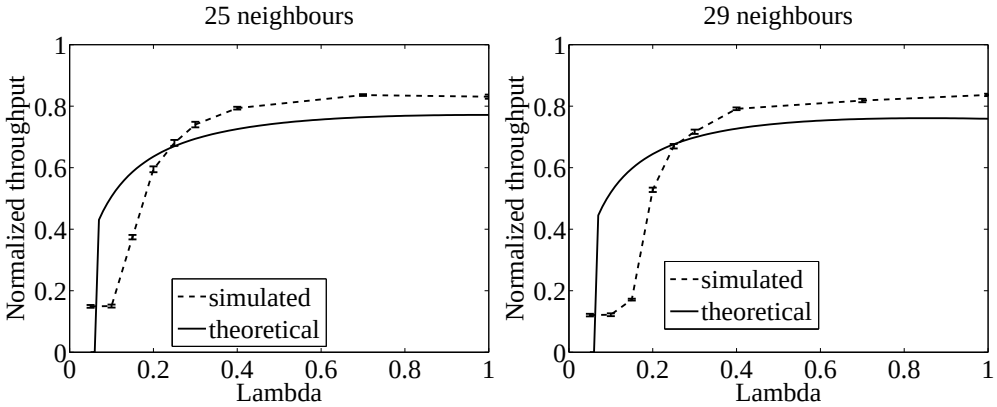

FIGURE 3.24: Normalized throughput as a function of λ for N=25 and $N = 29$.

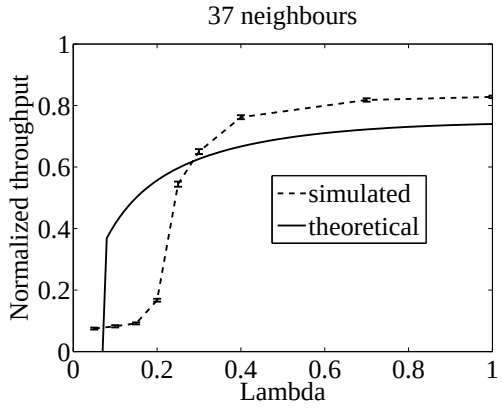

FIGURE 3.25: Normalized throughput as a function of λ for N=37.

3.4.6 Summary and conclusions

A theoretical model for an IEEE 802.11e ad hoc network in non saturation conditions has been proposed in this Section. This model facilitates to test the achievable capacity in this type of networks. It can be verified that it follows the trend of the simulation results.

The model accounts for the hidden terminal problem in non saturation conditions in ad hoc networks, one of the most important issues in this kind of networks. It can be used to seek the best parameters to provide a collision free MAC protocol. A maximum value of the AT close to 0.8 is achievable for the headers, collisions, and the SIFS and DIFS.

Future work includes to extract results for delay and number of collisions, as well as to seek improvements for the ad hoc system.

3.5 Conclusions

This Chapter addressed the optimization of IEEE 802.11e infrastructure and ad hoc mode. In the ad hoc mode an analytical model was developed that allows for investigating collision free communications in a distributed environment. For the infrastructure mode the optimization was done by:

- studying the effect that the buffer size has on the immediate Block Acknowledgement (BA) policy;
- doing cross-layer design that uses the PHY and link layer information, together with the application layer to schedule users in the utilization of the medium.

BA acknowledgement policy decreases delays and ensure a stable system. Although, for lower values of the number of stations, the use of BA leads to a slightly worst system performance, the BA procedure provides an improvement in highly loaded scenarios. The improvement, in single service scenario, is of 2 Mb/s and 2.2 Mb/s in average, for BK and VI traffic, respectively. In a scenario with mixture of services the most advised block size is 12 since it is the one that provides lower delays in a highly loaded scenario while the users are still within the capacity of the AP. The number of supported users increases from 30 to 35.

This Chapter also proposed an algorithm that uses cross layer design that changes the size of the AIFS and the CW length dynamically according to a periodically obtained fairness measure based on the SINR and transmission time, a delay constraint and the collision rate of a given machine. The proposed algorithm has showed improvements providing highest goodput, lowest delays, whilst supporting more users than the standard with higher QoS. The throughput was increased in 2 Mb/s for all the values of the load tested. It supports more users than the original standard while ensuring the appropriate grade of service. Although the delay for background traffic is never manageable into the IEEE 802.11e standard for the values of the load tested, with our algorithm the background traffic only starts being delayed when more than 20 stations are in the scenario.

Chapter 4

Common Radio Resource Management

As current trends drive towards increased number of users and bandwidth starving applications and services, efficient radio resource management in wireless networks is increasingly becoming a necessity.

In this Chapter, the main concepts are addressed for targeting this capacity challenge: cooperative/localization based radio resource management and dynamic spectrum assignment. Cooperation refers to the concept of a sole entity responsible for managing radio resources for heterogeneous networking environments, and herein we explore an HSDPA with an overlay WiFi/IEEE 802.11e network. If a multimode terminal supports several radio access technologies the question arises, which one should be used for a particular communication? To answer this question, first one needs to investigate which systems are available, and what is the required criteria to select the most suitable network based on service, capacity and current load.

One important enabling factor is the availability of bandwidth, which is also related to the assignment of frequency spectrum bands for IMT-A different technologies. This is impeded by the existing highly fragmented radio frequency spectrum that does not match the actual demand for transmission and network resources. Such fragmentation poses a challenge during dynamic spectrum use where multiple frequency bands can be assigned in support of the users and the mobile transmission systems ability to support a wide range of services across all elements of the network (i.e. core, distribution and access [1]).

The fragmented available spectrum can be virtually joined through the SA technique suggested by IMT-A and LTE-A [3], [4], [5]. Information about how to aggregate contiguous and non contiguous parts of the highly fragmented spectrum to be used and how to allocate users over

the dedicated and shared bands of an operator, can improve the overall system capacity. The idea of the proposed Multiband Scheduler is to explore the integration of spectrum and network resource management functionalities to the benefit of achieving higher performance and capacity gains in an IMT-A scenario

The first part of this Chapter investigates the application of suitability based RAT selection using positioning information for enhanced throughput performance in heterogeneous networking environments. In the second part of this Chapter an Integrated CRRM (iCRRM) is proposed. The iCRRM performs classic CRRM functionalities jointly with SA, being able to switch users between non-contiguous frequency bands. The SA scheduling is obtained with an optimised GMBS algorithm with the aim of cell throughput maximization. In particular, it is investigated the dependence of the throughput on the cell coverage distance for the allocation of users over the 2 and 5 GHz bands for a single operator scenario under a constant average SINR. For the performed evaluation, the same type of RAT (HSDPA) is considered for both frequency bands. The operator has the availability of a non-shared 2 GHz band and has access to part (or all) of a shared frequency band at 5 GHz. The performance gain, analysed in terms of data throughput, depends on the channel quality for each user in the considered bands which, in turn, is a function of the path loss, interference, noise, and the distance from the Base Station (BS). Enablers of SA are the advances in the area of smart antenna design, spread-spectrum technologies, Software-defined Radio (SDR), cooperative communications, and Cognitive Radio (CR) systems. Cognitive capabilities, such as sensing, access to database (in connection with geolocation), use of Cognitive Pilot Channel (CPC), transmission power control, etc, can form a CR system capability toolbox and could facilitate coexistence/sharing in bands, where it was previously determined to be not feasible.

In the third part a hybrid network is considered whose goal is to serve ad hoc stations using WiFi with high quality video and audio content, may the existing HSDPA and architecture. The aim of the IEEE 802.11e ad hoc part of the network is to optimally route the packets to/from the users while considering physical and link layer information, in a cross-layer approach. SA is applied to decide if the HSDPA backbone communications is performance either in the 2 GHz band and 5 GHz band whilst giving access to the users trough the IEEE 802.11e ad hoc network.

This Chapter is divided into three Sections that consider CRRMs in different perspectives. In the first Section, the CRRM has the capacity to schedule users in completely different RATs: one is centralized, HSDPA, whilst the other is distributed, WiFi. The interworking scenario is

proposed, and the positioning based suitability policy is described, in terms of the RAT selection procedures and of the identification of suitable metrics for normalized load whilst WiFi and HSDPA. The numerical results accounting for localization in RAT selection are then addressed. Finally, the conclusions are drawn.

In the second Section, one addresses a CRRM that is capable of scheduling users in different bands within the same RAT. First, the objective of the work and system model are presented, followed by the GMBS as a GAP. Then, a formulation to obtain the average SINR, with unitary reuse pattern is proposed and its dependence on the cell coverage distance is analyzed. Finally, the SA results with the proposed iCRRM are discussed, and conclusions are drawn.

In this chapter it is also proposed a scenario for interoperability between HSDPA and WiFi in which the end-user is travelling in public transportation system and requesting multimedia services to the operator. It was sought the most efficient way to manage routing packets inside the WiFi network. Finally, it is discuss the challenges that need to be addressed in order to materialise the envisaged cognitive radio scenario in public transportation.

4.1 CRRM in the coordination of different RATs

The paradigm for networks of the future envisage a network-of-wireless networks to support the market drive towards ubiquitous and seamless services, and to ensure the user is always connected to the best available system. Furthermore, in an era when spectral resources are a premium, it is essential for operators to explore new technologies that can maximize the spectral efficiency of the system in order to deliver these services at low cost. Hence, there is a need for future systems to cooperate to allow effective management of available radio resources. System cooperation can be achieved by a CRRM entity that is responsible for the assignment of mobiles in each RAT, where the assignment is based on an operator specific criterion and utilizes cross-system information to decide on the most optimal RAT assignment for each mobile.

Interworking architectures already exist between WiFi and Universal Mobile Telecommunication Systems (UMTS)/HSDPA like the loose and tight coupling approaches proposed by European Telecommunications Standards Institute (ETSI)/Broadband Radio Access Networks (BRAN) [81] and 3rd Generation Partnership Project (3GPP) [5]. Furthermore, [82], [83], [84],

[85] have investigated architectures and platforms for cooperation schemes between heterogeneous Radio Access Network (RAN), mainly between UMTS/HSDPA and WiFi. In [86] the requirements and algorithms for cooperation of several radio access networks are presented.

However, these works have not considered the effects of positioning information on network cooperation performance. Although research on the area of localization, wireless or cellular geo-location or positioning has been conducted since the late sixties [87], localization attracted much more interest after the U.S. Federal Communications Commission (FCC) announced that it is mandatory for all wireless service providers to be able to provide location information to public safety services in case of an emergency [88], [89].

Nevertheless, that was just the initial motivation, since researchers soon envisioned new commercial services that could become feasible if the exact location of the mobile user is known to the provider. Inspired by the difficulty of the localization problem and motivated by the aforementioned new commercial services, research exploited the nature of the wireless channel in an attempt to estimate meaningful parameters that could in turn be used for geo-location. Amongst the numerous techniques that were developed, the most commonly used and accepted are the geometrical ones and especially those based on the estimation of the Angle of Arrival (AoA), the Time of Arrival (ToA), the Time Difference of Arrival (TDoA), or a combination of two or maybe three of the above, or even the estimation of the Received Signal Strength (RSS) [90], [91].

Cooperation between networks based on the load suitability for delay constrained services was investigated in [17]. The notion of suitability is based on the most preferred access system to accommodate the service, but this concept, suitability, can change as load increases in order to maintain the quality of service across the networks. So the goal should be to optimize the load in each RAT without loss of QoS guarantee. In this work, we extend the concept of suitability to exploit localization information to enhance the RAT selection procedures between WiFi and HSDPA. Assuming that Near Real Time Video (NRTV) services can be serviced by both wireless systems, existing techniques assume the once the load threshold is breeched on HSDPA, excess users are allocated to the WiFi systems in order to support the increased demand for services. This approach can lead to reduced system throughput since the subset of users that increasingly become more suited for WiFi connectivity are transferred, but are dropped since they fall outside the WiFi coverage hotspot. However, by using localization information, the RAT selection procedure will have a priori knowledge of the user location in addition to its suitability

identifier, and will only perform vertical handover to WiFi if it is more suitable and the user shares the common coverage zone.

4.1.1 Interworking scenario

We explore the impact of positioning an interworking scenario between WiFi (IEEE 802.11e [20]) and HSDPA (rel. 6) that target a common coverage as depicted in Figure 4.1. An IP-based core network exists that acts as the networking bridge between WiFi and HSDPA. The CRRM entity is part of the network convergence platform that is able to direct traffic through different paths. It has full knowledge of the load in each system and the position of each user in the grid. The CRRM is responsible for i) gathering system and user specific information, ii) processing this information according to operator specific criteria, and iii) triggering a new handover event according to the load balancing criteria and position. In this work, we extend [17] to address the impact of positioning data on RAT selection. Moreover, it is assumed that a common operator deploys either both systems, or the system operators share a service level agreement. This scenario addresses the delivery of NRTV services that can be streamed either over HSDPA or WiFi systems. The end user is currently subscribing to an IP TV service, which may also be delivered over the WiFi hotspot. All the user equipment is multimode terminals that are able to support either WiFi or HSDPA. An handover triggered by the mobile terminal it is not a solution because it has no knowledge about the network load, it might know which are the available RATs but it does not know which are the overall network conditions like, load in the RATs, mobility support, etc.

The study will mainly be focused on the criteria for handling a handover event whilst neglecting architectural aspects of the intersystem handover (tight/loose coupling, centralized or decentralized), including signaling aspects. It is assumed that the values for the metrics are available and can be obtained with no errors. By using position and load measurements for both systems, based on the obtained suitability value, the algorithm selects the most preferred/suitable RAT as the best available connection.

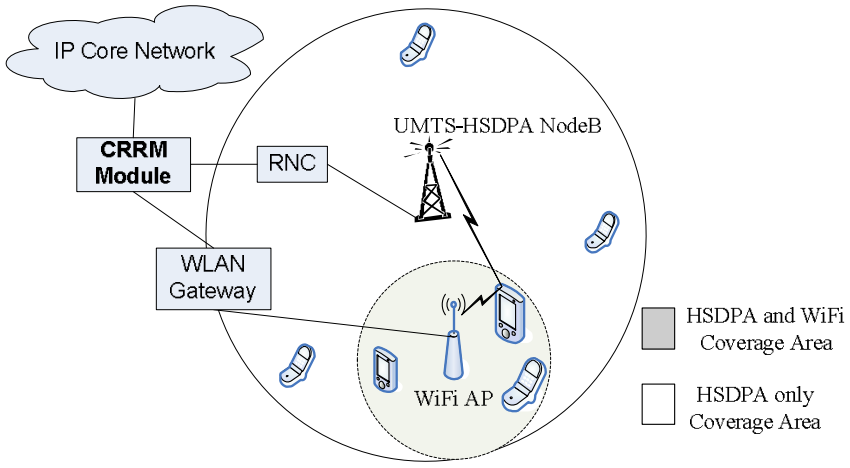

FIGURE 4.1: Interoperability scenario targeting WiFi and HSDPA.

4.1.2 Positioning based suitability policy

Suitability policy

An algorithm for selecting the most suitable RAT is proposed with the aim of balancing the load in critical loading situations. The rationale behind the algorithm is the following: a preferable RAT is selected by default to handle a service, assuming in this case that the service traffic is flexible and can be handled by more than one RAT. Cross-layer studies show that concave and convex functions are more suitable when flexibility and limited conditions are required [92], [93]. An empirical algorithm for load balancing among cells of different RATs is proposed when a new call is requested. The algorithm is targeted to flexible traffic and imposes certain flexibility on the system, meaning that the service can be held by each RAT. The algorithm for the suitability, *S*, is expressed by the following equation and depicted graphically in Figure 4.2

$$S(L(cell_{i,j})) = \begin{cases} 1 & if \quad L(cell_{i,j}) \leq LTh_j \\ \left(\frac{1-L(cell_{i,j})}{1-LTh_j}\right)^2 & if \quad L(cell_{i,j}) > LTh_j \end{cases} \tag{4.1}$$

where $cell_{i,j}$ represents the cell or access point i belonging to the RAT j, $L(cell_{i,j})$ is the normalized load in the $cell_{i,j}$, LTh_j is the load threshold for RAT j, and $S(L(cell_{i,j}))$ is the suitability value for accepting a new user in $cell_{i,j}$.

The preferable RAT, e.g. HSDPA for NRTV, should be selected in the case of equal suitability values obtained for cells of different RATs.

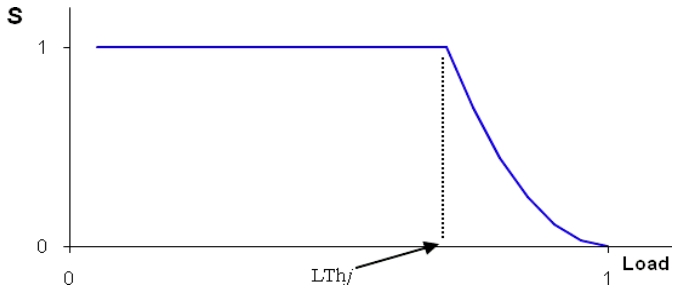

FIGURE 4.2: Suitability profile.

LTh_j is the parameter of the algorithm and characterizes the amount of load reserved for preferable traffic. So the operator should 'optimize' this threshold value in order to set the amount of traffic that a RAT will use for preferable services.

Normalized load estimation

The normalized load estimation in any cell is obtained as the ratio between the active load in the cell and the overall cell load capacity as described by the following equation

$$L_{normalized} = \frac{L_{active}}{L_{capacity}} \tag{4.2}$$

L_{active} is the active load in the cell and can be directly obtained by the sum of average service rate associated to each user while $L_{capacity}$ is the actual capacity of cell taking into account the radio propagation conditions.

Load estimation in HSDPA

Due to the HSDPA characteristics, i.e., constant power transmission and link adaptation based on adaptive modulation and coding, the load is estimated based on the resources available for the cell, and actually consumed by user connections. The normalized load in HSDPA is estimated as follows

$$L_{normalized}(i) = \frac{\sum_{n=1}^{N} Load\,(n)}{R_{HSDPA}} \tag{4.3}$$

where N is the number of HSDPA user, R_{HSDPA} is the number of High Speed Physical Downlink Shared Channel (HS-PDSCH) [94] allocated in the cell, and $Load(n)$ is the average number of

TABLE 4.1: Transport block size and bit rate associated to CQI

CQI	**Modulation**	**Transport Block size (bits)**	**Number of HS-PDSCH**	***R*(CQI) [kb/s]**
CQI5	QPSK	377	1	188.5
CQI8	QPSK	792	2	396.0
CQI15	QPSK	3319	5	1659.5
CQI22	16-QAM	7168	5	3584.0

HS-PDSCH required by user n to support its service rate, $R(n)$. This number is given by the following equation

$$Load\,(n) = \frac{R\,(n)}{R(CQI_n) \cdot N_{HS-PDSCH}\,(CQI_n)} \tag{4.4}$$

where the average propagation condition determines the channel quality indicator ID, CQI_n, $R(CQI_n)$ is the achieved bit rate when one CQI_n block is allocated in every frame and $N_{HS-PDSCH}(CQI_n)$ is the number of HS-PDSCH associated to CQI_n as defined in[94]. Table 4.1 presents the transport block size and the bit rate associated to each CQI.

Load estimation in WiFi

For the WiFi system, the standard considered was the IEEE 802.11e [20], [40]. The normalized load associated to the AP should be estimated also based on the available system and cell resources. Furthermore, in the intermediate phase, an amount of bandwidth is determined in the system (one AP and several nodes). This bandwidth is shared among nodes according to the service bandwidth. It should be noticed, however, that the errors in the packet transmission occur when there are collisions, since the IEEE 802.11e EDCA mode of the MAC protocol was completely implemented in the simulator [34]. The normalized load for the WiFi system in optimum conditions is given by:

$$
\begin{aligned}
&L_{normalizedWiFi} = \\
&\sum_{n=1}^{4}\left(\begin{array}{l} frame\_duration\,[payload\_RTS, R_{MCS}(n)]\cdot 2+ \\ frame\_duration\,[payload\_RES, R_{MCS}(n)]\cdot 3+ \\ frame\_duration\,[payload\_BK/3, R_{MCS}(n)]\cdot 3+ \\ \frac{DIFS+6\cdot SIFS}{\text{inter}arrival\_time_{BK}[s]} \end{array}\right)+ \\
&\sum_{n=1}^{4}\left(\begin{array}{l} frame\_duration\,[payload\_RES, R_{MCS}(n)] \\ +frame\_duration\,[payload\_VO, R_{MCS}(n)]+DIFS+SIFS \\ \hline \text{inter}arrival\_time_{VO}[s] \end{array}\cdot 2\right) \\
&+\sum_{n=1}^{N}\left(\begin{array}{l} frame\_duration\,[payload\_RES, R_{MCS}(n)] \\ +frame\_duration\,[payload\_VI, R_{MCS}(n)]+DIFS+SIFS \\ \hline \text{inter}arrival\_time_{VI}[s] \end{array}\right)
\end{aligned}
\tag{4.5}
$$

where N is the number of WiFi user, and $R_{MCS}(n)$ is the rate for the modulation and coding scheme available for user n (of the WiFi AP). SIFS is the Short interframe space, DIFS is the Distributed Coordination Function Interframe Space. *Frame_duration* returns the frame duration having as an input the payload and $R_{MCS}(n)$, adding the physical layer headers transmission (TX) time. *payload_VO, payload_VI, payload_BK, payload_RES, payload_RTS,* are the payload of the voice, video, background, acknowledgement and RTS packets. The other terms are self explanatory. This equation accounts for the four background users, the four voice users, and the N video users. These classes of traffic have different characteristics regarding packets payload and inter-arrival time, Table 4.3.

Voice (VO) and NRTV packets do not require "request to send/clear to send" (RTS/CTS) negotiation as it depends on the packet payload. Besides, no fragmentation is required; only an ACK. Background (BK) packets, in turn, require an acknowledgement, as they have a high payload, and RTS/CTS negotiation and fragmentation has to occur. Through the use of fragmentation, a packet is divided into three packets, for each fragment, an acknowledgement is required. The MAC and PHY parameters used for WiFi simulation are available in Table 4.3. *CWmin* and *CWmax* stand for minimum and maximum contention window value, respectively.

TABLE 4.2: WiFi traffic parameters [2]

AC	**Voice (VO)**	**Background(BK)**
Packet size	1280 bit	18430 bit
Packet interarrival	20 ms	12.5 ms
Symmetry	Symmetric	Asymmetric (downlink)

TABLE 4.3: WiFi MAC and PHY parameters

Slot time	0.009 ms
ACK size	112 bit
SIFS	0.016 ms
DIFS	0.034 ms
RTS threshold	4000 bit
RTS size	160 bit
CTS size	112 bit
CWmin	31 slots
CWmax	1280 slots
Collisions threshold	8
Fragmentation threshold	8192 bit

Positioning enhancements

It has been shown by [95], [96], [97] that positioning can be used to enhance communication protocol performance by including the spatial distribution of users and assets for communications (e.g., routing) and intersystem handover. An indispensable precondition to achieve integration of different networks is the possibility to allow for execution of handover between these systems. Positioning has also been applied to enhance cooperative relaying techniques [98]. A scheme is presented where each relay, assuming knowledge of its own location information, could assess its proximity toward source and destination and based on that proximity; contend for the channel with the rest of the relays.

In this work, in order to explore the possible enhancements, we propose the use of positioning together with the RAT selection for CRRM proposed in [91].

4.1.3 Numerical results

Simulation scenario and models

The scenario assumes an HSDPA network overlaid by WiFi hotspots assuming high-priority NRTV video traffic at 64 kb/s characterized by the 3GPP model [99]. The generation of NRTV calls is modeled by a Poisson distribution while the call duration is exponentially distributed

TABLE 4.4: HSDPA and WiFi simulation parameters.

Parameter	HSDPA	WiFi
Mode	FDD (Tx mode)	EDCA (MAC Tx mode)
CRRM Algorithm load threshold	0.6	0.53
Scheduler	MaxCI	Round-Robin
Link Adaptation	BLER 10 %	-
Radio propagation model	3GPP indoor + FF	ITU 2GHz propagation (PathLoss)
Cell type	Omnidirectional	Omnidirectional
Number HS-PDSCH (data codes)	15	-
Connection data rate	-	Variable with the user SINR

with average 180 s. The specifications of the HSDPA and WiFi simulators are given in [100] and [34], respectively. The simulation parameters are presented in Table 4.4. Users are distributed uniformly over the HSDPA cell area, which is larger than the WiFi coverage zone. In the best case scenario WiFi covers 50 % (50m of HSDPA cell radius) of HSDPA area, and in the worst case scenario around 13 % (100m cell radius). It is assumed that initially NRTV users prefer to use HSDPA, but after the given HSDPA load threshold is exceeded, the user will become more suited to connect to the WiFi access, depending on whether it lies within the coverage area of WiFi. Furthermore, the scenario considers 11 initial users in WiFi.

Evaluation metrics

The implementation of the proposed CRRM algorithm uses in each decision time instant, i.e., when a new session is requested, a measure of the load from each system. The output from the CRRM decision block is the target Node B (or AP) to which the new device should be attached. In order to evaluate the efficiency of the proposed load-balancing algorithm, performance evaluation metrics, e.g., the throughput are considered for the communication within the cell:

- Over the Air throughput (*OTA_thr*) - *OTA_thr* is proportional to the number of bits that have been transmitted by the given cell, b_{OTA}, in a given period p=kT, where k is the number of Time Transmission Intervals (TTIs) and T the size of the TTIs. To obtain $OTA\_thr_{[b \cdot s^{-1}]}$ one divides b_{OTA}, in a given period p with similar conditions regarding load, by k times T:

$$OTA\_thr_{[b \cdot s^{-1}]} = \frac{b_{OTA}(p)}{k \cdot T} \tag{4.6}$$

- Service throughput/goodput (*Serv_thr*) - the ratio between number of bits that have been transmitted and correctly received in the cell without packet errors, b_{serv}, and the duration

of k TTIs, and is obtained by:

$$Serv\_thr_{[b \cdot s^{-1}]} = \frac{b_{serv}(p)}{k \cdot T} \tag{4.7}$$

- QoS throughput/goodput (*QoS_thr*) - the ratio between the number of bits correctly received without packet errors within the allowed delay, b_{QoS}, and the duration of k TTIs, and is obtained by:

$$QoS\_thr_{[b \cdot s^{-1}]} = \frac{b_{QoS}(p)}{k \cdot T} \tag{4.8}$$

- Packet delay - the amount of time since a packet is generated up to the time it is correctly received. The maximum allowed delay is 300ms for NRTV, 10000ms for BK, and 30ms for VO.

- Dropped calls - calls that are dropped due to bad positioning information.

T is the transmit time interval, k is the number of steps in a period p, while b_{OTA}, b_{serv}, and b_{QoS} are the number of bits that have been transmitted, correctly received, and correctly received within the allowed delay in the simulation during period p, respectively.

Simulation results

The 95 % confidence interval is represented in the curves by the vertical bars. The x axis always accounts for the total number of users taking into account both systems.

One found that the most appropriate load thresholds, presented in Table IV are LTh_0=0.6 for HSDPA (RAT 0) and LTh_1 =0.53 for WiFi (RAT 1). These values were obtained by verifying when the QoS starts to decrease in each system. Figure E.1 presents results for LTh_0 =0.6 and LTh_0 =0.7. The values 0.7 and 0.8 are presented in the the Appendix E for LTh_0 resulted in users exceeding their QoS delay threshold, i.e., 300 ms. Results are only presented for a load higher than 31 users in the system because it is closer to the point of overload of the HSDPA system.

Figure E.2 presents the HSDPA throughput *vs.* users in the absence of CRRM for an HSDPA cell radius of 50 m. For 75 and 100m are presented in Appendix E. The results show typical performance and baseline trends for *OTA_thr*, service and QoS throughput. Moreover, it can be seen that in this scenario the QoS throughput starts to decrease after 37 users in the system (11 in WiFi and 26 in HSDPA). At this point, the system start to become overloaded, and QoS throughput is mainly lost due to longer packet delays and erroneous packets due to users at the

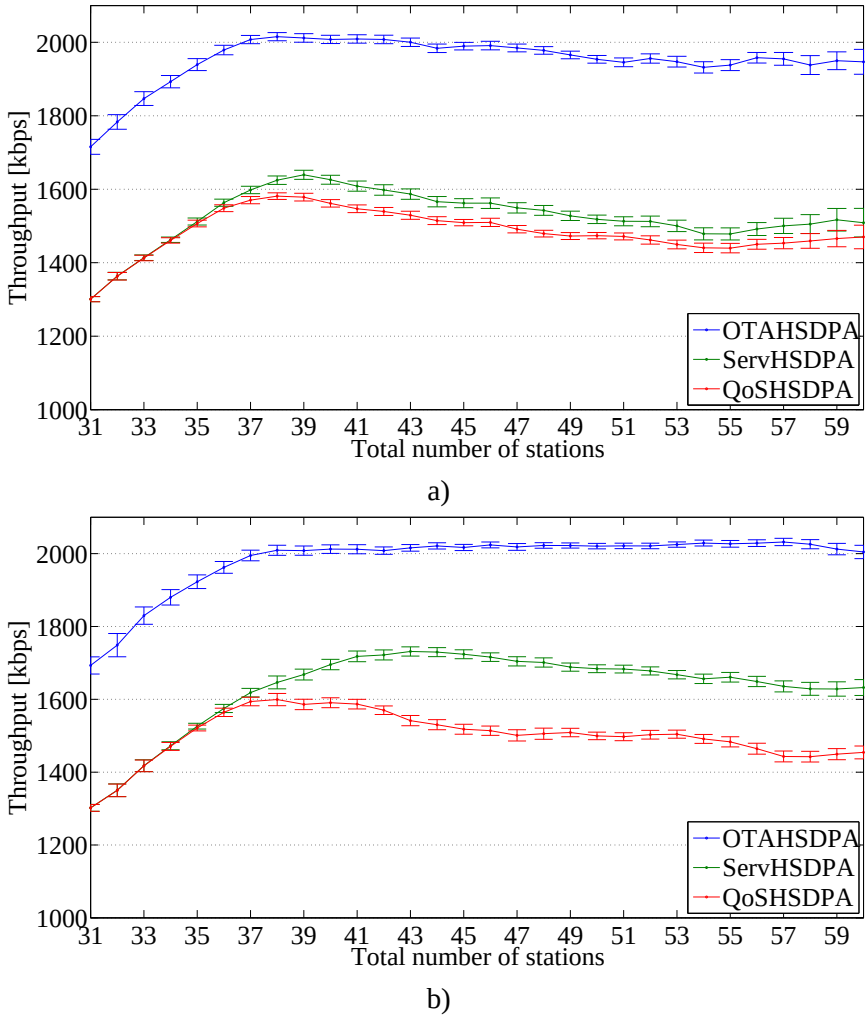

FIGURE 4.3: Throughput in HSDPA with CRRM entity exploring the diversity gain for a radius equal to 50 m, a) for load thresholds equal to 0.6, and b) for load thresholds equal to 0.7.

cell edge. For 60 active users (11 in WiFi and 49 in HSDPA), (64 kb/s·49users-1300 kb/s)/64 kb/s≈ 28 users (approximately 57 %) are unsatisfied.

The absence of localization (or positioning) information in the CRRM entity limits the performance of the cooperative systems since users that are potentially more suited for WiFi are switched and then dropped since they fall outside the coverage area of WiFi. The use of positioning information facilitates the decision since the vertical handover will only occur when the users fall within the area of the WiFi cell coverage. Indeed, Figure 4.5 presents the rate: dropped calls/number of session start attempt without localization data for HSDPA radii equal to 50, 75, and 100 m. These low values of cell radii are the ones for HSDPA micro-cells, e.g., the typical ones in micro-cellular offices environments.

As the HSDPA radius (scenario radius) increases there is a higher likelihood of users to be

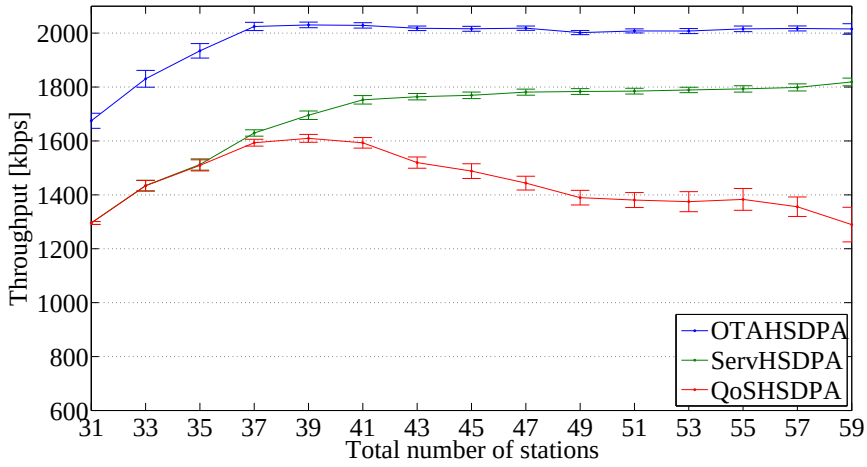

FIGURE 4.4: HSDPA throughput vs. number of users without CRRM entity.

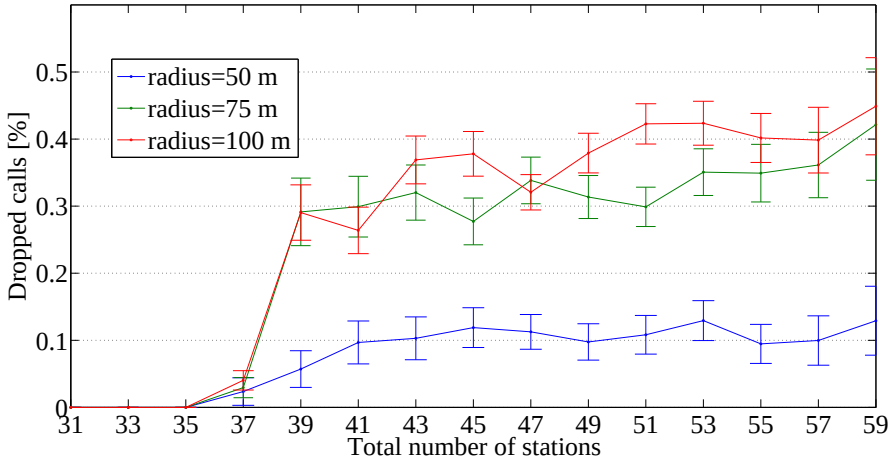

FIGURE 4.5: Accumulated dropped sessions vs. users.

located outside the WiFi coverage zone as the WiFi coverage area is fixed. Consequently, their sessions may be dropped. When localization information is used this effect is reduced. As the cell radius increases the probability of vertical handover dropping also increases, for 59 active NRTV sessions, we obtain 12, 41 and 44 % of dropped calls for 50, 75 and 100m HSDPA cell radii, respectively.

Figure 4.6 presents the results for the NRTV QoS goodput *vs* users. The performance range is bounded by the NRTV offered load and stand alone HSDPA baseline performance for a cell radius of 50 m, the latter being the worst case scenario. In the first instance, the benefits of CRRM based on suitability (without localization) compared to the HSDPA standalone scenario are shown. It leads to vastly improved QoS throughput. More specifically, without localization, as we increase the cell radius, and thus decrease the area of overlap between the cooperative

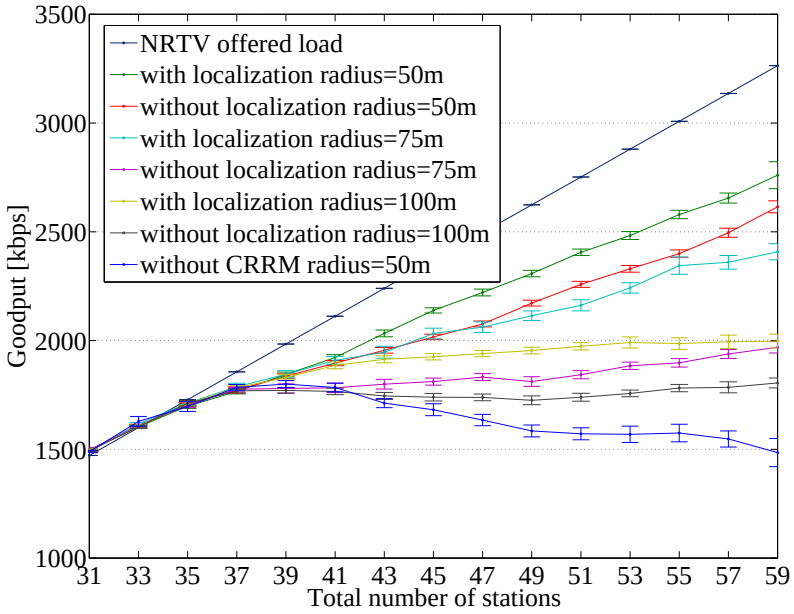

FIGURE 4.6: Throughput results vs. number of user for several values of the cell radius (with and without the use of localization information).

systems (for cell radii of 50, 75, 100 m), the goodput is reduced by an amount up to 700 kb/s for 53 users.

Foremost, it can be seen that there is a significant gain from using localization information in RAT selection. Comparing the simulation scenarios “with and without localization” for HSDPA cell radii of 50, 75 and 100 m, it can be seen in Figure 4.6 that localization can provide a marginal gain of up to 200, 450 and 200 kb/s, respectively. This simple inclusion of the use of positioning information on top of CRRM RAT selection may therefore lead to a clear improvement in system performance by means of the increase in the supported throughput in highly loaded operation conditions.

4.1.4 Summary and conclusions

This Section addresses the impact of positioning information for enhanced RAT selection. We consider a CRRM entity that acts as the cooperative platform between HSDPA rel. 6 and the WiFi/IEEE 802.11e standard. This entity has full knowledge of the load in both systems and perfect knowledge of all user positions within the simulation grid. It is able to trigger handovers between systems and redirect traffic through HSDPA or WiFi according to system suitability criteria based on traffic type and positioning information. Simulation results have shown that,

for high system loads, exploiting localization can provide a marginal gain of up to 450 kb/s goodput.

4.2 Spectrum aggregation

4.2.1 Overview

A key challenge for IMT-A infrastructures is the ability to operate in the preferred frequency bands, as announced in WRC-07 [101], while maximising network performance and maintaining intra-systems compatibility. The current problem of spectrum fragmentation requires a different approach to enabling the bandwidth required by IMT-A systems. Spectrum and Carrier Aggregation are two enabling techniques proposed for Long LTE-A [5] and IMT-A [4], [3] for achieving the advanced technical requirements identified for those systems. The physical layer aspects of LTE-A have been captured in [102], [103], [104].

SA consists in aggregating several (and possibly) fragmented bands. The concept of spectrum aggregation consists of exploiting multiple, small spectrum fragments simultaneously (aggregation) to yield to a (virtual) single larger band and ultimately deliver a wider band service (i.e., not otherwise achievable when using a single spectrum fragment. Further, SA allows that new high data rate wireless communication systems can coexist while reusing the spectrum of legacy systems.

There are two possible scenarios for SA: aggregation of contiguous bands and aggregation of non-contiguous bands. The non-contiguous approach may provide larger flexibility as well as diversity but on the other hand is more difficult to achieve in integrated devices.

The possibility to benefit from SA increases the freedom and the complexity in the RRM strategy. Some of the key features of LTE-A, Release 9, is the simple protocol architecture and moving the network intelligence down to the BS level [102]. The added functionalities should enable the mobile operators to provide services in a more effective manner, as well as to improve the Quality of Experience (QoE). The proposed shared channel gives instantaneous access to high rate, the envisioned scheduler exploits the channel in time and frequency, and there would be a very high number of "always-on" users.

SA requires modifications, both, at the MS side, namely, in the transceiver, and at the network side. For example, it has been proposed for LTE-A and IMT-A, that the BSs have the capability

to autonomously manage the radio resource allocation. This requires that novel approaches to benefit from the SA feature must be defined. As a result, SA could be investigated at least from these two perspectives: at the lower layer to solve implementation issues and at the upper layers to derive advanced resource management schemes to fully benefit from SA.

There are several SA studies that have been described in the literature [105], [106], [107] and [108]. The modelling and simulation aspects of SA in the context of LTE-A have been addressed in [105], including different scheduling strategies. A summary of the Carrier Aggregation (CA) types and the technical challenges in terms of various LTE-A system functionalities, such as control signalling, handover control, guard band settings, can be found in [106]. In [107] the authors analyse in more details the load balancing aspects and related scheduling solutions under various traffic conditions in a LTE-A system utilizing CA. The work in [108] further extends the studies in [107] by addressing the feedback schemes needed for channel aware scheduling over multiple component carriers. The studies in [103] and [104] are the main baseline for the L1-L2 radio resource management.

The best choice of a frequency band for a mobile communications system depends on many different factors. Once the spectrum has been obtained, there is still the remaining problem of managing the shared band, which implies proper allocation mechanisms for allocating users based on the specific user requirements and radio channel quality. In general, the lower frequency bands are better suited to longer range, higher mobility, lower capacity systems, while higher frequency bands are better suited to shorter range, lower mobility, and higher capacity systems. Therefore, for any given network the optimum frequency would vary depending on the required range, mobility and capacity [109].

The scheduling of users over multiple frequency bands can be modelled in its most general form as a GMBS problem [110]. A multi-band scheduler to manage the balance between the data pipe and the obtained extra source of spectrum was proposed in [111]. When the bandwidth from the shared band becomes available, the scheduler must be capable of realizing such a change in the spectrum pipe and shift some of the traffic load from the dedicated band to the shared band or vice versa. The scheduler must also be capable of further load balancing by actively monitoring the forthcoming changes in the spectrum and traffic data in order to shift the load from the shared band to dedicated one and vice- versa, if so required.

In LTE, LTE-A and IMT-A, a key feature of the RAN architecture is the CRRM entity in charge of distributing resources for inter- and intra-system radio resource management purposes. In

this way, the CRRM is the entity enabling the successful cooperation of the above mentioned systems with legacy systems (e.g., WiMAX, UMTS, GSM).

This work investigates a non-contiguous SA from an upper layer point of view and proposes an iCRRM entity where CRRM and SA functionalities are done together, performing the scheduling via the optimal solution of a GMBS problem. The employed Resource Allocation (RA) allocates the user packets to the available radio resources in order to satisfy the user requirements, and to ensure efficient packet transport to maximize spectral efficiency. The RA, an entity within the set of RRM algorithms, is envisioned to have an inherent tuning flexibility to maximise the spectral efficiency of the system for any type of traffic QoS requirements. The RA adopted here maps packets of variable size into variable length radio blocks for transmission over the PHY layer, and the length is dependent on the channel quality. The novelties of the approach compared to the current state-of-the art are that the proposed iCRRM enables the integration of spectrum and network resource management functionalities leading to higher performance and system capacity gains. The key to such integration is the pooling of the resources together; the integration allows for mapping of the service requirements onto an available spectrum amount and translates the latter into network load. The iCRRM uses the widely separated frequency bands for achieving lower delays and jitters and higher user throughput by exploiting the channel diversity [112]. These show independent Channel Quality Indicators (CQIs) over time and space, which becomes a source of diversity at the Physical (PHY) layer, with an important chance to achieve higher spectrum efficiency. Information from the network about the system state (e.g., received signal strength, transmitted power, MS velocity, etc) and used in RRM procedures such as load, admission and congestion control can successfully be combined with dynamic spectrum use and reduce the need of spectrum aggregation in some cases.

The integration of dynamic spectrum use and SA, achieved with the use of iCRRM techniques is shown to provide significant throughput gain compared to a system where the iCRRM is not used. A formulation is proposed for the average SINR that allows for setting the basic limits for the dependence of SA with multi-band scheduling on the coverage distance with an optimal solution.

4.2.2 Objective and system model

In the context of SA, there are two or more frequency bands available for the operator. A CRRM framework is proposed in this work which facilitates the best user allocation over a set of m

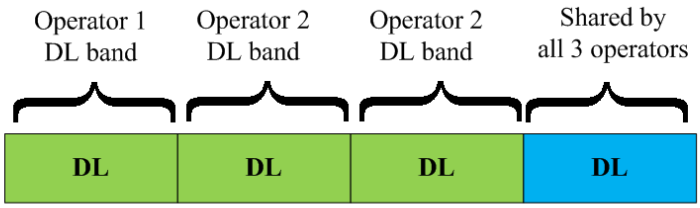

FIGURE 4.7: Scenario of common frequency pool [1].

frequency bands, $b \in \{1,2,\ldots m\}$. The objective is to maximise the total network throughput. Without loss of generality, two bands are considered ($m = 2$). The operator has exclusive access to the channels in the 2 GHz band and may access the shared frequency pool at 5 GHz.

The amount of radio resource available at 5 GHz is determined by spectrum trading (or bargaining) among all the operators that have access to the common frequency pool, Figure 4.7. Since spectrum sharing mechanisms are beyond the scope of this work, it is assumed here that the operator gains access to the frequency pool with a fixed portion of the available spectrum. Once a part of the spectrum has been obtained, the operator still faces the problem of allocating users on the available bands. Depending on the capabilities at the MSs, each user may be allocated to a single frequency band or simultaneously to both frequency bands. In the latter case, MSs need to have multi-radio transceivers; here, single-transceiver MSs are considered that enable the selection of one carrier at a time.

An HSDPA radio access network operating in the 2 GHz and 5 GHz bands is simulated in a context of multi-user allocation [113]. CRRM is adopted from [114], as shown in the simulation setup in Figure 4.8. It is responsible for allocating the available radio resources to the user traffic in a cost-effective manner, and includes a scheduling mechanism, link adaptation, code allocation policy, and an Hybrid Automatic Repeat Request (H-ARQ) scheme, to increase service throughput for users at the cell edge. In the considered scenario, inter-frequency handover between Wideband Code Division Multiple Access (WCDMA) carriers is possible, which is performed as in [115]. Besides all the common functionalities inherent to the CRRM entity, in this work it was given extra intelligence to the CRRM entity. By using an Integer Programming (IP) based algorithm, the inter-frequency handovers are performed in an optimised way, offering additional intelligence to the CRRM unit maximising system capacity.

The network is deployed with omnidirectional hexagonal cells and with frequency reuse pattern one. The results are presented only for the central cell. The session activity is modelled by the NRTV streaming traffic model from [99], with a service rate $S_{rate} = 64$ kb/s. The RRM includes

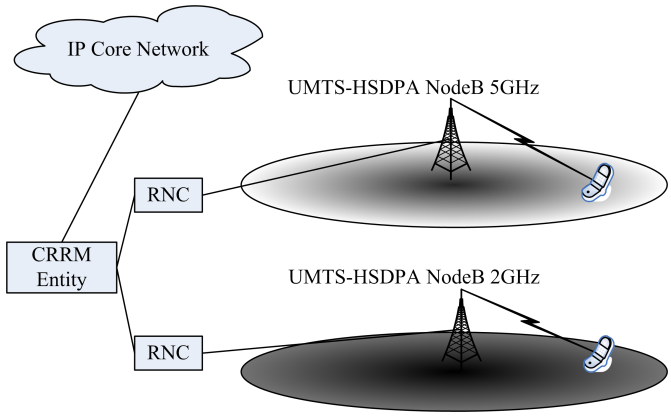

FIGURE 4.8: CRRM in the context of SA with two separated frequency bands.

TABLE 4.5: Parameters and Models used for 2 and 5 GHz bands

Carrier frequency	2 GHz	5 GHz
Bandwidth	5 MHz	5 MHz
Path loss model [dBW]	$128.1 + 37.6 \cdot \log(d_{[km]})$	$141.52 + 28 \cdot \log(d_{[km]})$
Shadowing de-correlation length	5 m	20 m

the following functionalities: Adaptive Modulation and Coding (AMC), *n*-parallel channel H-ARQ using chase combining and a Round Robin (RR) scheduling algorithm.

The radio channel follows the ITU radio propagation models, as summarised in Table 4.5. The channel loss between the MS and the BS is modelled by using a shadowing loss with log-normal distribution and by considering fast fading with Jakes model, as in [116]. The interference in the MS is calculated with the signal strength received from the first ring of neighbouring BSs and the thermal noise [117].

Each TTI is associated with a sub-frame duration, that corresponds to an HSDPA frame duration of 2 ms, with three time slots of 0.67 ms. The available data rates are summarised in Table 4.6. The CQI is a mapping of the averages of the CQIs recorded over time; a direct mapping between CQI_{bu} and the available rate at the physical layer, in kb/s, $R(CQI_{bu})$ is considered:

$$R(CQI_{bu}) = \begin{cases} 188.5 & \text{if } CQI_{bu} = 5 \\ 198.0 & \text{if } CQI_{bu} = 8 \\ 331.9 & \text{if } CQI_{bu} = 15 \\ 716.8 & \text{if } CQI_{bu} = 22 \end{cases} \tag{4.9}$$

where b is the band index ($b \in \{1,2\}$) and u is the user index ($u \in \{1,2,...,n\}$, n being the number of users).

TABLE 4.6: Transport block size and bit rate associated to CQI.

CQI	**Modulation**	**Transport Block size [bits]**	***R(CQI)* [kb/s]**
CQI 5	QPSK	377	188.5
CQI 8	QPSK	396	198.0
CQI 15	QPSK	663.8	331.9
CQI 22	16-QAM	1433.6	716.8

The RRM allocates the user packets to the available radio resources in order to satisfy the user requests, while ensuring efficient packet transport and maximising spectral efficiency. The RRM should have inherent tuning flexibility, to maximise the spectral efficiency of the system for any type of traffic QoS requirements. Depending on the radio channel quality, the CRRM maps data packets into variable length radio blocks, for transmission. The following events occur:

1. User packets awaiting transmission are prioritised according to the scheduling algorithm criteria;
2. A CQI identifier is selected according to the link adaptation algorithm, using the available CQI options from the physical layer;
3. An idle ARQ channel j is selected to hold and manage the ARQ transmission;
4. The packet is transmitted and received at the MS. Soft retransmissions are combined with previous packet transmissions (chase combining) and the ARQ messages are generated accordingly. These messages are then signalled to the BS, and the ARQ processes are released if the messages are positive ACKs.

Figure 4.9 illustrates the mechanism used to sense the CQI over the various frequency bands. The sensing is based on quality measurements of the Common Pilot Channel (CPICH) performed by the MS. In fact, the MS performs a prediction of the ratio between the received power and the received inter-cell interference. Several approaches may be followed.

The MS can be either in the active or passive mode. In the active mode, the user is continuously measuring the received CQI over both frequencies. In the passive mode, the measurements are periodically sent to the Radio Network Controller (RNC). The CQI measurements are communicated to the HSDPA RNC through the High-Speed Dedicated Physical Control Channel (HS-DPCCS). Although the active mode has the advantage of self-detection, allowing for an aggressive exploitation of radio channel capacity, the passive mode may be preferred

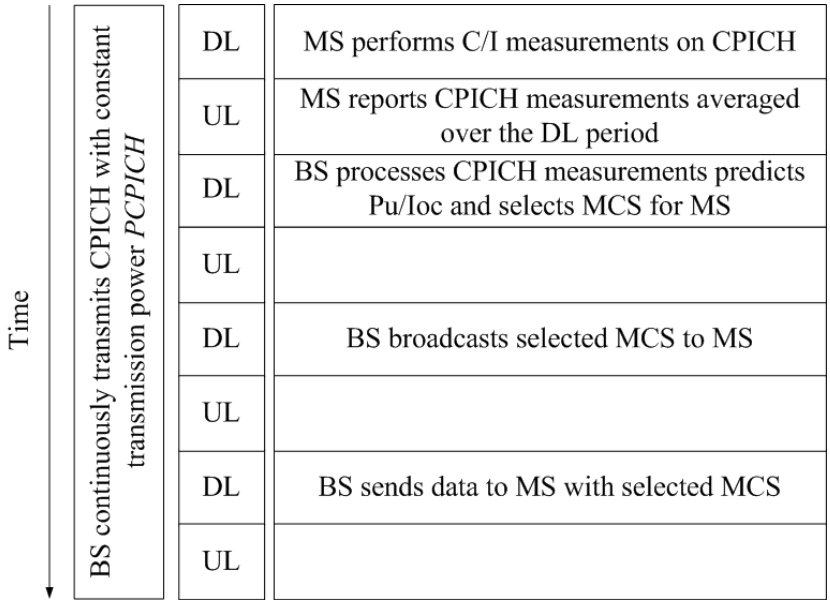

FIGURE 4.9: Channel Quality measurements and MCS selection cycle.

when the purpose is energy saving at the MS and reduced signalling overhead. If no transmission has been previously attempted in a given band, the best CQI is optimistically assumed. Instead, if a transmission has already occurred, the value for the CQI is calculated from the average of the last transmissions within a given period, i.e., moving average calculation.

4.2.3 General Multi-Band Scheduling

SA offers an added dimension for user scheduling and poses an optimization problem for the best network resource exploitation. The scheduling problem can be formulated as a General Assignment Problem [118]. In this specific scenario, the user allocation problem is referred to as GMBS. The proposed Profit Function (PF) maximises the total throughput of the operator via a single objective problem[1].

The GMBS problem can be solved with IP. The GMBS PF is defined considering the ratio between the rate available on a single Downlink (DL) channel and the requested rate by the service flow and is expressed as follows:

$$(PF) \quad \sum_{b=1}^{m} \sum_{u=1}^{n} W_{bu} x_{bu} \tag{4.10}$$

[1]However, multiple objectives can be easily introduced,as in [119], with a Multiple Objectives GAP (MO-GAP). Several objectives, such as fairness and QoE requirements, can be included via a linear combination, also referred to as "scalarization" [120].

where x_{bu} is the allocation variable and the normalised metric W_{bu} is given by:

$$W_{bu} = \frac{[1 - PER(CQI_{bu})] \cdot R(CQI_{bu})}{S_{rate}} \tag{4.11}$$

where S_{rate} is the NRTV service rate, $PER(CQI_{bu})$ is the average Packet Error Rate (PER) occurred in previous transmissions that the DL channel for user u on band b is suffering for the Modulation and Coding Scheme (MCS) supported (0 in the case no transmissions has ever occurred), and $R(CQI_{bu})$ is the DL channel throughput for user u on band b, as a function of the MCS supported.

The constraints for GMBS vary, depending on the ability of the MSs to simultaneously transmit and receive in multiple frequencies (multiple transceivers at the MS), or just over a single band at the time. HSDPA physical layer [121] provides a set of orthogonal codes available for data transmission within a sub-frame. Codes may be allocated to service flows/users[2] in a flexible manner. More than one code can be assigned to a single user or a single code can be assigned to more than one user. The users on the same code adopt a time-division multiple-access which is managed by the packet scheduler. The allocation variable x_{bu} reflects the code allocation per users and is either a boolean value in the case of single code allocation, or a positive integer, $x_{bu} \in \{0, \max(N_{codes})\}$, in the case of multi-code allocation.

An example of multi-code allocation is shown in Figure 4.10, where a RR packet scheduler is used in which all the users are satisfied within three TTIs. Two iterations of three TTIs are presented: user 1, allocated to band 1, has $x_{11} = 5$, while user 14, allocated to band 2, has $x_{214} = 3$.

In the following explanation, a single-frequency single-code allocation will be explored with a RR scheduler. The RR scheduler was selected since it is the one with least interference on upper layer algorithms[3].

In single-frequency single-code allocation, the GMBS presents the following constraints:

[2] Each user in the network is assumed to bear only one service flow. With this assumption, the terms service flow and user can be used interchangeably.

[3] For instance, in the case of a maximum C/I scheduler, the users with worst channel conditions would not have been served and the full extent of the proposed algorithm would not be thoroughly revealed.

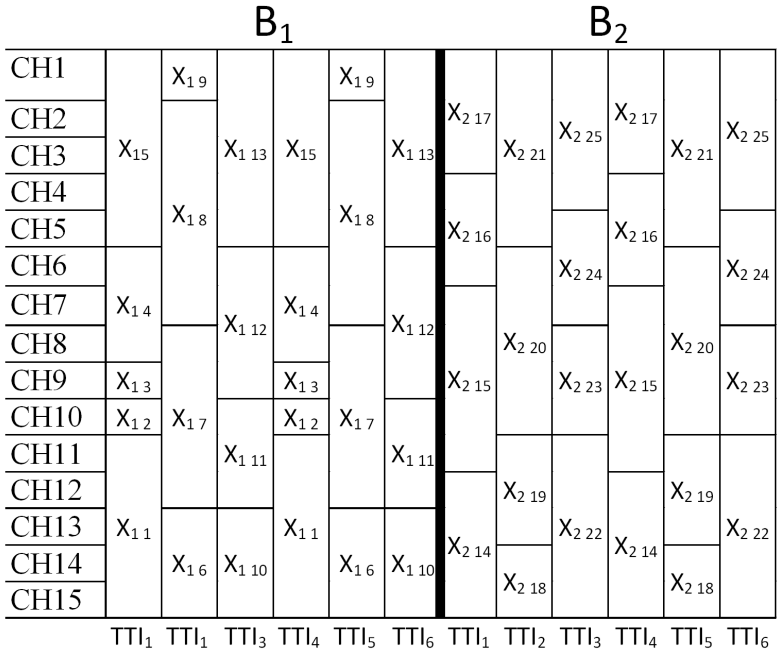

FIGURE 4.10: Allocation matrix example over two frequency bands.

1. Allocation Constraint (ACt): each user can be allocated only to a single frequency band with a single orthogonal code:

$$(ACt) \qquad \sum_{b=1}^{m} x_{bu} \leq 1, \qquad x_{bu} \in \{0,1\} \quad \forall u \in \{0,...,n\} \tag{4.12}$$

2. Bandwidth Constraint (BC): the total number of users on each band is upper bounded by the maximum normalised load that can be handled in the band, $L_b^{max} \in [0,1]$:

$$(BC) \qquad \sum_{u=1}^{n} \frac{S_{rate} \cdot (1 + R_{Tx} \cdot PER(CQI_{bu}))}{R(CQI_{bu}) \cdot N_{codes}} \cdot x_{bu} \leq L_b^{max} \quad \forall b \in \{1,\ldots,m\} \tag{4.13}$$

where the first term is the requested service data rate for user u, including the packet loss, normalized with the maximum data rate that the network can offer to the user u on band b which is $R(CQI_{bu}) \times N_{codes}$ where N_{codes} is the maximum number of parallel codes available in HSDPA. $R_{Tx} = 2$ is the number of H-ARQ retransmissions. BC accounts for the user traffic requirement, DL capacity and overhead caused by packets lost. The load constraint for each band, L_b^{max}, is lower than one because of the padding caused when the packets from upper layers are fragmented, to fit the MPDU and signalling overhead.

b \ u	1	2	3	...	n
1	1	0	1	...	0
2	0	1	0	...	0
3	0	0	0	...	0
⋮	⋮	⋮	⋮	...	⋮
m	0	0	0	....	0
↓	↓	↓	↓	↓	↓
$\sum_b x_{bu}$	1	1	1	1	1

FIGURE 4.11: Example of an allocation matrix X for single-frequency single-code GMBS.

Figure 4.11 presents one example, for a given case, for the allocation matrix $X = [x_{bu}]$, with $b = \{1,...,m\}$ and $u = \{1,...,n\}$. With two bands, $m = 2$ and $L^{max} = [L_1^{max}, L_2^{max}]^T$.

After several tests performed to find the best load threshold, a load factor of 75 % has been chosen. This value was found through extensive simulation. It is a parameter that should be tuned by the operator. To find an heuristic that outputs this parameter is out of the scope of this work.

4.2.4 Average SINR analysis with unitary frequency reuse pattern

The SA gain has been evaluated for several inter-cell distances with a frequency reuse pattern one. In order to have comparable results, SA needs to be analysed at constant average SINR. To obtain the average SINR, a method similar to the described in chapter 12 from [122] was applied. By tuning the BSs transmitter power, the average SINR was kept constant.

SINR at a given position

In general, given a BS transmitter power P_{Tx}, the MS SINR at a position (x,y) can be expressed as:

$$SINR(P_{Tx},x,y) = \frac{P_{ow}(P_{Tx},x,y)}{(1-\alpha)\cdot P_{ow}(P_{Tx},x,y) + P_{nh}(P_{Tx},x,y) + P_{noise}} \tag{4.14}$$

where P_{noise} is thermal noise power, α is the orthogonality level of the codes [123], P_{ow} is the power received from the own cell, and P_{nh} is the total amount of interfering power coming from the neighbour cells (6 cells in the case of hexagonal cell deployment).

At 2 GHz, P_{ow} can be expressed as:

$$P_{ow}(P_{Tx},x,y) = P_{Tx}G_{Tx}G_{Rx}10^{-\frac{128.1+37.6\cdot\log\sqrt{y^2+x^2}}{10}} \tag{4.15}$$

where G_{Tx} and G_{Rx} are the antenna gains.

P_{nh} is the interfering power received by a MS from the first ring of six neighbours cells, as illustrated in Figure 4.12. It is given by:

$$P_{nh}(P_{Tx},x,y) = \sum_{i=1}^{6} I_i(P_{Tx},x,y) \quad \text{with,} \quad I_1 = I_6,\ I_2 = I_5,\ I_3 = I_4 \tag{4.16}$$

where $I_i(P_{Tx},x,y) = P_{Tx}G_{Tx}G_{Rx}10^{-\frac{PL(x,y)^i}{10}}$ and the following functions for the path loss, PL, at 2 GHz band stand as:

$$\begin{aligned} PL(x,y)^{1,6} &= 128.1 + 37.6 \cdot \log\sqrt{(\tfrac{3}{2}R - x)^2 + \left(\tfrac{\sqrt{3}}{2}R\right)^2} \\ PL(x,y)^{2,5} &= 128.1 + 37.6 \cdot \log\sqrt{\left(\sqrt{3}R\right)^2 + x^2} \\ PL(x,y)^{3,4} &= 128.1 + 37.6 \cdot \log\sqrt{(\tfrac{3}{2}R + x)^2 + \left(\tfrac{\sqrt{3}}{2}R\right)^2} \end{aligned} \tag{4.17}$$

The geometry symmetries have been considered and I_i is the i^{th} cell interference.

Figure 4.13 shows the variation of the SINR as a function of the MS-BS distance, $d\,(0 \leq d \leq R)$. Results are presented for a cell radius of 300 and 1500 m.

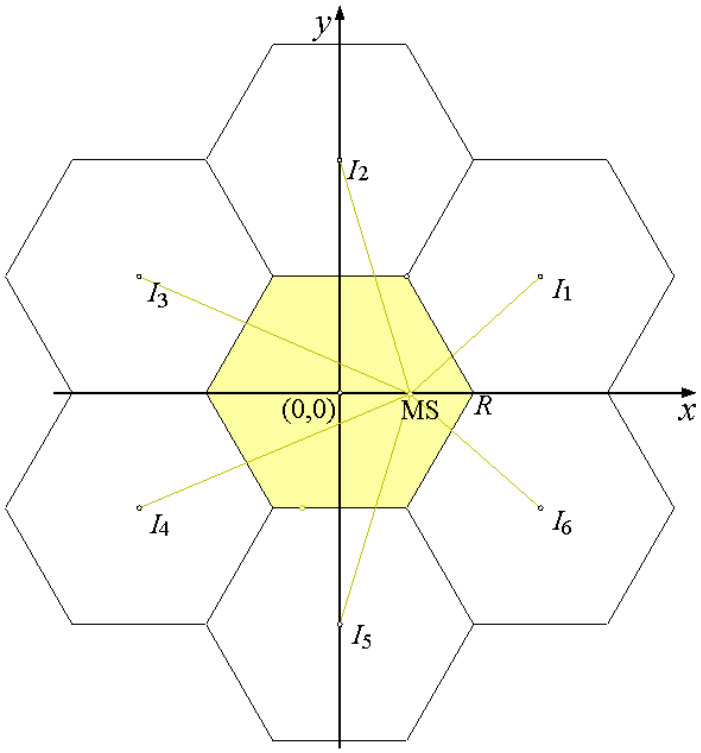

FIGURE 4.12: Simulation topology of the HSDPA networks.

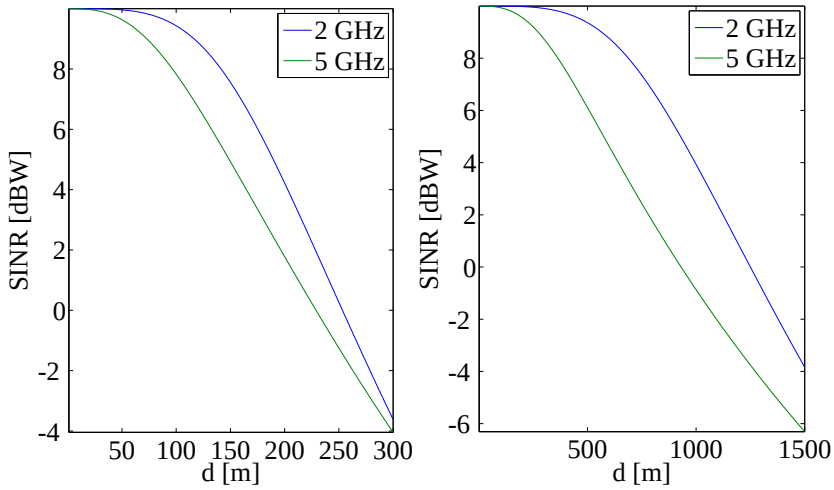

FIGURE 4.13: From left to right, SINR as a function of the MS-BS distance for two cell radii ($R \in \{300, 1500\}$ m) and P_{Tx}=1 dBW.

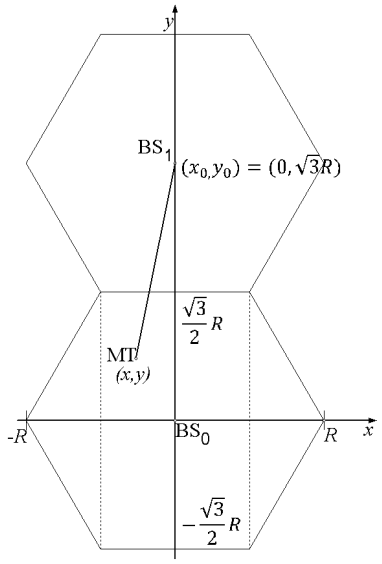

FIGURE 4.14: Interference received from neighbouring cells.

Average cell SINR

The average SINR within a cell is the SINR measured by a MS with uniform probability density function for its deployment over the cell area. It depends on the cell radius, R, and on the BS transmitter power, P_{Tx}, as follows:

$$\overline{SINR}(R, P_{Tx}) = \frac{\overline{P}_{ow}(R, P_{Tx})}{(1-\alpha)\overline{P}_{ow}(R, P_{Tx}) + \overline{P}_{nh}(R, P_{Tx}) + P_{noise}} \tag{4.18}$$

where $\overline{P}_{nh}(R, P_{Tx})$ is the average interference power from the six neighbouring cells. The average interference generated by a neighbour cell can be calculated by integrating each fraction of the interfering power over the area of the affected cell. Figure 4.14 shows one affected cell in the

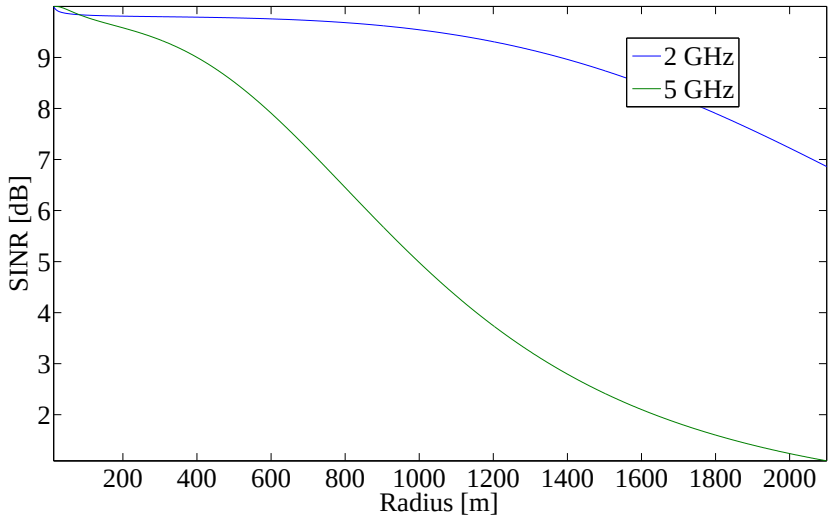

FIGURE 4.15: Average SINR [dB] as a function of the cell radius in meters.

origin of the coordinates and one interfering cell, at (x_0, y_0). By integrating over the hexagonal cell area, the average level of received power from a neighbour cell $\bar{I}$ may be calculated as:

$$\bar{I}(R, P_{Tx}) = \int_y \int_x f_I(P_{Tx}, x, y) dxdy = \int_y \int_x \frac{P_{Tx} G_{Tx} G_{Rx}}{A_{Cell}} PL(x, y) dxdy \tag{4.19}$$

where A_{Cell} is the total affected cell area. $\bar{P}_{nh}(R, P_{Tx}) = 6 \cdot \bar{I}(R, P_{Tx})$ as the surrounding interfering neighbours are all at the same distance, $\sqrt{3}R$. The variation of the average received interference with the cell radius is shown in Figure F.1, in the Appendix F. The details for the calculation of the average interference are also reported in the Apendix.

$\bar{P}_{ow}(R, P_{Tx})$ is the average signal power within a cell. It may be obtained following an approach similar to the used for the average interference calculation, with a different integrand function, f_p, which, due to the geometry of the problem, has a simpler expression. The following integrand function is reported for the 2 GHz channel model:

$$f_{P_{ow}}(P_{Tx}, x, y) = \frac{P_{Tx} G_{Tx} G_{Rx}}{A_{ow}} 10^{-\frac{128.1 + 37.6 \cdot \log\sqrt{y^2 + x^2}}{10}} \tag{4.20}$$

A detailed calculation is reported in the Appendix F and the results for the average power within the cell are shown in Figure F.1. The average SINR results are shown in Figure 4.15. The average SINR at 5 GHz band decreases faster after 300 m, as it suffers higher pathloss effect. After 2000 m, the network in the 5 GHz band starts to be noise-limited and the impact of interference is lower.

TABLE 4.7: Values for the normalized transmitter power P_{Tx,R_0} [dBW], for the 2 and 5 GHz bands.

Radius [m] / **Bands**	300	600	900	1200	1500	1800
2 GHz	-8.14	5.92	14.09	19.85	24.29	27.90
5 GHz	2.26	15.00	22.92	29.22	35.21	43.28

Transmitter Power Normalization Procedure

The goal of the Average SINR analysis is to determine a set of transmitting powers P_{Tx} in order to have a constant average SINR for all the cell radii. From (4.18), assuming the antenna gains are constant, the average SINR for a given radius, R_0, in the cell only depends on P_{Tx}.

In order to determine the values for the power that should be used at 2 and 5 GHz, we first found the transmitter power that corresponds to the maximum average SINR (with a difference lower than 0.01 dB to such a maximum) for R_0= 1800 m, P_{Tx,R_0}, in each of the frequency bands. Then, for $R \in \{300, 600, 900, 1200, 1500, 1800\}$, we found $P_{Tx,R}$ such that :

$$\overline{SINR}(R, P_{Tx}) = \overline{SINR}(R_0, P_{Tx,R_0}) \tag{4.21}$$

which provided the values for the transmitter power from Table 4.7, for the selected values of the cell radius. As these values for the power correspond to the maximum average SINR, the 5GHz band non-covered area was kept to the minimum, less than 0.88 % for $R \geq 600$ m and less than 1.08 % for $0 \leq R \leq 600$ m.

4.2.5 Results

The performance of the SA user allocation is assessed by using the total Service Throughput (ST) metric, which is the total number of bits that have been transmitted and correctly received by all the users in the cell:

$$\mathrm{ST}_{[bits/s]} = \frac{b_{serv}(p)}{k \cdot T} \tag{4.22}$$

where $b_{serv}(p)$ is the number of bits received in a given period p, T is the transmit time interval, and $k \cdot T$ is the total simulation time. Users are deployed on the cell with an uniform spatial distribution, within the cell radius R. Simulations were performed by considering the set of cell radii $R = \{300, 600, 900, 1200, 1500, 1800\}$ m, with overlapping 2 GHz and 5 GHz bands coverage, as shown in Figure 4.8. The NRTV calls are modelled by a Poisson distribution, and

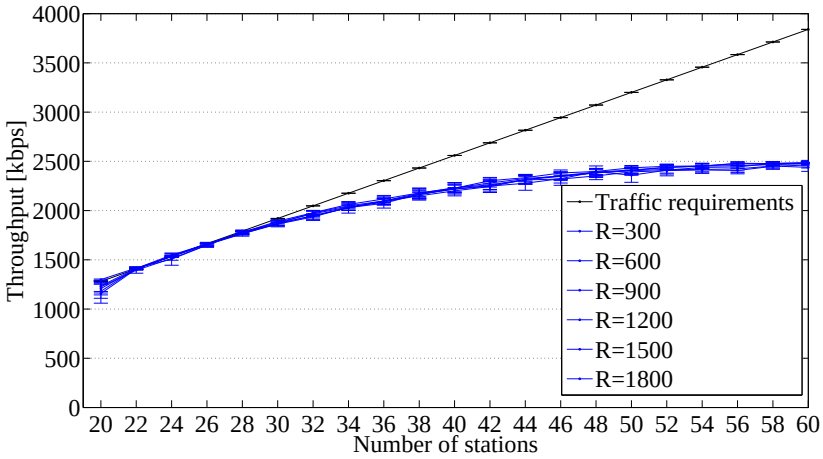

FIGURE 4.16: Average throughputs without the iCRRM.

the call duration is exponentially distributed with an average of 180 s. The 95 % confidence interval is represented in the curves by the vertical bars.

Figure 4.16 reports the total ST for a system without iCRRM, using the standard CRRM from [114]. In such system, each one of the two frequency bands are managed separately. NRTV session requests are expressly assigned to one of the two bands and it is not possible to switch a session from one band to the other. The results show approximately the same network capacity for variable cell radius. The ST reported in Figure 4.16 is the sum of the service throughput in both frequency bands, 2 and 5 GHz. The traffic requirement is the traffic needed to satisfy all the users (i.e., the NRTV required data rate, times the number of users in the system).

The system can achieve better performance if MSs are allowed to be switched between bands. Figure 4.17 shows the results in the presence of the iCRRM with the GMBS algorithm proposed in subsection 4.2.3, for several cell radii with normalized power. Due to the power normalization procedure, the performance of the iCRRM is almost constant for all the cell radii. In the saturation point which is located around 60 active MSs, for R=1500 m, the total throughput increases from 2430 kpbs to 3170 kpbs: a gain of 30 % compared to the absence of iCRRM. Figure 4.18 presents the throughput gain in percentage and the absolute gain as a function of the cell radius under a constant average SINR: the power normalization procedure proposed in the previous subsection allows for fair results comparison with variable cell radius. The almost constant gain demonstrates the potentiality of iCRRM over a wide range of cell coverage distances.

Figure 4.19 shows the load variation depending on the number of active MSs in the cell for both frequency bands and R=300, 900 and 1500 m. Since the path loss is lower at 2 GHz compared to the 5 GHz band, in the case of low cell load, the iCRRM entity will mainly allocate the MSs

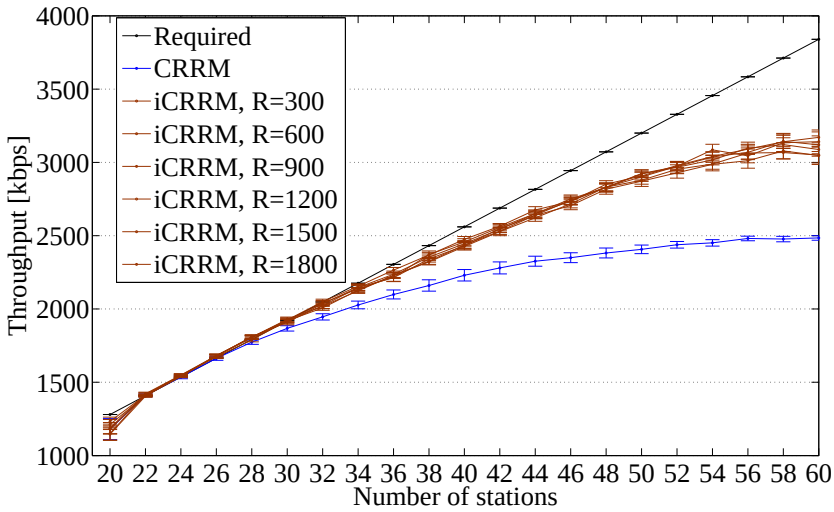

FIGURE 4.17: Average service throughput with the iCRRM with normalized power.

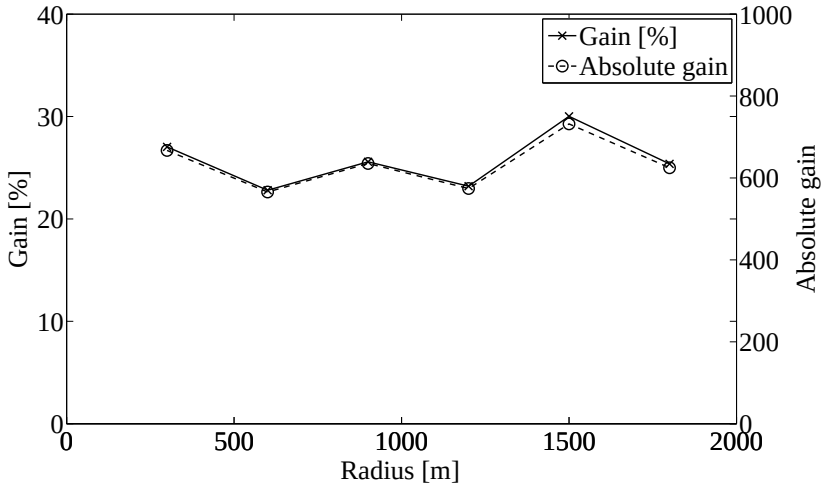

FIGURE 4.18: Gain between the presence of and the iCRRM and just a CRRM as a function of the cell radius for 60 users.

to the 2 GHz band. Furthermore, the load management interventions are not frequent, as it is evident in Figure 14 for the group of 20-29 users. As the load raises, the bandwidth constraint for the 2 GHz band becomes stringent and the iCRRM entity optimises the use of resources with more frequent MS switching between bands. Both bands have a higher throughput due to the switching of the user between the two bands, based on their respective channel qualities. When the system gets close to the load threshold level, both bands are equally populated with allocated MSs.

As the signalling overhead arising from SA may be an issue, it is worth analysing the number of frequency band exchanges that result from SA. Figure 4.20 presents the average number of exchanges, among simulations, as a function of the MS-BS distance with the number of active

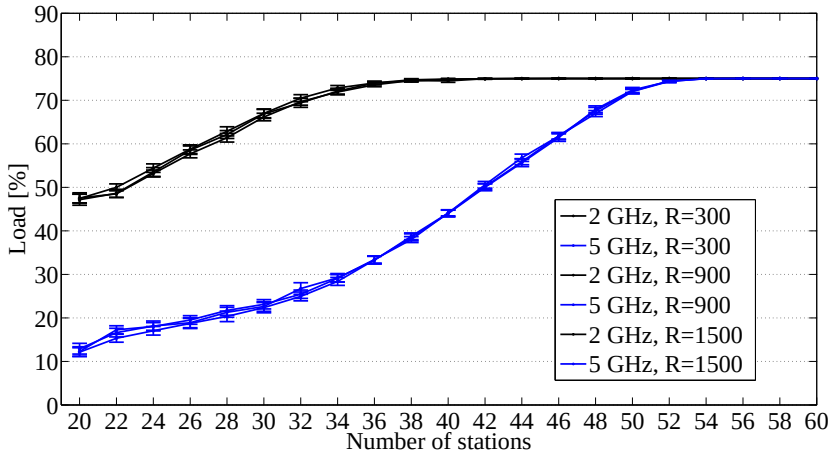

FIGURE 4.19: Variation of the load with the number of stations for both frequency bands and *R*=300, 900 and 1500 m.

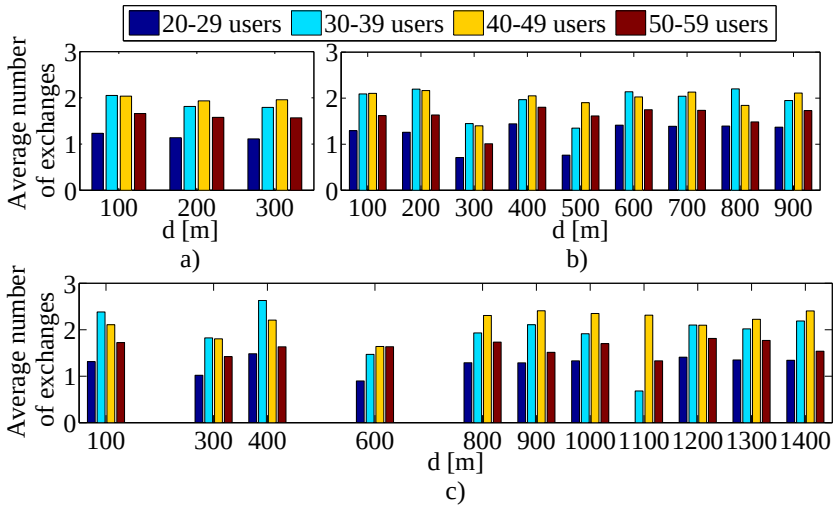

FIGURE 4.20: Exchanges between frequency bands for cell radius a) *R*=300, b) *R*=900 and c) *R*=1500 m .

MSs as parameter. The MS-BS distance varies up to the cell radius *R*. Values are presented in different charts for a cell radius of *R*=300, 900 and 1500 m. The number of the iCRRM interventions is higher for medium loaded systems and it is lower when the active MSs are in the range of 20-29 and 50-59. Furthermore, the number of MSs switched between bands grows with the cell radius.

The two input parameters to the GMBS problem were analysed in Figures 4.21 and 4.22. Figure 4.21 presents the percentage of users that use CQI15, one of the four MCSs available in the HSDPA system for *R*=300, 900, 1500 m. CQI15 is the one presented as it is dominant in the absence and presence of the iCRRM. However, when using iCRRM the set of MSs using CQI15 increases 20 %. This is directly related to the capacity gain plotted in Figure 4.17.

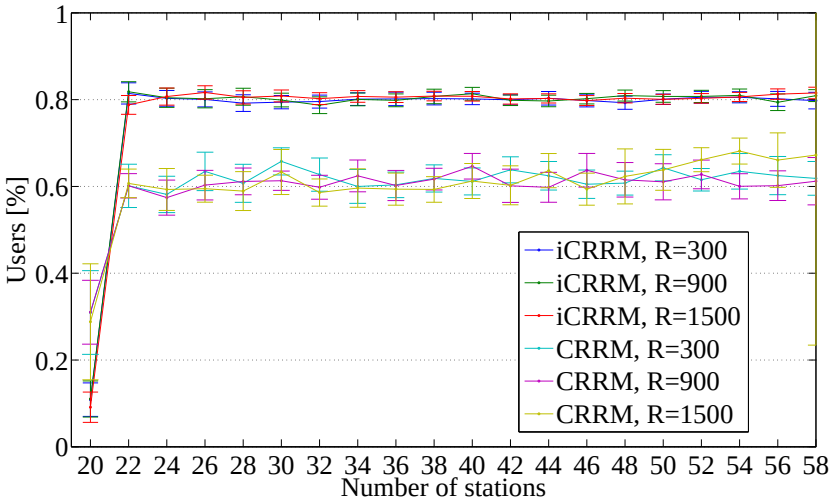

FIGURE 4.21: CQI15 usage for a cell radius *R*=300, 900 and 1500 m.

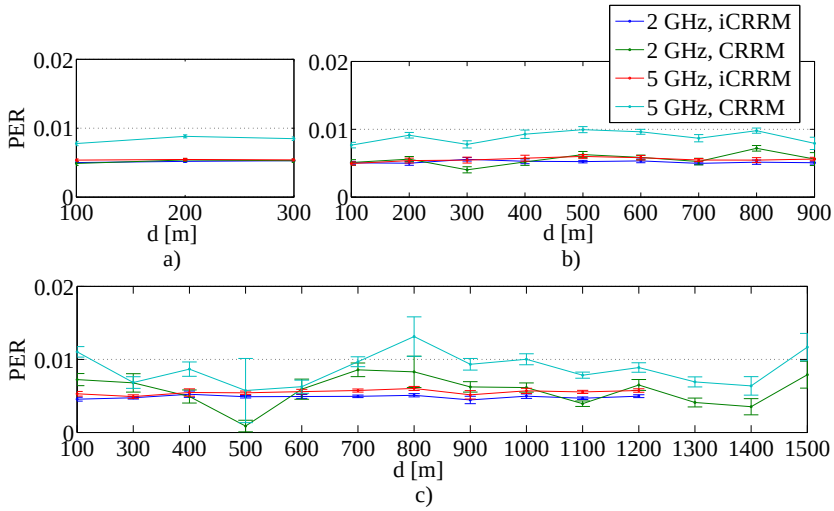

FIGURE 4.22: PER variation for a cell radius a) *R*=300, b) *R*=900 and c) *R*1500 m.

Figure 4.22 presents the average PER as a function of the MS-BS distance for three cell radii: *R*=300, 900 and 1500 m; the use of iCRRM shows a significant reduction of PER, especially for the 5 GHz band. For all the cell radii, the GMBS is able to reduce the PER from 0.01 to 0.005 via an accurate selection of the MSs to be moved between 2 and 5 GHz, based on their channel quality in each frequency band.

4.2.6 Summary and conclusions

This Section proposes an Integrated CRRM entity that has control over a pool of frequency resources. It assigns these resources to the active Mobile Stations with the solution of an

optimization problem with the objective of total Service Throughput maximization. The proposal is in the scope of currently on-going work within the ITU-R towards International Mobile Telecommunications-Advanced systems, and in particular the use of Spectrum Aggregation. The hypotheses of these work consider that Spectrum Aggregation can be successfully combined with Radio Resource Management techniques for an optimised performance.

In order to test the Integrated CRRM with several cell radii with comparable conditions, a formulation was developed that gives the average SINR in the cell considering frequency reuse pattern one. The transmitter powers were obtained for different cell radii in order to achieve a constant average SINR for variable cell radius and derive comparable results for iCRRM performance evaluation.

At the load saturation point, the iCRRM system has shown a gain of 23 up to 30 %, compared to a system where the allocated Mobile Station cannot be switched between bands and the system cannot opportunisticaly exploit the variable channel qualities of the Mobile Stations.

With Integrated CRRM, the intra-operator Spectrum Aggregation procedure is able to support a higher number of Near Real Time Video users, due to the ability of scheduling their traffic according to the radio channel quality in different parts of the radio spectrum. The achieved improvement is relative to scenarios where users are uniformly deployed on the cell.

Future work will analyse the impact of the spatial distribution of the users over the cell and the consideration of multi-service scenario. In this work, the General Multi-Band Scheduling Profit Function is based on the total throughput. Quality of Service requirements will be also included, in a scheduling problem with a linear combination of multiple objectives (scalarisation). A combined solution integrating the packet and the spectrum schedulers is foreseen to be able to greatly reduce the average delays and jitters, which are parameters of paramount importance for real-time services. Mobility patterns will also be analysed, showing the effectiveness of an Integrated CRRM to counter-fight shadowing in the support of the aforementioned real-time services and applications.

4.3 IEEE 802.11e ad hoc networking

It is worthwhile to address a network of wireless networks, consisting of a backbone infrastructure provided by HSDPA radio towers hierarchically bonded with a flexible wireless ad hoc

network running IEEE 802.11e standard. The purpose of this hybrid network is to serve users with high-quality video and audio content, using the already existing infrastructure. In the context of the WiFi network, the effects of changing the routing metrics in the service quality for an ad hoc network are studied, mostly the number of packets delivered and latency. This study manages to find the best approach, which is used to compute the paths for the hierarchical HSDPA/WiFi scenario that is being suggested and will be simulated in the future.

In this Section, we present several approaches to determine the best path for packets flowing in an IEEE 802.11e ad hoc network. Unlike the infrastructure mode, the IEEE 802.11e ad hoc mode does not use an entity responsible for managing the communications within the network. As so, the role of the AP is distributed by all the stations that are part of the network. Hence, it is up to each station which receives a packet to know to where it should be forwarded to. This is known as the routing problem, and its optimization is very important so that packets flow through the best path possible, enabling them to reach destination efficiently (meaning arriving safely and with a low delay). If the routing does not work efficiently, packets will start to get lost or taking longer paths and/or entering loops, which generates problems to the upper layers. There are several approaches that can be used in order to obtain the best path for the packets. In this work, all the stations have global knowledge of the network, meaning that they know all the connections that exist between the stations. This is done by impelling each station to perform a transmission in full power, and make all the others read the received SINR. This gives information not only about which neighbors each station has, but also what type of modulation and coding schemes can be used in each link. We use that information to compute the routing table for all stations, whose entries indicate the next hop for each destination.

In this study, we focus not on how the information about the links quality is spread across the network, but on the best way to, given a table of the connections between all the stations, determine which path the packets should take to arrive promptly at the destination. For this purpose, we address the optimization problem in two different ways: the empirical approach, and the Genetic Algorithm (GA) one. In the empirical approach, we manually define the cost functions for each link. In turn, GAs are an optimization approach that enables to reach the optimal solution without having to study the entire space of possible solutions.

All the results presented in this section were obtained by running the simulations in the custom-made IEEE 802.11e simulator from [9]. The details on the IEEE 802.11e standard are presented in Chapter 2. QoS support is achieved by mapping all packets into one of the four existing access

categories (VI, VO, BK, and BE), and unequally treating them according to this classification. This means that the MAC layer scheduling will give, for example, priority to a packet marked as video over another one marked as background.

4.3.1 Empirical approach

In our first approach, we manually assign a cost to each link. Then, Dijkstra's Algorithm (DA) [124] is run in a table containing the cost of all links, which allows for getting the least-cost path from each station to all the others. This information is inserted in the routing table which, for each pair source/destination, indicates the ID of the "next hop". For the first tests we wanted to verify how the signal strength in each link could be used to compute the best path. If a link has a strong signal, it is more robust to the outside interference, and it can use a modulation (and coding rate) that allows for transmitting at a higher data rate, allowing for faster transmissions, as shown in Table 4.8. However, strong signal can only be achieved if the stations are close to each other, which means that the overall progress of the packet towards the destination will be slower than if a longer link was used. Of course, the use of a longer link implies a lower data rate, and since the signal is weaker, more interference will exist.

TABLE 4.8: The relation between the SINR, modulation and data rate.

Mode	Modulation	Code rate	Min. SINR	Link throughput [Mb/s]
1	BPSK	1/2	4.1	6
2	BPSK	3/4	-	9
3	QPSK	1/2	7.9	12
4	QPSK	3/4	11.0	18
5	16-QAM	1/2	14.8	24
6	16-QAM	3/4	17.8	36
7	64-QAM	2/3	22.8	48
8	64-QAM	3/4	24.2	54

In order to define if the best approach was to use longer, robuster, or intermediary links, we proposed the following cost function:

$$cost = abs(data\_rate - setpoint) \tag{4.23}$$

The setpoints used are presented in Table 4.9. Three types of traffic sources were chosen. The traffic sources parameters are presented in Table 2.7, as well as the Access Categories (AC) of

TABLE 4.9: The setpoints in study.

Function	Setpoint [Mb/s]	Privileges
Alfa	$(data\_rate + 1)$	Paths with less hops/longer links
Beta	21	Intermediary links
Gama	30	Intermediary links
Delta	56	Robuster links

TABLE 4.10: Results for each cost function.

Function	Latency [ms]	Packets delivered	Packets delivered [%]
Alfa	6547	74	74/1500=0.049(3)
Beta	5675	197	197/1500=0.131(3)
Gama	5704	98	98/1500=0.065(3)
Delta	5361	282	282/1500=0.188

each type of traffic. Seven traffic streams were put in the scenario, one VI, three VO, and three BK streams. VI and BK traffic are unidirectional, while VO is bidirectional.

Simulations were run for a random deployment of 30 stations on a 150×150 m^2 field. The obtained results for a simulation time of 15 s are summarised in Table 4.10. These results are only for the video traffic that is being generated in station 3 and has station 10 as the destination.

From the results, one can conclude that the approach which privileges links with higher SINR allows to deliver more packets and with a lower latency.

4.3.2 Genetic Algorithms approach

In the second approach, we replaced the determination of the best path for the GAs approach. The challenges presented by GAs are the following ones:

Codification: the chromosomes are the paths. A chromosome is a vector of integers that represents the set of node IDs through which a packet has to go from the origin to the destination. The first locus of the chromosome is the origin while the last one is the destination. The ones in the middle have an order that the packet being transmitted needs to follow. For example, the chromosome [A N1 N2 B] establishes that a packet going from A to B has to go first to node N1, then to N2, and finally to B. The maximum size of the chromosomes is the maximum number of stations in the scenario.

Fitness metric: the fitness represents chromosome quality. it must reflect as precisely as possible the quality of a chromosome. In our case, the fitness value has some noise provided by

the randomization features of the simulator. To reduce this noise and not discard a good chromosome (or use a bad chromosome as a parent more often), we evaluate a chromosome with a given degree of freedom. In this work, the fitness value is provided by the number of packets delivered in a given period. However, we could have considered the delay or any other metric for the fitness parameter, and the algorithm would work the same way.

Population initialisation: an heuristic method in which the costs of the links in the DA follow an exponential distribution, was used.

Selection procedure: the selection procedure chooses the chromosomes to be parents of an offspring. The parents with best fitness will give the best offspring [125]. Therefore, if we want to increase the fitness while getting closer to the optimal solution, the chromosomes with higher fitness should have higher probability of being selected, i.e., the selection procedures focus on the exploitation of promising areas of the solution space. From the several tested the Rank Selection was the one that presented better results. It involves the following steps:

1. The chromosomes are ranked according to the fitness;
2. The top 1/4 of the chromosomes are selected;
3. To generate offspring, two chromosomes are selected randomly from the set found in step 2.

Crossover between genes: two chromosomes are two solutions for the problem. The crossover brings a new solution derived from them. In our case, the crossover is done by exchanging partial route of two chosen chromosomes (paths).

Mutations: a mutation is performed by randomly changing the genes in the chromosome. The mutation in our case is not a standard case since we cannot change a given locus randomly without any constraint; otherwise we could get a path without connection. Mutation is only possible if, when requested, there is an alternative path to the one being used from the locus over which the mutation was requested.

Results for the Rank/List and Tournament selection algorithms were obtained from three seconds simulations, and are presented in Figure 4.23 for the same topology as in the previous test. Several simulation runs were considered for the List selection (dashed lines) and for the Tournament selection (solid lines) algorithms.

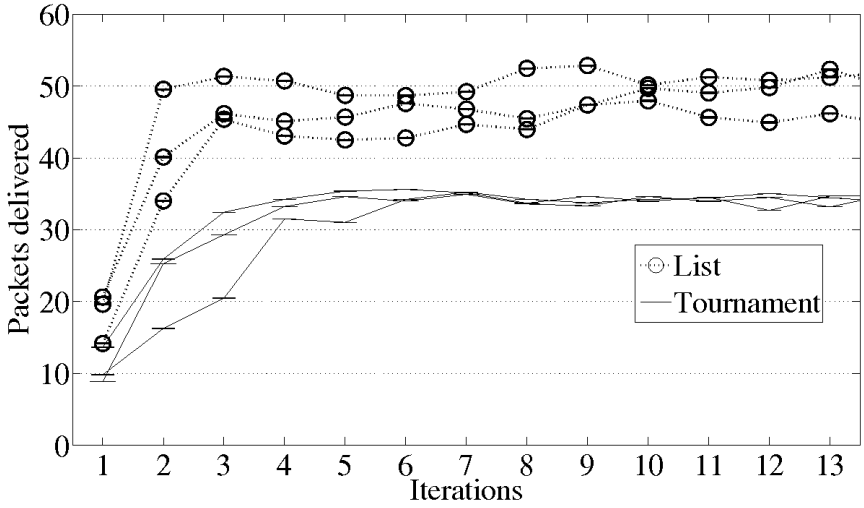

FIGURE 4.23: Packets delivered in topology 1 with the Tournament selection (solid lines) and List selection (dashed lines) algorithms.

It can be observed that the List selection algorithm presents better results than the Tournament selection algorithm, as it delivers more packets. The List selection algorithm also converges faster than the Tournament selection one. The List selection algorithm delivers approximately 16 % of the packets, but its performance is not as high as the Delta function from the empirical approach, which delivers 18.8 % of the packets (but it can be improved).

4.3.3 Conclusions and future work

The goal of the routing algorithms proposed in this Section was to find a path that delivers the highest number of packets in an IEEE 802.11e ad hoc network with the lowest delay. This optimization was tested for a single video stream whilst considering background and voice traffic streams, to increase the network load. A novel hybrid method to initialise the GA chromosomes was proposed. The simulations with the best initial population size (40) and the best selection algorithm (List/Rank) always converge to a single solution. In this case, the GA approach did not manage to reach better results than the best empirical one, but from our simulations in more random generated topologies in most of the cases GA outperformed the other approach. However, we are only presenting the initial results in this Section. As a future work, we intend to use the QoS feature of the simulator to attribute a different cost function to different traffic types. For example, a function that delivers more packets, but with larger delay, can be used for background traffic, while another with more packet drops, but with lower delay, can be used to compute the path for video traffic. In this case, the fitness function of GA could account for

more than the packets delivered like a weighted function that accounts for packets delivered and other metrics like jitter, and delay that will enhance the quality of experience of the users. More topologies will also be tested, to check which metrics are more suitable.

4.4 Challenges for hierarchical HSDPA/WiFi scenario

In our envisaged scenario we are looking for a way to provide the best service to the end user. One possibility for our scenario is depicted in Figure 4.24.

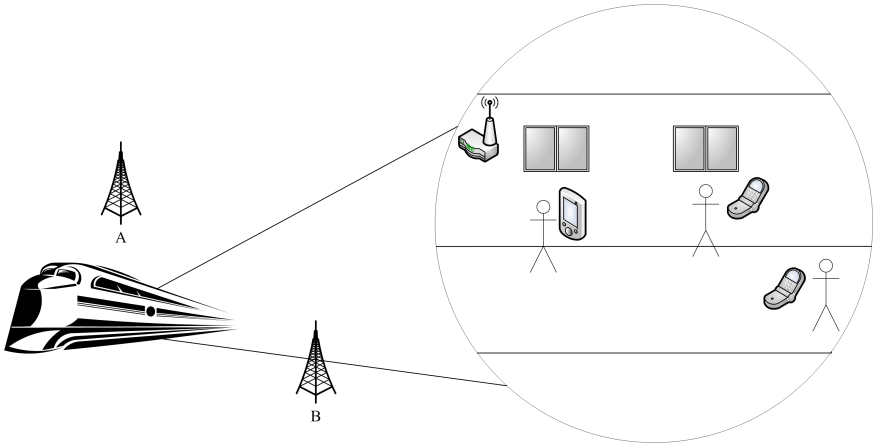

FIGURE 4.24: The scenario under study: users get access to services from a WiFi or an HSDPA connection, depending on which one is more suitable.

The user is requesting NRTV while moving on a public transportation service. This can be a bus moving inside the town, or a train in the suburbs. On the one hand, the mobility (which is higher in the train scenario) is presented as a great challenge, since it requires frequents handover as the user travels outside the area that was covered by the antenna he was connected to. On the other hand, the natural and man-made (e.g., buildings) obstacles interfere with the signal, also requiring a well planned handover strategy since a massive building can temporary block the connection between the user and his serving antenna. The service must be provided with QoS assurance, meaning that the video displayed on the user terminal must have enough quality (which include acceptable throughput and no service interruptions). For that purpose, it can be served by an HSDPA BS, or by a nearby WiFi hotspot, or even another user that is closer, depending on which can provide the (best) service. The train has an efficient outdoor receiver that can better receive the signal than any of the user terminals inside, and is connected to the WiFi hotspot in the coach. If the train is passing some problematic spots, e.g., very tall buildings or mountain area, the user terminal may start getting a lousy signal from the BS, and to ensure

the QoS it can be switched to the WiFi network. In this process, SA is applied to decide if the HSDPA backbone communications is performed either in the 2 GHz band and 5 GHz band whilst giving access to the users trough the IEEE 802.11e ad hoc network.

For users that are far from the wireless router, for example if they are in another coach, the connection can be made by using another terminal as a relay.

Nowadays, the technology allows mobile phones to have 3G, WiFi, and even WiMAX communications capabilities, all integrated into one equipment. As so, the availability of different technologies in the end user equipment is not an issue for our scenario. The true issue is how to decide to which technology should the terminal be connected to, and how to make the different RATs cooperate and not interfere. This is integrated in the larger challenge which is the routing one: the packets have to be routed through several hops, each one using its own technology, before arriving into the core network. We designate these routes as cognitive paths (CPs). The entity that controls the flow of information and define the CPs must have accurate and up-to-date information regarding all the users in the network, their connections quality and user requirements. This involves a good amount of information flowing to the routing coordination entity, and enough processing capacity required to it, in order to efficiently serve all the network. The algorithm that generates the CPs may involve complex calculations if the network has to serve a large number of users and several connection options. However, nowadays both software and hardware solutions are enough developed to materialise this scenario.

4.5 Conclusions

This Chapter addresses CRRM and SA that aims at providing the best service possible to a user requesting high quality and time dependent services, such as video or voice. In the considered scenario of interoperability, the core of the service access is provided by standard HSDPA BSs, whose coverage is improved indoor by using WiFi ad hoc connections. The WiFi network uses the IEEE 802.11e standard to prioritise the delay sensitive traffic. We provide isolated tests for each component of the system. First, the interoperability between two wireless technologies, HSDPA and WiFi, was studied. Since the operation is performed in different frequency bands, these technologies can co-exist without interfering with each other. From the tests run in our simulator, we demonstrated that the WiFi improves the coverage of the HSDPA without the need for a complex management system, providing a better service to the users. Simulation results

show that, for high system loads, exploiting localization can provide a marginal gain of up to 450 kb/s in the goodput. These results show that, for optimized decisions in such an environment, to utilize mobile positioning leads to enhanced system performance.

HSDPA was also studied in the context of cognitive radio, by considering two co-located BSs operating at different frequencies (in the 2 and 5 GHz bands) in the same cell. The system automatically chooses the frequency to serve each user with an optimal GMBS algorithm. It was shown that enabling the access to a secondary band may increase the throughput of the system, while serving more users. By using the proposed iCRRM, an almost constant gain near 30 % was obtained with the proposed optimal solution, compared to a system where users are first allocated in one of the two bands and later not able to handover between the bands.

In the WiFi ad hoc network, the goal was to find the path that delivered the highest number of packets and with the lowest delay. The optimization was tested for a video stream, whilst considering background and voice traffic streams to increase the network load. We first defined our cost functions manually, but ended-up by using an automatic optimization procedure in the form of GAs. Choosing the path that minimises the delay whilst maintaining the delivery ratio is very important to provide QoS to the user, and our optimal approach manages to reach these two objectives.

The main challenge for our cognitive radio scenario for public transportation is to discover and maintain the paths between the service provider and the end user, which we call the cognitive paths. We have shown that, isolated, each piece of the network can be optimised to provide the best performance possible, and we expect to use the optimization performed in the global management entity. The simulator to be used is being conceived and adapted for the tests, and we expect to obtain results soon.

Chapter 5

Conclusions and future research

The future wireless ecosystem will certainly be a heterogeneous network of networks, which integrates a number of overlapped Radio Access Technologies (RATs), such as High Speed Downlink Packet Access (HSDPA), Wireless Metropolitan Area Network (WMAN) and Wireless Local Area Network (WLAN), through a common platform. A major challenge arising from the heterogeneous network is the Radio Resource Management (RRM) strategy. Currently, RRM strategies are implemented independently in different kinds of RATs. Individually, these RRM strategies work well in the RATs that they are designed for. However, none of them is suitable for the heterogeneous network because each RRM only considers the peculiarities of one particular RAT. A common RRM module is needed instead in order to provide a step toward network convergence to hide this heterogeneity between operators and technologies.

The objectives of this thesis are two-fold. On the one hand, the optimization of a distributed WLAN is considered that provides multi-service with a given assured QoS whilst cooperating with HSDPA network whenever it is having difficulties to satisfy the traffic demand in a given area. The proposed suitability-based algorithm facilitates the interoperability between the two different RATs in an efficient manner. On the other, the addition of extra frequency spectrum bands and a so-called integrated Common Radio Resource Management (CRRM) that enables spectrum aggregation was addressed, through the integration of spectrum and network resource management functionalities. In this context, future cognitive radio scenarios where ad hoc modes will be essential for giving access to the mobile users have been proposed.

The QoS behaviour of the IEEE 802.11e medium access protocol has been investigated. By considering different access categories and user priorities, considerable enhancements can be

achieved in the network performance. While some modifications on the protocols are low impact ones (e.g., Block Acknowledgements), enhancements that have high impact implementation on the IEEE 802.11e standard in hardware (e.g., cross-layer design) but are able to ensure ameliorated QoS and increased system capacity.

A Common Radio Resource Management (CRRM) entity was proposed to manage communication resources, either from a different RAT or from a pool of spectrum resources. User terminals will be able to freely roam from the coverage area of one radio access technology to another one, thereby bringing benefits in terms of the experienced quality of service and user experience while optimizing network operation.

The developed IEEE 802.11e event driven simulator has been presented in Chapter 2. It is a tool that allows for tuning-up several parameters like the ones dealing with the use block acknowledgement, normal acknowledgement, and no acknowledgement policies. Policies have been tested that provide access to the medium, that ensure a given grade of service, based on the channel SINR, delays, and bit error rate. This C++ simulator was developed for many practical reasons since it allows avoiding interactions with the higher levels of the protocol stack and fully controlling and tracing the MAC protocol operations and performance figures. Its development allowed for creating a simulation framework which fully supports fragmentation [36]. Besides, our simulator also supports the ad hoc mode [37], which is not the case of the OMNet++ simulator [38]. This MAC layer simulator also facilitates to evaluate the service quality in IEEE 802.11e in order to enable simulations accounting for interoperate with HSDPA with QoS support. This interoperability is supported in the context of the IT-MOTION tool [39] whilst improving scheduling algorithms performance and CRRM techniques [18].

Chapter 3 addresses the optimization of IEEE 802.11e infrastructure and ad hoc mode.

In the infrastructure mode the optimization was done by:

- studying the effect that the buffer size has on the immediate Block Acknowledgement (BA) policy;
- doing cross layer design that uses the Physical Layer (PHY) and link layer information, together with the application layer to schedule users in the utilization of the medium.

BA policy decreases delays and ensures a stable system. Although, for lower values of the number of stations, the use of BA leads to a slightly worst system performance, the BA procedure

provides an improvement in highly loaded scenarios. The improvement, in single service scenario, is of 2 Mb/s and 2.2 Mb/s in average, for BK and VI traffic, respectively. In a scenario with mixture of services the most advised block size is 12 since it is the one that provides lower delays in a highly loaded scenario while the users are still within the capacity of the Access Point (AP). The number of supported users increases from 30 to 35. In Chapter 3, an algorithm was also proposed that uses cross layer design that changes the size of the Arbitration Interframe Space (AIFS) and the Contention Window (CW) length dynamically according to a periodically obtained fairness measure based on the SINR and transmission time, a delay constraint and the collision rate of a given machine. The proposed algorithm has showed improvements providing the highest goodput and lowest delays, whilst supporting more users than the standard with higher QoS. The throughput was increased in 2 Mb/s for all the values of the load that have been tested. It satisfies more users than the original standard while ensuring the appropriate grade of service. Although the delay for background traffic is never manageable into the IEEE 802.11e standard, for the values of the load that have been tested, with our algorithm, the background traffic only starts being delayed when more than 20 stations are in the scenario.

In the ad hoc mode an analytical model was developed that allows for investigating collision free communications in a distributed environment.

Chapter 4 addresses CRRM and SA that aims at providing the best service possible to a user requesting high quality and time dependent services, such as video or voice. In the considered scenario of interoperability, he core of the service access is provided by standard HSDPA BSs, whose coverage is improved indoor by using WiFi ad hoc connections. The WiFi network uses the IEEE 802.11e standard to prioritise the delay sensitive traffic. We provide initial isolated tests for each component of the system. First, the interoperability between two wireless technologies, HSDPA and WiFi, was studied. Since the operation is performed in different frequency bands, these technologies can co-exist without interfering with each other. From the tests run in our simulator, we demonstrated that the WiFi improves the coverage of the HSDPA without the need for a complex management system, providing a better service to the users. Simulation results show that, for high system loads, exploiting localization can provide a marginal gain of up to 450 kb/s in the goodput. These results show that, for optimized decisions in such an environment, to utilize mobile positioning leads to enhanced system performance. HSDPA was also studied in the context of cognitive radio, by considering two co-located BSs operating at different frequencies (in the 2 and 5 GHz bands) in the same cell. The system automatically chooses

the frequency to serve each user with an optimal General Multi-Band Scheduling (GMBS) algorithm. It was shown that enabling the access to a secondary band may increase the throughput of the system, while serving more users. By using the proposed Integrated CRRM (iCRRM), an almost constant gain near 30 % was obtained with the proposed optimal solution, compared to a system where users are first allocated in one of the two bands and later not able to handover between the bands.

In the WiFi ad hoc network, the goal was to find the path that delivered the highest number of packets and with the lowest delay. The optimization was tested for a video stream, whilst considering background and voice traffic streams to increase the network load. We first defined our cost functions manually, but ended-up by using an automatic optimization procedure in the form of Genetic Algorithms (GA). Choosing the path that minimizes the delay whilst maintaining the delivery ratio is very important to provide QoS to the user and our optimal approach manages to reach these two objectives.

The results presented in this thesis reveal the importance of an appropriate design of cross-layer and cross-system optimization algorithms for future heterogeneous wireless networks. They also reinforce the idea of deploying such future networks in which the user terminals will be able to roam freely from the coverage area of one radio access technology to another one, thereby bringing benefits in terms of the optimization of the experienced quality of service in network operation. Although a vast number of issues in the interesting field of cross-layer and cross-system optimization remain open for further research today, this thesis has given innovative contributions on the following issues:

- cross-layer functions and weights for the optimization of the IEEE 802.11e performance in the context of multi-service;
- a model for the computation of the throughput of IEEE 802.11 e in ad hoc mode;
- a model for the computation of SINR in HSDPA in an iCRRM/Spectrum Aggregation context;
- an optimal load suitability RAT selection algorithm between HSDPA and IEEE 802.11e;
- the incorporation of a new entity for spectrum and resource management, the so-called Integrated CRRM.

Besides, it has contributed towards a better understanding of the complex interactions between different radio access technologies based on system level simulation tools.

5.1 Suggestions for future research

For further research, one suggests to address handover policies between APs In this context,a scenario using more than one cell needs to be considered. As the parameters found for the cross-layer algorithm proposed in Section 3.3 best suit a specific case scenario, a dynamic procedure based on genetic algorithms is being developed in order to perform weight optimization real time so that this procedure will always be optimized in a given scenario.

Regarding the CRRM entity proposed in Chapter 4, the impact of the spatial distribution of the users over the cell and the consideration of multi-service scenario needs to be analyzed int he future. In this work, the GMBS Profit Function is based on the total throughput. Quality of Service requirements will be also included, in a scheduling problem with a linear combination of multiple objectives (scalarisation). A combined solution integrating the packet and the spectrum schedulers is foreseen to be able to greatly reduce the average delays and jitters, parameters of paramount importance for real-time services and applications. Mobility patterns will also be analysed, showing the effectiveness of an iCRRM to counter-fight shadowing in the support of the aforementioned real-time services and applications.

The main challenge for the cognitive radio scenario proposed for public transportation is to discover and maintain the paths between the service provider and the end user, the so-called cognitive paths. As a future work, the intention is to use the QoS feature of the simulator build to attribute a different cost function to different traffic types. For example, a function that delivers more packets, but with larger delay, can be used for background traffic, while another one (enabling more packet drops, but with lower delay) can be used to compute the path for video traffic. In this case, the fitness function of GA could account for more parameters than the packets delivered, for example, a weighted function that accounts for packets delivered and other metrics like jitter and delay, and will enhance the users' quality of experience. Different topologies will be tested to check which metrics are the most suitable ones.

Appendices

Appendix A

Distributed Coordination Function overview

The basic medium access protocol is a DCF that allows for automatic medium sharing between compatible PHYs through the use of CSMA-CA and a random backoff time following a busy medium condition. In addition, all directed traffic uses immediate positive acknowledgment where retransmission is scheduled by the sender if no ACK is received.

The CSMA-CA protocol is designed to reduce the collision probability between multiple STAs accessing a medium, at the point where collisions would most likely occur. Just after the medium becomes idle following a busy medium (as indicated by the CS function) is when the highest probability of a collision exists. This is because multiple STAs could have been waiting for the medium to become available again. This is the situation that necessitates a random backoff procedure to resolve medium contention conflicts.

Carrier Sense (CS) shall be performed both through physical and virtual mechanisms. The virtual CS mechanism is achieved by distributing reservation information announcing the impending use of the medium. The exchange of RTS and CTS frames prior to the actual data frame is one means of distribution of this medium reservation information. The RTS and CTS frames contain a Duration/ID field that defines the period of time that the medium is to be reserved to transmit the actual data frame and the returning ACK frame. All STAs within the reception range of either the originating STA (which transmits the RTS) or the destination STA (which transmits the CTS) shall learn of the medium reservation. Thus a STA can be unable to receive

from the originating STA, yet still know about the impending use of the medium to transmit a data frame.

Another means of distributing the medium reservation information is the Duration/ID field in directed frames. This field gives the time that the medium is reserved, either to the end of the immediately following ACK, or in the case of a fragment sequence, to the end of the ACK following the next fragment.

The RTS/CTS exchange also performs both a type of fast collision inference and a transmission path check. If the return CTS is not detected by the STA originating the RTS, the originating STA may repeat the process (after observing the other medium-use rules) more quickly than if the long data frame had been transmitted and a return ACK frame had not been detected. Another advantage of the RTS/CTS mechanism occurs where multiple BSSs utilizing the same channel overlap. The medium reservation mechanism works across the BSS boundaries. The RTS/CTS mechanism may also improve operation in a typical situation where all STAs can receive from the AP, but cannot receive from all other STAs in the BSS. The RTS/CTS mechanism cannot be used for MPDUs with broadcast and multicast immediate address because there are multiple destinations for the RTS, and thus potentially multiple concurrent senders of the CTS in response. The RTS/CTS mechanism should not be used for every data frame transmission because the additional RTS and CTS frames add overhead inefficiency, the mechanism is not always justified, especially for short data frames. The use of the RTS/CTS mechanism is under control of the dot11RTSThreshold attribute. This attribute may be set on a per-STA basis. This mechanism allows STAs to be configured to use RTS/CTS either always, never, or only on frames longer than a specified length. A STA configured not to initiate the RTS/CTS mechanism shall still update its virtual CS mechanism with the duration information contained in a received RTS or CTS frame, and shall always respond to an RTS addressed to it with a CTS.

The medium access protocol allows for STAs to support different sets of data rates. All STAs shall receive all the data rates in aBasicRateSet and transmit at one or more of the aBasicRateSet data rates. To support the proper operation of the RTS/CTS and the virtual CS mechanism, all STAs shall be able to detect the RTS and CTS frames. For this reason the RTS and CTS frames shall be transmitted at one of the aBasicRateSet rates.

A.1 Carrier Sense mechanism

Physical and virtual CS functions are used to determine the state of the medium. When either function indicates a busy medium, the medium shall be considered busy; otherwise, it shall be considered idle.

A physical CS mechanism shall be provided by the PHY. A virtual CS mechanism shall be provided by the MAC. This mechanism is referred to as the NAV. The NAV maintains a prediction of future traffic on the medium based on duration information that is announced in RTS/CTS frames prior to the actual exchange of data. The duration information is also available in the MAC headers of all frames sent during the CP other than Power Save-Poll Control frames.

The CS mechanism combines the NAV state and the STA's transmitter status with physical CS to determine the busy/idle state of the medium. The NAV may be thought of as a counter, which counts down to zero at a uniform rate. When the counter is zero, the virtual CS indication is that the medium is idle; when nonzero, the indication is busy. The medium shall be determined to be busy whenever a STA is transmitting.

A.2 Interframe Space

The time interval between frames is called the IFS. A STA determines that the medium is idle through the use of the CS function for the interval specified. Four different IFSs are defined to provide priority levels for access to the wireless media. Figure A.1 presents some of these relationships:

1. Short Inter-Frame Space (SIFS);
2. PCF Interframe Space (PIFS);
3. Distributed Inter-Frame Space (DIFS);
4. Arbitration Interframe Space (AIFS), used by the QoS facility;

The different IFSs are independent of the STA bit rate. The IFS timings are defined as time gaps on the medium, and the IFS timings except AIFS are fixed for each PHY (even in multirate capable PHYs). The IFS values are determined from attributes specified by the PHY.

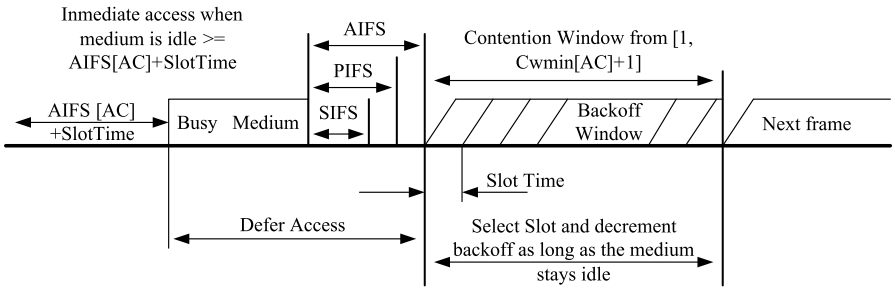

FIGURE A.1: Different IFS.

Short Inter-Frame Space

The SIFS are used for an ACK frame, a CTS frame, the second or subsequent MPDU of a fragment burst, and by a STA responding to any polling by the PCF. It may also be used by a PC for any types of frames during the CFP. The SIFS is the time from the end of the last symbol of the previous frame to the beginning of the first symbol of the preamble of the subsequent frame as seen at the air interface.

PCF Interframe Space (PIFS)

The PIFS are used only by STAs operating under the PCF to gain priority access to the medium at the start of the CFP. A STA using the PCF is allowed to transmit contention-free traffic after its CS mechanism determines that the medium is idle.

Distributed Inter-Frame Space

The DIFS are used by STAs operating under the DCF to transmit data frames MPDUs and management frames MMPDUs. A STA using the DCF is allowed to transmit if its CS mechanism determines that the medium is idle a DIFS after a correctly received frame, and its backoff time has expired.

Arbitration Interframe Space

The AIFS is used by QSTAs to transmit all MPDUs, all MMPDUs, and the following control frames: Power Save Pol, RTS, CTS (when not transmitted as a response to the RTS), BlockAckReq, and Block ACK (when not transmitted as a response to the BlockAckReq). A QSTA using the EDCA obtains a TXOP for an AC if the QSTA's CS mechanism determines that the medium is idle a AIFS[AC] after a correctly received frame, and the backoff time for that AC has expired.

Extended Interframe Space

The EIFS is used by the DCF, and the EIFS-DIFS+AIFS[AC] shall be used by the EDCA mechanism under HCF, when the PHY has indicated to the MAC that a frame transmission was begun that did not result in the correct reception of a complete MAC frame with a correct Frame Check Sequence (FCS) value. The EIFS interval begins following indication by the PHY that the medium is idle after detection of the erroneous frame, without regard to the virtual CS mechanism. The EIFS is defined to provide enough time for another STA to acknowledge what was, to this STA, an incorrectly received frame before this STA commences transmission. Reception of an error-free frame during the EIFS resynchronizes the STA to the actual busy/idle state of the medium, so the EIFS is terminated and normal medium access (using DIFS or AIFS as appropriate and, if necessary, backoff) continues following reception of that frame.

A.3 Random backoff time

A STA desiring to initiate transfer MPDUs and/or MMPDUs invokes the CS mechanism to determine the busy/idle state of the medium. If the medium is busy, STA defers until the medium is determined to be idle without interruption for a period of time equal to a DIFS when the last frame detected on the medium was received correctly, or after the medium is determined to be idle without interruption for a period of time equal to an Extended IFS when the last frame detected on the medium was not received correctly. After this DIFS medium idle time, the STA then generates a random backoff period for an additional deferral time before transmitting, unless the backoff timer already contains a nonzero value, in which case the selection of a random number is not needed and not performed. This process minimizes collisions during contention between multiple STAs that have been deferring to the same event.

$$BackoffTime = Random() \times aSlotTime \tag{A.1}$$

where $Random()$ is a Pseudorandom integer drawn from a uniform distribution over the interval [0,CW], where CW stands for contention window and it is an integer within the range of values of the PHY characteristics $aCWmin$ and $aCWmax$, $aCWmin \leq CW \leq aCWmax$. $aSlotTime$ is a slot time and it varies according to the PHY.

The *CW* parameter takes an initial value of *aCWmin*. The *CW* takes the next value in the series every time an unsuccessful attempt to transmit an MPDU occurs it causes a STA retry counter to increment until the *CW* reaches the value of *aCWmin*. Once it reaches *aCWmin*, the *CW* remains at the value of *aCWmax* until it is reset, Figure A.2. The *CW* is reset to *aCWmin* after every successful attempt to transmit an MSDU or MMPDU. The set of *CW* values are sequentially ascending integer powers of 2, minus 1, beginning with a specific *aCWmin* value, and continuing up to *aCWmax* value.

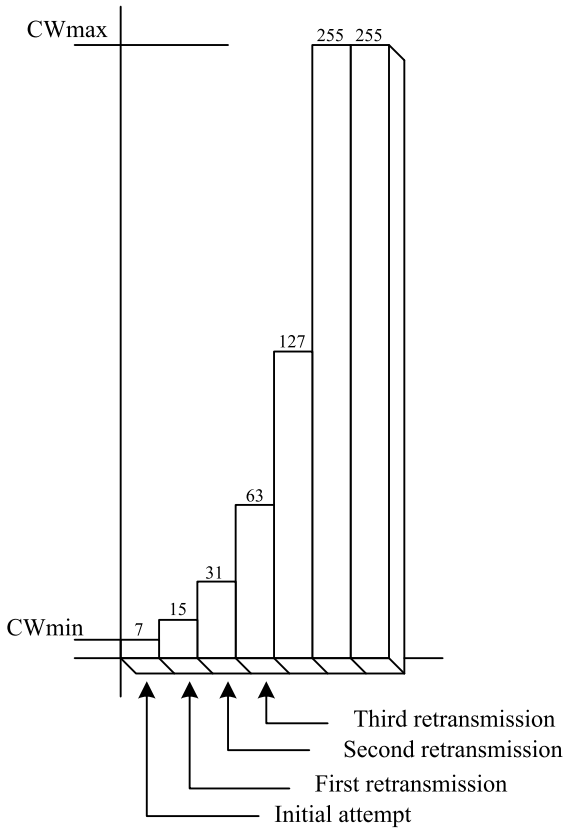

FIGURE A.2: Exponential increase of the *CW*.

A.4 Backoff procedure

The backoff procedure is invoked by a STA to transfer a frame when finding the medium busy as indicated by either the physical or virtual CS mechanism. The backoff procedure is also invoked when a transmitting STA infers a failed transmission. To begin the backoff procedure, the STA sets its Backoff Timer to a random backoff time using the equation before all backoff slots occur following a DIFS period during which the medium is determined to be idle for the duration of the DIFS period following detection of a frame that was not received correctly.

A STA performing the backoff procedure uses the CS mechanism to determine whether there is activity during each backoff slot. If no medium activity is indicated for the duration of a particular backoff slot, then the backoff procedure decrements its backoff time by *aSlotTime*. If the medium is determined to be busy at any time during a backoff slot, then the backoff procedure is suspended; that is, the backoff timer does not decrement for that slot. The medium is determined to be idle for the duration of a DIFS, before the backoff procedure is allowed to resume. Transmission commences whenever the backoff timer reaches zero.

In the case of unsuccessful transmissions requiring acknowledgment, this backoff procedure begins at the end of the ACK timeout interval. If the transmission is successful, the *CW* value reverts to *aCWmin* before the random backoff interval is chosen, and the STA short retry count and/or STA long retry count are updated. This assures that transmitted frames from a STA are always separated by at least one backoff interval.

The effect of this procedure is that when multiple STAs are deferring and go into random backoff, then the STA selecting the smallest backoff time using the random function will win the contention.

A.5 Setting and resetting the Network Allocation Vector

STAs receiving a valid frame shall update their NAV with the information received in the Duration/ID field, but only when the new NAV value is greater than the current NAV value and only when the frame is not addressed to the receiving STA. Various additional conditions may set or reset the NAV

Figure A.3 indicates the NAV for STAs that may receive the RTS frame, while other STAs may only receive the CTS frame, resulting in the lower NAV bar as shown (with the exception of the STA to which the RTS was addressed). The “CTS_Time” is calculated using the length of the CTS frame and the data rate at which the RTS frame used for the most recent NAV update was received.

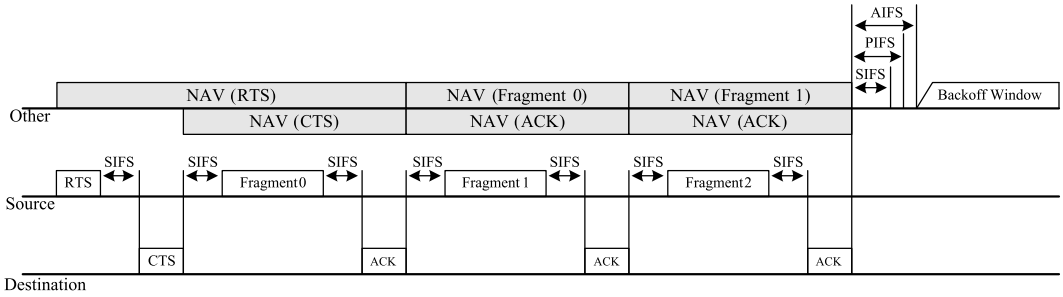

FIGURE A.3: NAV and RTS/CTS with fragmentation.

A.6 RTS/CTS usage with fragmentation

The following is a description of using RTS/CTS for a fragmented MSDU or MMPDU. The RTS/CTS frames define the duration of the following frame and acknowledgment. The Duration/ID field in the data and ACK frames specifies the total duration of the next fragment and acknowledgment, as is presented in Figure A.3.

Each frame contains information that defines the duration of the next transmission. The duration information from RTS frames are used to update the NAV to indicate busy until the end of ACK 0. The duration information from the CTS frame is also used to update the NAV to indicate busy until the end of ACK 0. Both Fragment 0 and ACK 0 contain the duration information to update the NAV to indicate busy until the end of ACK 1. This is done by using the Duration/ID field in the Data and ACK frames. In the case where an acknowledgment is sent but not received by the source STA, STAs that heard the fragment, or ACK, will mark the channel busy for the next frame exchange due to the NAV having been updated from these frames. If an acknowledgment is not sent by the destination STA, STAs that can only hear the destination STA will not update their NAV and may attempt to access the channel when their NAV updated from the previously received frame reaches zero. All STAs that hear the source will be free to access the channel after their NAV updated from the transmitted fragment has expired.

After transmitting an RTS frame, a STA waits for a *CTSTimeout* interval. If a CTS is not received during the *CTSTimeout* interval, the STA shall conclude that the transmission of the RTS has failed, and this STA invokes its backoff procedure upon expiration of the *CTSTimeout* interval.

Appendix B

Hybrid Coordination Function overview

This Section describes the QoS enhancements to the MAC functional description implemented by the IEEE 802.11e amendment. QSTAs may access the channel in a more controlled manner, compared to a non-QSTA, to transmit MPDUs. Under HCF, the basic unit of allocation of the right to transmit onto the WM is the TXOP. Each TXOP is defined by a starting time and a defined maximum length. The TXOP may be obtained by a QSTA winning an instance of EDCA contention during the CP or by a non-AP QSTA receiving a QoS (+) CF- Poll (frame requesting polling) frame during the CP or CFP. The former is called EDCA TXOP, while the latter is called HCCA TXOP or polled TXOP.

Reference Implementation

The channel access protocol is derived from the DCF procedures. A model of the reference implementation is presented in Figure 2.3 and illustrates a mapping from frame type to AC: the four transmit queues and the four independent EDCAFs, one for each queue. The mapping of UP to the AC is described in Figure 2.3.

EDCA TXOPs

There are two modes of EDCA TXOP defined, the initiation of the EDCA TXOP and the multiple frame transmission within an EDCA TXOP. An initiation of the TXOP occurs when the EDCA rules permit access to the medium. A multiple frame transmission within the TXOP

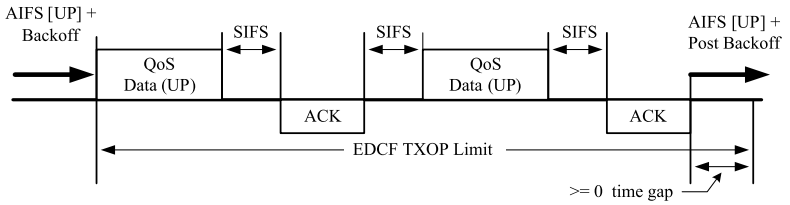

FIGURE B.1: TXOPLimit.

occurs when an EDCAF retains the right to access the medium following the completion of a frame exchange sequence, such as on receipt of an ACK frame.

The TXOP limit duration values are advertised by the QAP in the EDCA Parameter Set information element in Beacon and Probe Response frames transmitted by the QAP. A TXOP limit value of 0 indicates that a single MSDU or MMPDU, in addition to a possible RTS/CTS exchange or CTS to itself, may be transmitted at any rate for each TXOP.

Non-AP QSTAs ensure that the duration of a TXOPs obtained using the EDCA rules do not exceed the TXOP limit as shown in Figure B.1. The duration of a TXOP is the duration during which the TXOP holder maintains uninterrupted control of the medium, and it includes the time required to transmit frames sent as an immediate response to the TXOP holder's transmissions.

A QSTA fragments a unicast MSDU so that the transmission of the first MPDU of the TXOP does not cause the TXOP limit to be exceeded at the PHY rate selected for the initial transmission attempt of that MPDU. The TXOP limit may be exceeded, when using a lower PHY rate than selected for the initial transmission attempt of the first MPDU, for a retransmission of an MPDU, for the initial transmission of an MPDU if any previous MPDU in the current MSDU has been retransmitted, or for broadcast/multicast MSDUs. When the TXOP limit is exceeded due to the retransmission of an MPDU at a reduced PHY rate, the STA do not transmit more than one MPDU in the TXOP.

Obtaining an EDCA TXOP

Each channel access timer maintains a backoff function (timer), which has a value measured in backoff slots. The duration $AIFS[AC]$ is a duration derived from the value $AIFSN[AC]$ by the relation:

$$AIFS[AC] = AIFSN[AC] \times aSlotTime + aSIFSTime \tag{B.1}$$

The value of $AIFSN[AC]$ is greater than or equal to 2 for non-AP QSTAs and is advertised by the QAP in the EDCA Parameter Set information element in Beacon and Probe Response frames

transmitted by the QAP. The value of $AIFSN[AC]$ is greater than or equal to one for QAPs. An EDCA TXOP is granted to an EDCAF when the EDCAF determines that it shall initiate the transmission of a frame exchange sequence. Transmission initiation is determined according to some rules.

On specific slot boundaries, each EDCAF makes a selection to perform one and only one of the following functions:

- Initiate the transmission of a frame exchange sequence for that access function;
- Decrement the backoff timer for that access function;
- Invoke the backoff procedure due to an internal collision;
- Do nothing for that access function.

The specific slot boundaries at which exactly one of these operations is performed are defined as follows, for each EDCAF:

1. Following $AIFSN[AC] \times aSlotTime$ of idle medium after SIFS after the last busy medium on the antenna that was the result of a reception of a frame with a correct FCS.
2. Following $DIFS + AIFSN[AC] \times aSlotTime + aSIFSTime$ of idle medium after the last indicated idle medium as determined by the physical CS mechanism that was the result of a frame reception that has resulted in FCS error, or PHY- RXEND.indication (RXERROR) primitive where the value of RXERROR is not NoError.
3. When any other EDCAF at this QSTA transmitted a frame requiring acknowledgment, the earlier of:
   (a) The end of the ACK-Timeout interval timed from the PHY_TXEND.confirm primitive, followed by $AIFSN[AC] \times aSlotTime + aSIFSTime$ of idle medium, and
   (b) The end of the first $AIFSN[AC] \times aSlotTime$ of idle medium after SIFS when a transmission successful occurs.
4. Following $AIFSN[AC] \times aSlotTime$ of idle medium after SIFS after the last busy medium on the antenna that was the result of a transmission of a frame for any EDCAF and which did not require an acknowledgment.

5. Following $AIFSN[AC] \times aSlotTime + aSIFSTime$ of idle medium after the last indicated idle medium as indicated by the CS mechanism that is not covered by a) through d).

6. Following *aSlotTime* of idle medium, which occurs immediately after any of these conditions, a) through f), is met for the EDCAF.

At each of the above-described specific slot boundaries, each EDCAF initiates a transmission sequence if:

- there is a frame available for transmission at that EDCAF, and
- the backoff timer for that EDCAF has a value of zero, and
- initiation of a transmission sequence is not allowed to commence at this time for an EDCAF of higher UP.

At each of the above-described specific slot boundaries, each EDCAF decrements the backoff timer if the backoff timer for that EDCAF has a nonzero value.

At each of the above-described specific slot boundaries, each EDCAF invokes the backoff procedure due to an internal collision if:

- there is a frame available for transmission at that EDCAF, and
- the backoff timer for that EDCAF has a value of zero, and
- initiation of a transmission sequence is allowed to commence at this time for an EDCAF of higher UP.

Multiple frame transmission in an EDCA TXOP

Multiple frames may be transmitted in an acquired EDCA TXOP if there are more than one frame pending in the AC for which the channel has been acquired. However, those frames that are pending in other ACs shall not be transmitted in this EDCA TXOP. If a QSTA has in its transmit queue an additional frame of the same AC as the one just transmitted and the duration of transmission of that frame plus any expected acknowledgment for that frame is less than the remaining medium occupancy timer value, then the QSTA may commence transmission of that frame at SIFS after the completion of the immediately preceding frame exchange sequence. The

intention of using the multiple frame transmission is indicated by the QSTA through the setting of the duration/ID values in one of the following two ways:

1. Long enough to cover the response frame, the next frame, and its response frame;
2. Long enough to cover the transmission of a burst of MPDUs subject to the limit set by dot11EDCATableTXOPLimit.

No other AC at the QSTA transmits before the expiration of the NAV set by the frame that resulted in a transmission failure. All other ACs at the QSTA treat the medium as busy until the expiration of the NAV set by the frame that resulted in a transmission failure, just as they would if they had received that transmission from another QSTA.

Note that, as for an EDCA TXOP, a multiple frame transmission is granted to an EDCAF, not to a non-AP QSTA or QAP, so that the multiple frame transmission is permitted only for the transmission of a frame of the same AC as the frame that was granted the EDCA TXOP.

EDCA backoff procedure

Each EDCAF maintains a state variable $CW[AC]$, which is initialized to the value of the parameter $CWmin[AC]$. If a frame is successfully transmitted by a specific EDCAF, indicated by the successful reception of a CTS in response to an RTS, the successful reception of an ACK frame in response to a unicast MPDU or a BlockAck, the successful reception of a BlockAck or ACK frame in response to a BlockAckReq frame, or the transmission of a multicast frame or a frame with No ACK policy, the $CW[AC]$ shall be reset to $CWmin[AC]$. The backoff procedure is invoked for an EDCAF when any of the following events occurs:

- A frame with that AC is requested to be transmitted, the medium is busy as indicated by either physical or virtual CS, and the backoff timer has a value of zero for that AC.
- The final transmission by the TXOP holder initiated during the TXOP for that AC was successful.
- The transmission of a frame of that AC fails, indicated by a failure to receive a CTS in response to an RTS, a failure to receive an ACK frame that was expected in response to a unicast MPDU, or a failure to receive a BlockAck or ACK frame in response to a BlockAckReq frame.

- The transmission attempt collides internally with another EDCAF of an AC that has higher priority, that is, two or more EDCAFs in the same QSTA are granted a TXOP at the same time.

If the backoff procedure is invoked for reason a) above, the value of $CW[AC]$ is left unchanged. If the backoff procedure is invoked because of reason b) above, the value of $CW[AC]$ is reset to $CWmin[AC]$. If the backoff procedure is invoked because of a failure event (the two last cases above), the value of $CW[AC]$ is updated as follows before invoking the backoff procedure:

1. If the QoS Short Retry Counter (QSRC) or the QoS Long Retry Counter (QLRC) of a given AC for the QSTA has reached dot11ShortRetryLimit or dot11LongRetryLimit respectively, $CW[AC]$ is reset to $CWmin[AC]$.
2. Otherwise,
   - If $CW[AC]$ is less than $CWmax[AC]$, $CW[AC]$ is set to the value $(CW[AC] +1)\times$2-1.
   - If $CW[AC]$ is equal to $CWmax[AC]$, $CW[AC]$ remains unchanged for the remainder of any retries.

The backoff timer is set to an integer value chosen randomly with a uniform distribution taking integer values in the range [0,$CW[AC]$]. All backoff slots occur following an $AIFS[AC]$ period during which the medium is determined to be idle for the duration of the $AIFS[AC]$ period, or following an DIFS + $AIFS[AC]$ period during which the medium is determined to be idle for the duration of the DIFS + $AIFS[AC]$ period following detection of a frame that was not received correctly.

Appendix C

Channel model

This appendix presents a brief overview of the main factors that affect the SINR in wireless networks, as well as some mathematical models that were useful for the simulations presented in this thesis.

If the received signal power, P_r, and the background noise power, N, are known, it is possible to calculate the instantaneous SINR as:

$$SINR = \frac{P_r}{N} \tag{C.1}$$

The ratio between signal and noise can also be expressed as the ratio between the average energy-per-bit, E_b, or energy-per-symbol, E_s, and the positive-frequency noise power spectral density (N_0). If B is the transmission bandwidth of the system, we have:

$$SINR = \frac{P_r}{N} = \frac{R_b}{B} \cdot \frac{E_b}{N_0} = \frac{R_b}{\log_2(M) \cdot B} \cdot \frac{E_s}{N_0} \tag{C.2}$$

where R_b is the bit-rate, considering a given modulation, and M is the number of symbols of the modulation.

In practical terms, if a signal is transmitted with power P_t, it arrives at the receiver with power P_r given by the following expression:

$$P_r[\text{dBm}] = P_t[\text{dBm}] - PL(d)[\text{dB}] + \alpha^2[\text{dB}] \tag{C.3}$$

where $PL(d)$ is the path loss between sender and receiver for a distance d and α^2 is the instantaneous gain of small-scale fading. The latter deals with random variations of the received signal amplitude and phase as a result of small changes in the spatial separation and speed between the transmitter and receiver. $PL(d)$ varies slowly over a large area as a function of distance and hence it is termed large-scale fading.

C.1 Path Loss

A simple and very common path loss model is the free space propagation model, also designated the Friis model [71]. This ideal model assumes that there is a line of sight path between the transmitter and receiver, without taking into account multipath effects. According to this model, the received power is calculated as follows:

$$P_r(d) = \frac{P_t \times G_t \times G_r \times \lambda^2}{(4\pi^2) \times d^2 \times l} \tag{C.4}$$

where $P_r(d)$ is the received power at distance d, G_t and G_r are the transmit and receive antenna gains, λ is the carrier wavelength (in meters) and l is the system loss factor. The Friis model is only valid for distances that stay on the far-field of the transmitting antenna, which starts at reference distance d_0. The latter should respect the following relation:

$$d_0 > \frac{2D^2}{\lambda} \tag{C.5}$$

where D is the largest physical dimension of the antenna (in meters).

The Friis model calculates the received power as a deterministic function of distance. In reality the received power is a random variable that can be affected by shadowing obstacles and multipath fading. A more realistic and widely-used model that takes into account these phenomena is the Log-distance path loss model [71] given by the following expression:

$$PL(d)[\text{dB}] = PL(d_0)[\text{dB}] + 10 \cdot n \cdot \log_{10}\left(\frac{d}{d_0}\right) + X_\sigma \tag{C.6}$$

The considered path loss exponent is typically n=3 for office environment models [71]. $PL(d_0)$, or path loss experienced at the reference distance is calculated with the Friis free space propagation model.

Surrounding objects may introduce location dependent propagation effects, which also affect the received power. This is called shadowing, X_σ, and can be modelled as a log-normal random variable (i.e., it forms a Gaussian distribution if measured in dB units) with zero mean and standard deviation $\sigma_{[\mathrm{dB}]}$ designated the shadowing deviation.

Nevertheless, the Log-distance path loss model is still not realistic for indoor scenarios where walls and floor partitions can introduce significant attenuation. In such scenarios the Log-distance path loss model must be complemented with partition attenuation factors [71]:

$$PL(d)[\mathrm{dB}] = PL(d_0)[\mathrm{dB}] + 10 \cdot n \cdot \log_{10}\left(\frac{d}{d_0}\right) + FAF[\mathrm{dB}] + \sum WAF[\mathrm{dB}] \qquad \text{(C.7)}$$

where *FAF* represents a floor attenuation factor and *WAF* represents a wall attenuation factor.

C.2 Small-scale Fading

Small-scale fading is used to describe the rapid fluctuations of the amplitudes, phases or multipath delays of a radio signal over a short travel distance, in which variations in terms of large-scale path loss may be ignored [71]. These fluctuations are caused by the reception of multiple delayed versions of the signal at the receiver at slightly different times. Fading can be flat or frequency selective. Flat fading occurs when there is a constant gain and linear phase response over a bandwidth greater than the bandwidth of the transmitted signal. In this case the spectral characteristics of the transmitted signal are preserved at the receiver, with fading being translated as changes in the received signal strength caused by fluctuations in the gain of the channel. On the other hand, in frequency selective fading the channel possesses a constant gain and linear phase response over a bandwidth that is smaller than the bandwidth of the transmitted signal. This occurs when multiple versions of the transmitted signal are attenuated and delayed in time due to multipath, causing distortion at the receiver.

Only flat fading is considered in this thesis. The statistical time-varying nature of the received signal envelope is assumed to follow a Rayleigh distribution, which corresponds to a scenario

where there is no line-of-sight propagation path (the worst-case). Consider the example presented in [126], which consists of signal $s(t) = A\cos(2\pi f_c t)$ transmitted through a channel with M multipath components. If the line-of-sight component is discarded and the noise component is not taken into account, the received signal can be expressed as:

$$y(t) = A \cdot \sum_{i=1}^{M} a_i \cdot \cos(2\pi f_c t + \theta_i) \tag{C.8}$$

where a_i is the attenuation of the i^{th} multipath component and θ_i is its phase-shift. It should be noted that a_i and θ_i are random variables. Let Eq. C.8 be rewritten as:

$$y(t) = A\left\{\left(\sum_{i=1}^{M} a_i \cdot \cos(\theta_i)\right)\cos(2\pi f_c t) - \left(\sum_{i=1}^{M} a_i \cdot \sin(\theta_i)\right)\sin(2\pi f_c t)\right\} \tag{C.9}$$

Two random processes $X_1(t)$ and $X_2(t)$ are introduced such that Eq. C.9 becomes:

$$y(t) = A\{X_1(t) \cdot \cos(2\pi f_c t) - X_2(t) \cdot \sin(2\pi f_c t)\} \tag{C.10}$$

If the value M is large, invoking the Central-Limit Theorem, it comes that $X_1(t)$ and $X_2(t)$ are Gaussian random variables with zero-mean and variance σ^2. Eq. C.10 can be rewritten as:

$$y(t) = A \cdot \alpha(t) \cdot \cos(2\pi f_c t + \theta(t)) \tag{C.11}$$

where the amplitude of the received waveform $\alpha(t)$ given by:

$$\alpha(t) = \sqrt{X_1(t)^2 + X_2(t)^2} \tag{C.12}$$

Since $X_1(t)$ and $X_2(t)$ are Gaussian, it can be shown that $\alpha(t)$ has a Rayleigh distribution with probability density function:

$$f_\alpha(t) = \frac{r}{2\sigma^2} \cdot e^{\frac{-r^2}{2\sigma^2}}, \quad r > 0 \tag{C.13}$$

The phase of the received waveform $\theta(t)$ is given by:

$$\theta(t) = \tan^{-1}\left(\frac{X_2(t)}{X_1(t)}\right) \tag{C.14}$$

Distortion of the phase can be overcome with differential modulation. It is the amplitude distortion that severely degrades the performance of digital communication systems over fading channels.

It is usually assumed that the value of $\alpha(t)$ is constant during a time interval called the coherence time. The coherence time can be approximated by the following expression [71]:

$$T_c(t) = \frac{9 \cdot \lambda}{16 \cdot \pi \cdot v(t)} \tag{C.15}$$

where $v(t)$ is the speed along the line-of-sight between the sender and receiver at time t.

C.3 Noise and Interference

The primary source of performance degradation is thermal noise generated at the receiver. The thermal noise power, N_t, is determined by the product of Boltzman constant, k_B, the environmental temperature (given in Kelvin degrees) and the transmission bandwidth of the signal:

$$N_T = k_B \cdot T \cdot B = N_0 \cdot B \tag{C.16}$$

This type of noise is called Additive White Gaussian Noise (AWGN). AWGN is called "white" because its energy is distributed evenly across the frequency band and does not have any deterministic behaviour over time or frequency. It can be modelled as a Gaussian random process with zero mean and constant positive-frequency power spectral density N_0[127].

N_T is the theoretical noise floor for an ideal receiver. The noise floor for a real receiver will always be higher by a factor called the Noise Figure, *NF*. The latter accounts for the noise introduced by the receiver itself in the signal amplification and processing stages:

$$N = N_T \cdot NF \tag{C.17}$$

Besides the noise floor related to thermal noise, background noise at reception can additionally be caused by co-channel interference from other radiating sources (ΣI). Interference from other radiating sources usually consists of narrowband interference, with a specific behaviour in time and frequency. In this thesis it is assumed that all background noise is AWGN only, including interfering sources. The overall noise power at the receiver is given by the following expression:

$$N = k_B \cdot T \cdot B \cdot NF + \sum I \tag{C.18}$$

Appendix D

Topologies evaluated

Besides the topologies form Figure 3.20, the following topologies were considered to verify the validity of the throughput model for the IEEE 802.11e ad hoc network, Figures D.1, D.2, D.3 and D.4.

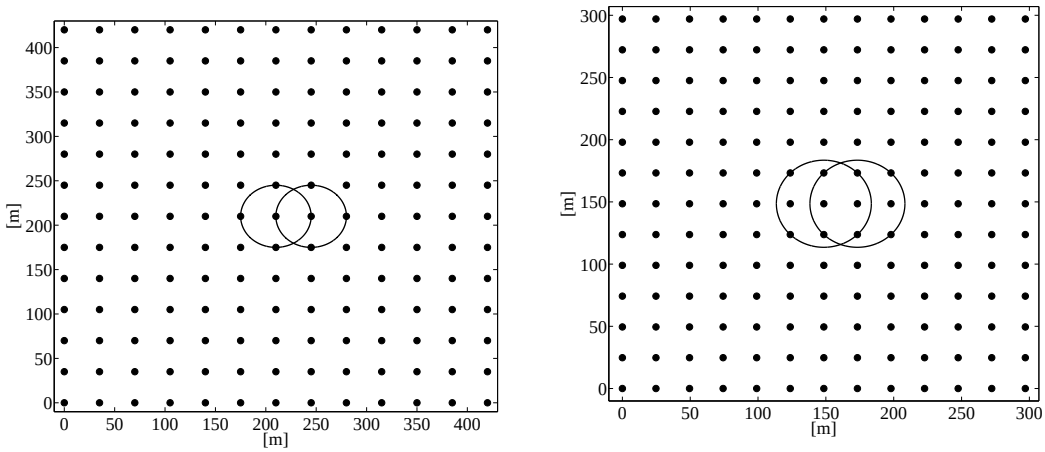

FIGURE D.1: Topologie for $\lambda = 9.5805 \cdot 10^{-4}$ and $\lambda = 1.916 \cdot 10^{-3}$.

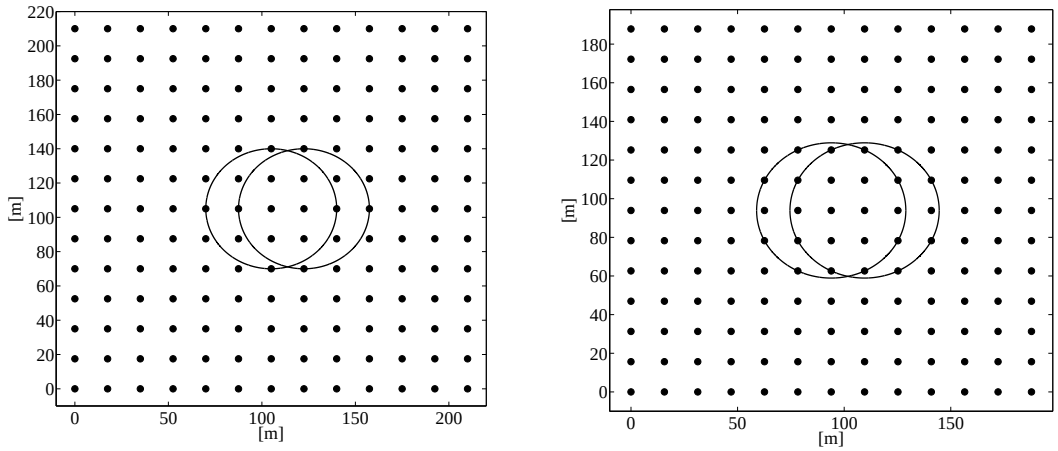

FIGURE D.2: Topologie for $\lambda = 3.832 \cdot 10^{-3}$ and $\lambda = 4.790 \cdot 10^{-3}$.

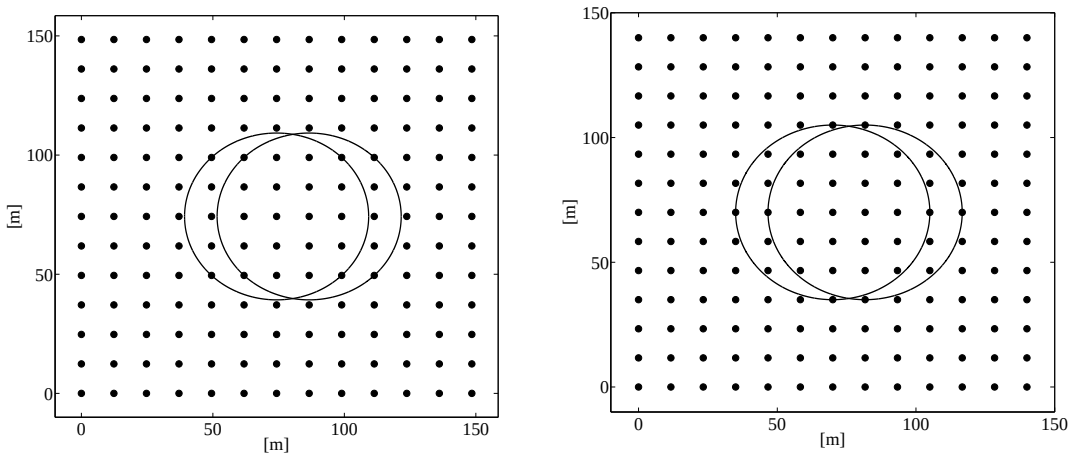

FIGURE D.3: Topologie for $\lambda = 7.665 \cdot 10^{-3}$ and $8.622 \cdot 10^{-3}$.

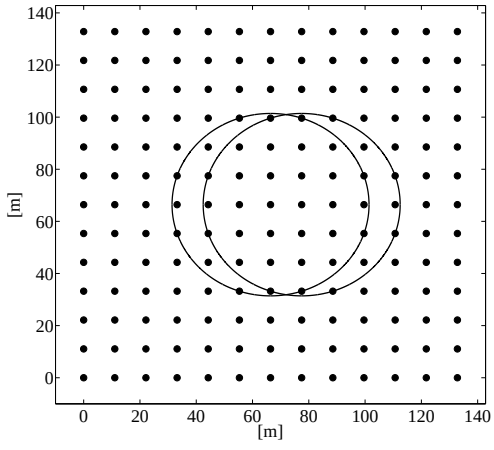

FIGURE D.4: Topologie for $\lambda = 9.580 \cdot 10^{-3}$.

Appendix E

Common Radio Resource Management extra results

This Appendix presents additional results for the RAT selection algorithm with the load suitability function applied for the interoperability between HSDPA and IEEE 802.11e. While Figure 4.3 considers a cell radius of 50 m and values for the load threshold of 0.6 and 0.7, the load thresholds considered in Figure E.1 are 0.5 and 0.8. Figure E.2 presents results in the absence of the use of the CRRM entity.

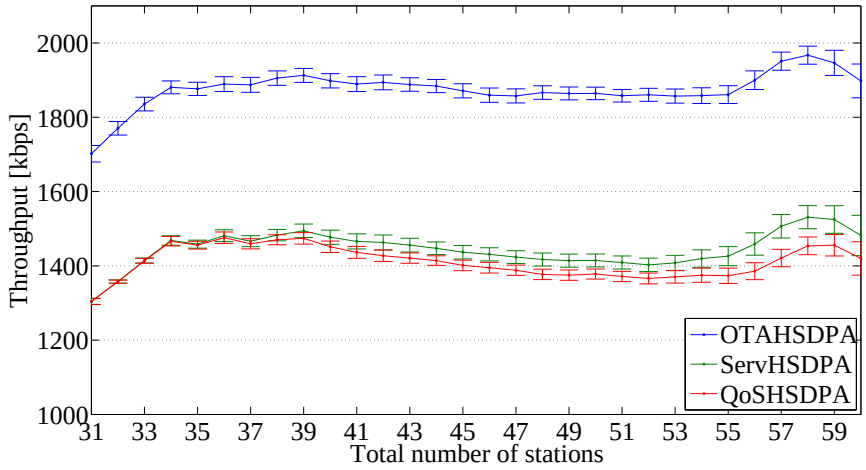

a)

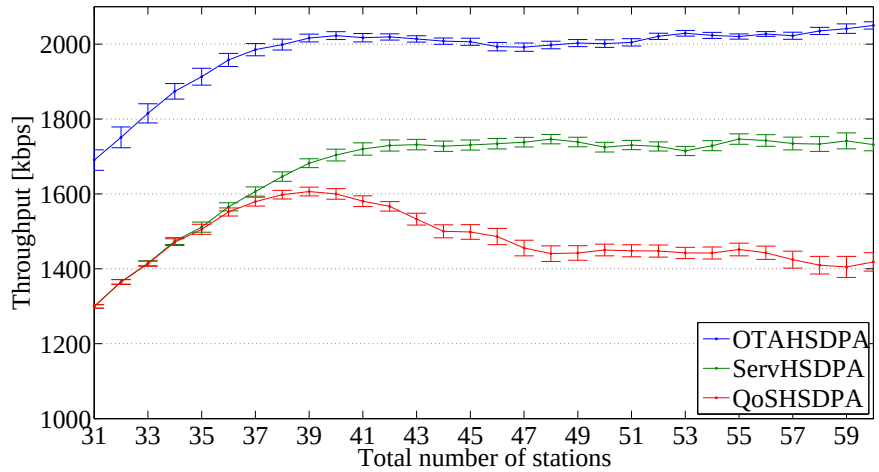

b)

FIGURE E.1: Throughput in HSDPA with CRRM entity exploring the diversity gain for a radius equal to 50 m, a) for load thresholds equal to 0.5 and b) for load thresholds equal to 0.8.

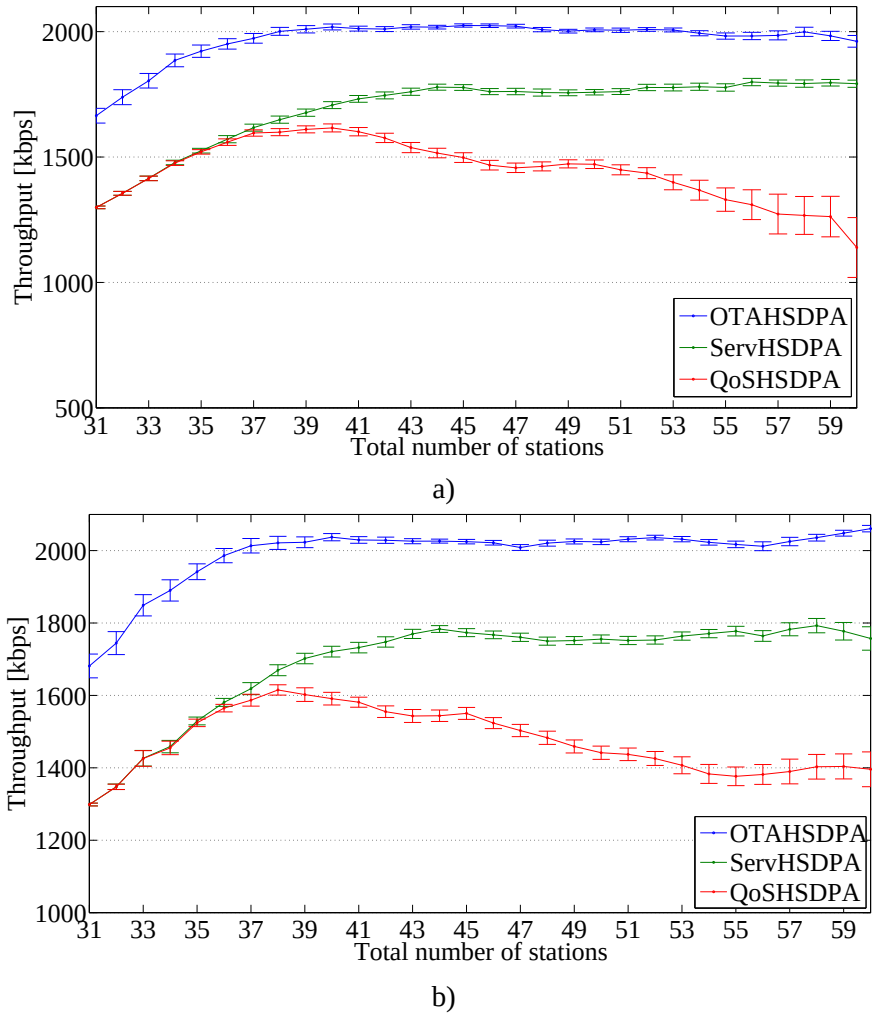

FIGURE E.2: HSDPA throughput vs. number of users without CRRM entity, a) for radius=75m and b) for radius=100m.

Appendix F

Cellular analysis for constant average SINR

In this appendix, detailed calculations of the average SINR are presented for various cell radii, in a cellular network of BSs with reuse pattern one. First, the average interference from a neighbour cell is presented. Then, the average signal power in the central cell is calculated in order to derive the SINR as function of the cell radius and transmit power.

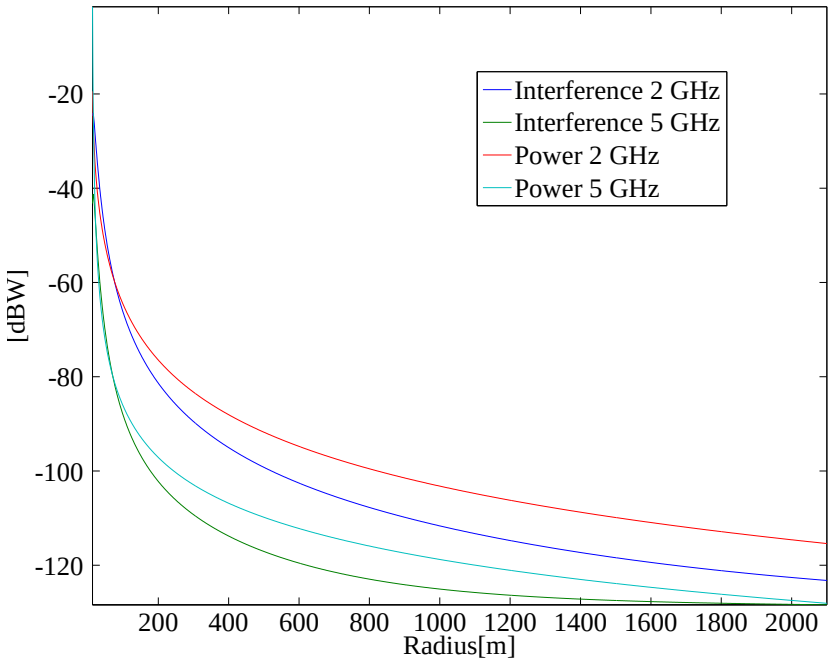

FIGURE F.1: Average power and interference [dBW] within a cell as a function of the inter-cell distance [m] with P_{Tx}1 dBW.

The average interference from one neighbour cell is obtained, referring to the coordinate system in Figure 4.14, as:

$$\bar{I}(R,P_{Tx}) = \int_x \int_y f_I(P_{Tx},x,y)dydx = \int_x \int_y \frac{P_{Tx}G_{Tx}G_{Rx}}{A_{Cell}} PL(x,y)dydx \tag{F.1}$$

where the area for an hexagonal cell is $A_{Cell} = \frac{3}{2}\sqrt{3}R^2$, the PL follows the models specified in Table 4.5, the distance being determined by $d = \sqrt{(y-y_0)^2 + (x-x_0)^2}$; $P_{Tx} = 1$ dBW, $G_{Tx} = 14$ dBi and $G_{Rx} = 0$ dBi. Figure 4.14 shows the division of the central hexagonal cell into three sub-regions. Assuming $x_0 = 0$, $y_0 = \sqrt{3}R$, we may calculate the average interference as:

$$\bar{I}(R,P_{Tx}) = \sum_{r=1}^{3} \int_{\Gamma_x^r} \int_{\Gamma_y^r} f_I(P_{Tx},x,y)dydx \tag{F.2}$$

where the integration regions are as follows:

$$\Gamma_x^r = \left\{ [-R, -\frac{R}{2}], [-\frac{R}{2}, \frac{R}{2}], [\frac{R}{2}, R] \right\}$$

and

$$\Gamma_y^r = \left\{ [-\sqrt{3}x - \sqrt{3}R, \sqrt{3}x + \sqrt{3}R], [-\frac{\sqrt{3}}{2}R, \frac{\sqrt{3}}{2}R] \right.,$$

$$\left. [\sqrt{3}x - \sqrt{3}R, -\sqrt{3}x + \sqrt{3}R] \right\}$$

For the 2 GHz band, $f_I(P_{Tx},x,y)$ is given by:

$$f_I(P_{Tx},x,y) = \frac{P_{Tx}G_{Tx}G_{Rx}}{A_{cell}} 10^{-\frac{128.1+37.6\cdot\log\sqrt{(y-\sqrt{3}R)^2+x^2}}{10}} \tag{F.3}$$

As R is positive (F.2) is solvable. Then:

$$\begin{aligned} &\textstyle\int_{\Gamma_{x,y}^r} f_I(P_{Tx},x,y)dydx = \\ &P_{Tx}G_{Tx}G_{Rx} \cdot 10^{-\frac{\sum_{r=1}^{3} \int_{\Gamma_{x,y}^r} \left(128.1+37.6\cdot\log\sqrt{(y-\sqrt{3}R)^2+x^2}\right)dydx}{10\cdot A_{cell}}} \end{aligned} \tag{F.4}$$

Considering that the distance in the path loss equation is expressed in kilometres and that:

$$\int_{\Gamma_{x,y}^1} dydx = \frac{\sqrt{3}}{4}R^2 \tag{F.5}$$

the steps for solving the integral in the second term of (F.4) over the region $\Gamma^1_{x,y}$ are as follows:

$$\begin{aligned}&\int_{\Gamma^1_{x,y}}\left(128.1+37.6\cdot\log\sqrt{(y-\sqrt{3}R)^2+x^2}\right)dydx=\\&\tfrac{37.6}{2}\int_{\Gamma^1_{x,y}}\log\left[\left(y-\sqrt{3}R\right)^2+x^2\right]dydx+\\&(128.1-37.6\cdot\log(1000))\tfrac{\sqrt{3}}{4}R^2.\end{aligned}\tag{F.6}$$

The solution for the integral in the second term of (F.6) is:

$$\begin{aligned}&\int_{\Gamma^1_{x,y}}\log\left[\left(y-\sqrt{3}R\right)^2+x^2\right]dydx=\int_{\Gamma^1_{x,y}}\frac{\ln\left[\left(y-\sqrt{3}R\right)^2+x^2\right]}{\ln(10)}dydx=\\&\ln(10)^{-1}\int_{\Gamma^1_x}\left(-4\sqrt{3}R-4\sqrt{3}x+\tfrac{2Rx}{3}+2x\cdot\arctan\left[\tfrac{\sqrt{3}(2R+x)}{x}\right]+\right.\\&\sqrt{3}x\cdot\ln\left(4x^2\right)+2\sqrt{3}R\cdot\ln\left[4\left(3R^2+3Rx+x^2\right)\right]+\\&\left.\sqrt{3}x\cdot\ln\left[4\left(3R^2+3Rx+x^2\right)\right]\right)dx.\end{aligned}\tag{F.7}$$

The average interference power can be obtained with the evaluation of a linear combination of the integrals of arctan, ln and polynomial functions. The integration over region $\Gamma^2_{y,x}$, by applying the method of integration by parts, are simple to obtain. Over region $\Gamma^3_{y,x}$, the steps to be followed are similar to the ones outlined in (F.5), (F.6) and (F.7). The average interference that comes from each of the surrounding cells is equal as the interfering BS is always at the same distance $\sqrt{3}R$ from the central cell, see Figure 4.12.

The average signal power in the intended cell can be calculated with the same approach used for the average interference power, substituting the integrand function f_I with f_P, which is reported for the 2 GHz as follows:

$$f_P(P_{Tx},x,y)=\frac{P_{Tx}G_{Tx}G_{Rx}}{A_{ow}}10^{-\frac{128.1+37.6\cdot\log\sqrt{y^2+x^2}}{10}}\tag{F.8}$$

The average power is calculated as:

$$\overline{P}_{ow}(R,P_{Tx})=\sum_{r=1}^{6}\int_{\Gamma^r_x}\int_{\Gamma^r_y}f_P(P_{Tx},x,y)dydx\tag{F.9}$$

where

$$\Gamma^r_x=\left\{[-R,-\frac{R}{2}],[-\frac{R}{2},-Fr],[-Fr,Fr],[-Fr,Fr],[Fr,\frac{R}{2}],[\frac{R}{2},R]\right\}$$

and

$$\Gamma_y^r = \left\{ [-\sqrt{3}x - \sqrt{3}R, \sqrt{3}x + \sqrt{3}R], [-\frac{\sqrt{3}}{2}R, \frac{\sqrt{3}}{2}R], [-\frac{\sqrt{3}}{2}R, -Fr], \right.$$
$$\left. [Fr, \frac{\sqrt{3}}{2}R], [-\frac{\sqrt{3}}{2}R, \frac{\sqrt{3}}{2}R], [\sqrt{3}x - \sqrt{3}R, -\sqrt{3}x + \sqrt{3}R] \right\}$$

Equation (F.9) is unsolvable if the integration region includes $(x,y) = (0,0)$ (where the BS is located). We adopted an approximation of the Fraunhofer distance, F_r, for an antenna radiator equal to 72 cm. If $R > F_r$ the integral is solvable. With a square approximation of the Fraunhofer region centered in (0,0), the total integration area is $A_{ow} = \frac{3}{2}\sqrt{3}R^2 - F_r^2$.

The average power calculation can thus be expressed as:

$$\begin{aligned} &\textstyle\int_{\Gamma_{x,y}^r} f_P(P_{Tx}, x, y) dydx = \\ &P_{Tx} G_{Tx} G_{Rx} \cdot 10^{-\frac{\sum_{r=1}^{6} \int_{\Gamma_{x,y}^r} \left(128.1 + 37.6 \cdot \log\sqrt{y^2+x^2}\right) dydx}{10 \cdot A_{ow}}} \end{aligned} \tag{F.10}$$

From all the integration regions in (F.10) the most complicated integrals to solve are the ones for r=1 and r=6. As their resolutions are similar, we outline the one for r=6. Considering that the distance in the path loss is expressed in kilometres, and that:

$$\int_{\Gamma_{x,y}^6} dydx = \frac{\sqrt{3}}{4}R^2$$

then:

$$\begin{aligned} &\textstyle\int_{\Gamma_{x,y}^6} \left(128.1 + 37.6 \cdot \log\sqrt{y^2+x^2}\right) dydx = \\ &\textstyle\frac{37.6}{2} \int_{\Gamma_{x,y}^6} \log(y^2+x^2) dydx + (128.1 - 37.6 \cdot \log(1000)) \frac{\sqrt{3}}{4} R^2 \end{aligned} \tag{F.11}$$

The solution to the integral in the second term in (F.11) is given by:

$$\begin{aligned} &\textstyle\int_{\Gamma_{x,y}^6} \log(y^2+x^2) dydx = \int_{\Gamma_{x,y}^6} \frac{\ln(y^2+x^2)}{\ln(10)} dydx = \\ &\ln(10)^{-1} \textstyle\int_{\Gamma_x^6} \left(2(-\sqrt{3}x + \sqrt{3}R) \ln\left[(-\sqrt{3}x + \sqrt{3}R)^2 + x^2\right]\right. \\ &\left. -4(-\sqrt{3}x + \sqrt{3}R) + 4x \cdot \arctan\left[\frac{-\sqrt{3}x + \sqrt{3}R}{x}\right]\right) dx. \end{aligned} \tag{F.12}$$

The second term of the last member of (F.12) it is a polynomial integration. The first and third terms of the last member of (F.12) are solved by using the method of integration by parts. The integration is shown for exemplification for the third term only:

$$\begin{aligned}&\int \arctan\left[\tfrac{-\sqrt{3}x+\sqrt{3}R}{x}\right]dx = \\ &2x^2\cdot\arctan\left[\tfrac{-\sqrt{3}x+\sqrt{3}R}{x}\right]+2\sqrt{3}R\left[\tfrac{1}{4}x-\tfrac{3}{4}R\cdot\right. \\ &\left.\left(-\tfrac{1}{2\sqrt{3}}\cdot\arctan\left[\tfrac{-3R+4x}{\sqrt{3}R}\right]-\tfrac{1}{4}\cdot\ln\left(3R^2-6Rx+4x^2\right)\right)\right]\end{aligned} \tag{F.13}$$

The second integration over regions $\Gamma^3_{x,y}$ and $\Gamma^4_{x,y}$ do not exist for $x=0$. Dividing the region Γ^3_x (equal to Γ^4_x) into two subregions, $[Fr,0[$ and $]0,Fr]$, the integral can be put in the improper integral form and then solved by parts:

$$\begin{aligned}&\textstyle\int_{\Gamma^3_x}\int_{\Gamma^3_y} f_P(P_{Tx},x,y)dydx = \\ &\lim_{\varepsilon\to 0^-}\int_{-Fr}^{\varepsilon}\int_{\Gamma^3_y} f_P(P_{Tx},x,y)dydx+\lim_{\varepsilon\to 0^+}\int_{\varepsilon}^{Fr}\int_{\Gamma^3_y} f_P(P_{Tx},x,y)dydx\end{aligned} \tag{F.14}$$

The average power can now be obtained for the whole hexagon, except in the square with the side length equal to the Fraunhofer distance and the average SINR in (4.18) can be finally calculated.

References

[1] (2008, Dec.) EU CELTIC Project WINNER+, Deliverable 3.1, IMT-Advanced: Requirements and Evaluation Criteria. [Online]. Available: http://projects.celtic-initiative.org/winner+/

[2] Q. Ni, "Performance analysis and enhancements for IEEE 802.11e wireless networks," *IEEE Network*, vol. 19, no. 4, pp. 21–27, July-Aug. 2005.

[3] EU CELTIC Project WINNER+. [Online]. Available: http://projects.celtic-initiative.org/winner+/

[4] FP6 IST Project WINNER and WINNER II. [Online]. Available: www.ist-winner.org

[5] Third Generation Partnership Project 3GPP. [Online]. Available: www.3gpp.org

[6] "D4.1.2 Final Specification of Algorithms for Cross-Layer and Cross-System Optimisation," Aegean, NCSR, Eurecom, FT, IT, UniS, CEA-LETI, IST Central Office, Brussels, Belgium, Tech. Rep. IST-4-026906, Jan. 2008, www.ist-unite.org.

[7] "D4.4.1 Final Results, Specifications and Design Guidelines," T, Eur, UniS, DEM, AEG, RS, CEA-LETI, IST Central Office, Brussels, Belgium, Tech. Rep., Feb. 2009, www.ist-unite.org.

[8] CROSSNET Progect. [Online]. Available: http://www.e-projects.ubi.pt/crossnet/

[9] O. Cabral, A. Segarra, and F. Velez, "Event-Driven Simulation for IEEE 802.11e Optimization," *IAENG International Journal of Computer Science*, vol. 35, no. 1, pp. 161–173, 2008.

[10] ——, "Implementation of IEEE 802.11e Block Acknowledgement Policies," *IAENG International Journal of Computer Science*, vol. 36, no. 1, pp. 85–93, Feb. 2009.

[11] O. Cabral, F. J. Velez, A. Mihovska, and N. R. Prasad, "Optimization of Multi-Service IEEE802.11e Block Acknowledgement," in *Proc. of IEEE Radio and Wireless Symposium (RWS09)*, San Diego, CA, USA, Jan. 2009.

[12] O. Cabral, F. Velez, and N. R. Prasad, "A cross-layer design of a weighted scheduling algorithm for IEEE 802.11e EDCA," *submitted to IET Communications.*, pp. –, Dec. 2010.

[13] J. Ferro, O. Cabral, and F. Velez, "A Cross-Layer Multi-Hop Simulator for IEEE 802.11e," *Wireless Personal Communications*, vol. 19, no. 1, Sep. 2010.

[14] J. M. Ferro, O. Cabral, and F. J. Velez, "Seeking for an Optimal Route in IEEE 802.11e Ad-Hoc Networks," in *Proc. of IEEE Semi Annual Vehicular Technology Conference (VTC2009-Fall)*, Anchorage, Alaska, USA, 2009.

[15] O. Cabral, J. M. Ferro, and F. J. Velez, *Cognitive Radio Mobile Ad Hoc Networks edited by Richard Yu*. Norwell, MA, USA: Springer, 2011, ch. Interoperability Between IEEE 802.11e and HSDPA: Challenges towards Cognitive Radio.

[16] V. Monteiro, J. Rodriguez, A. Gameiro, O. Cabral, and F. Velez, "RAT and Cell Selection Based on Load Suitability," in *Proc. of the 68th IEEE Vehicular Technology Conference (VTC08)*, Calgary, Canada, Sep. 2008, invited paper.

[17] V. Monteiro, O. Cabral, J. Rodriguez, F. Velez, and A. Gameiro, "HSDPA/WiFi RAT Selection Based on Load Suitability," in *Proc. of ICT Mobile and Wireless Summit*, Stockholm, Sweden, June 2008.

[18] O. Cabral, F. Velez, J. Rodriguez, V. Monteiro, A. Gameiro, and N. Prasad, "Optimal load suitability based RAT selection for HSDPA and IEEE 802.11e," in *Proc. of the 1st International Conference on Wireless Communication, Vehicular Technology, Information Theory and Aerospace Electronic Systems Technology, 2009. Wireless VITAE 2009.*, Aalborg, Denmark, May 2009, pp. 722 –726.

[19] O. Cabral, F. Meucci, A. Mihovska, F. J. Velez, N. R. Prasad, and R. Prasad, "Integrated Common Radio Resource Management with Spectrum Aggregation over Non-Contiguous Frequency Bands," *submitted to Wireless Personal Communications*, pp. –, -2011.

[20] *IEEE Std. 802.11e; Wireless LAN Media Access Control (MAC) and Physical Layer (PHY) Specifications*, IEEE, 2005.

[21] *IEEE Std. 802.11a; .Wireless LAN Media Access Control (MAC) and Physical Layer (PHY) Specifications: High-speed Physical Layer in the 5 GHz Band*, IEEE, 1999.

[22] P. Lettieri and B. Srivastava, "Adaptive Frame Length Control for Improving Wireless Link Throughput, Range, and Energy Efficiency," in *Proc. of IEEE International Conference on Computer Communications (INFOCOM98)*, San Francisco, CA, EUA, March 1998.

[23] D. Xu, B. Li, and K. Nahrstedt, "QoS-Directed Error Control of Video Multicast in Wireless Network," in *Proc. of 8th IEEE International Conference on Computer Communications and Networks (ICCCN99)*, Boston-Natick, MA, USA, Oct. 1999, pp. 257–262.

[24] A. Majumdar, D. Sachs, I. Kozintsev, and K. Ramchandran, "Multicast and Unicast Real-Time Video Streaming over Wireless LANs," *IEEE Transactions on CSVT*, vol. 12, no. 6, pp. 524–534, June 2002.

[25] G. Holland, N. Vaidya, and P. Bahl, "A Rate-Adaptive MAC Protocol for Multi-Hop Wireless Networks," in *Proc. of ACM/IEEE International Conference on Mobile Computing and Networking (MOBICOM01)*, Rome, Italy, July 2001.

[26] D. Qijao and S. Choi, "Goodput enhancement of IEEE 802.11a wireless LAN via link adaptation," in *Proc. of IEEE International Conference on Communications (ICC01)*, Helsinki, Finland, June 2001.

[27] D. Qijao, S. Choi, and K. Shin, "Goodput Analysis and Link Adaptation for IEEE 802.11a Wireless LANs," *IEEE Transactions on Mobile Computing*, vol. 1, no. 4, Oct.-Dec. 2002.

[28] M. Radimirsch, "An Algorithm to Combine Link Adaptation and Transmit Power Control in HIPERLAN Type 2," in *Proc. of IEEE International Symposium on Personal Indoor and Mobile Radio Conference 2002 (PIMRC02)*, Lisbon, Portugal, Sept. 2002.

[29] A. Kamerman and L. Monteban, "WaveLAN-II: A high-performance wireless LAN for the unlicensed band," *Bell Labs Technical Journal*, vol. 2, no. 3, pp. 118–133, Summer 1997.

[30] K. Balachandran, S. Kadaba, and S. Nanda, “Channel Quality Estimation and Rate Adaptation for Cellular Mobile Radio,” *IEEE Journal on Selected Areas in Communications*, vol. 17, no. 7, July 1999.

[31] K. Olszewski, *Channel Quality Measurement Method for 802.16ab PHY Layers*, IEEE 802.16abc-01/45, Oct. 2001.

[32] D. Qijao, A. Soomro, and K. Shin, “Energy-Efficient PCF Operation of IEEE 802.11a Wireless LAN,” in *Proc. of IEEE International Conference on Computer Communications (INFOCOM02)*, New York, NY, USA, June 2002.

[33] A. Myles, *IEEE 802.11h Draft Normative Proposal*, June 2002.

[34] O. Cabral, A. Segarra, and F. J. Velez, “Simulation of IEEE 802.11e in the context of interoperability,” in *Proc. of International Conference of Wireless Networks (ICWN07)*, London, United Kingdom, July 2007.

[35] N. Anastacio, F. Merca, and F. Velez, “QoS Metrics for Cross-Layer Design and Network Planning for B3G Systems,” in *Proc. of IEEE Third International Symposium on Wireless Communication Systems (ISWCS06)*, Valencia, Spain, Sep. 2006.

[36] *IEEE Std. 802.11; Wireless LAN Media Access Control (MAC) and Physical Layer (PHY) Specifications*, IEEE, 1999.

[37] J. Ferro and F. Velez, “Cross-Layer Multi-Hop Simulator for Ad-Hoc IEEE 802.11e,” in *Proc. of the 11th International Symposium of Wireless Personal Multimedia Communications (WPMC08)*, Lapland, Finland, Sep 2008.

[38] (2010) INET Framework for OMNEST/OMNeT++ 4.0. [Online]. Available: https://github.com/inetmanet/inetmanet

[39] D. Huy, T. Phan, V. Monteiro, A. Gameiro, X. Yang, J. Rodriguez, and R.Tafazolli, “System level performance evaluation of MATRICE air interface,” in *Proc. of the 13th IST Mobile Wireless Communications Summit*, Lyon, France, June 2004.

[40] A. R. Prasad and N. R. Prasad, *802.11 WLANs and IP Networking, security, QoS, and mobility*. Boston, MA, USA: Artech House, 2005.

[41] J. Luo, R. Mukerjee, M. Dillinger, E. Mohyeldin, and E. Schulz, “Investigation of radio resource scheduling in WLANs coupled with 3G cellular network,” *IEEE Communications Magazine*, vol. 41, no. 6, pp. 108–115, 2003.

[42] M. van Der Schaar and N. S. Shankar, "Cross-layer wireless multimedia transmission: challenges, principles, and new paradigms," *IEEE Wireless Communications*, vol. 12, no. 4, pp. 50 – 58, Aug. 2005.

[43] V. Srivastava and M. Motani, "Cross-layer design: a survey and the road ahead," *IEEE Communications Magazine*, vol. 43, no. 12, pp. 112 – 119, Dec. 2005.

[44] V. Kawadia and P. Kumar, "A cautionary perspective on cross-layer design," *IEEE Wireless Communications*, vol. 12, no. 1, pp. 3 – 11, Feb. 2005.

[45] M. Mitchell, *An introduction to genetic algorithms*. Cambridge, MA, USA: MIT Press, 1996.

[46] D. E. Goldberg, *Genetic Algorithms in Search, Optimization and Machine Learning*, 1st ed. Boston, MA, USA: Addison-Wesley Longman Publishing Co., Inc., 1989.

[47] T. Li, Q. Ni, T. Turletti, and Y. Xiao, "Performance Analysis of the IEEE 802.11e Block ACK Scheme in a Noisy Channel," in *Proc. of IEEE Second International Conference on Broadband Networks (BroadNets05)*, Boston, MA, USA, Oct. 2005.

[48] T. Li, Q. Ni, and Y. Xiao, "Investigation of the Block ACK Scheme in Wireless Ad-hoc Networks," *Wiley journal of Wireless Communications and Mobile Computing*, vol. 6, no. 6, Aug. 2006.

[49] I. Tinnirello and S. Choi, "Efficiency Analysis of Burst Transmissions with Block ACK in Contention-Based 802.11e WLANs," in *Proc. of IEEE International Conference on Communications (ICC05)*, Seoul, Korea, May 2005.

[50] V. Scarpa, G. Convertino, S. Oliva, and C. Parata, "Advanced Scheduling and Link Adaptation Techniques for Block Acknowledgement," in *Proc. of 7th IFIP International Conference on Mobile and Wireless Communications Networks (MWCN05)*, Marrakech, Morocco, Sep. 2005.

[51] A. Grilo, "Quality of Service in IP-based WLANs," Doctoral thesis, Instituto Superior Tecnico, Technical University of Lisbon, Lisbon, Portugal, June 2004.

[52] G. Bianchi, "Performance analysis of the IEEE 802.11 Distributed Coordination Function," *IEEE Journal Selected Areas in Communications*, vol. 18, no. 3, pp. 535–547, 2000.

[53] A. Grilo, M. Macedo, and M. Nunes, “A scheduling algorithm for QoS support in IEEE802.11 networks,” *IEEE Wireless Communications*, vol. 10, no. 3, pp. 36–43, 2003. [Online]. Available: http://dx.doi.org/10.1109/MWC.2003.1209594

[54] H. Kim and J. Hou, “ Improving protocol capacity with model-based frame scheduling in IEEE 802.11-operated WLANs,” in *Proc. of the Annual International Conference on Mobile Computing and Networking (MOBICOM03)*, San Diego, CA, USA, Sep. 2003, pp. 190–204.

[55] N. Vaidya, P. Bahl, and S. Gupta, “Distributed fair scheduling in a wireless LAN,” in *Proc. of Sixth Annual International Conference on Mobile Computing and Networking (MobiCom00)*, Boston, MA, USA, Aug. 2000, pp. 167–178.

[56] Y. Kwon, Y. Fang, and H. Latchman, “ A Novel MAC Protocol with fast collision resolution for wireless LANs,” in *Proc. of IEEE International Conference on Computer Communications (INFOCOM03)*, San Diego, CA, USA, March/April 2003, pp. 853–862.

[57] J. Robinson and T. Randhawa, “Saturation throughput analysis of IEEE 802.11e Enhanced Distributed Coordination Function,” *IEEE Journal on Selected Areas in Communications*, vol. 22, no. 5, pp. 917–928, 2004.

[58] J. L. Sobrinho and A. Krishnakumar, “Real-time traffic over the IEEE 802.11 Medium Access Control layer,” *Bell Labs Technical Journal*, vol. 1, no. 2, pp. 172–187, 1996.

[59] H. Wu, Y. Peng, K. Long, S. Cheng, and J. Ma, “Performance of reliable transport protocol over IEEE 802.11 wireless LAN: Analysis and enhancement,” in *Proc. of IEEE International Conference on Computer Communications (INFOCOM02)*, New York, NY, USA, June 2002, pp. 599–607.

[60] G. Bianchi and I. Tinnirello, “Kalman filter estimation of the number of competing terminals in an IEEE 802.11 Network,” in *Proc. of IEEE International Conference on Computer Communications (INFOCOM03)*, San Francisco, USA, Mar. 2003, pp. 844–852.

[61] R. O. Baldwin, N. Davis, and S. Midkiff, “A real-time medium access control protocol for ad hoc wireless local area networks,” *ACM Mobile Computing and Communications Review*, vol. 3, no. 1, pp. 20–27, Aug. 1999.

[62] F. Cali, M. Conti, and E. Gregori, “Dynamic tuning of the IEEE 802.11 protocol to achieve a theoretical throughput limit,” *IEEE/ACM Transactions on Networking*, vol. 8, no. 6, pp. 785–799, 2000.

[63] B. A. Venkatakrishnan and S. Selvakennedy, “An enhanced HCF for IEEE 802.11e wireless networks,” in *Proc. of the 7th ACM international symposium on Modeling, analysis and simulation of wireless and mobile systems (MSWiM04)*. New York, NY, USA: ACM, 2004, pp. 135–142.

[64] A. Ksentini, A. Guéroui, and M. Naimi, “Adaptive transmission opportunity with admission control for IEEE 802.11e networks,” in *Proc. of the 8th ACM international symposium on Modeling, analysis and simulation of wireless and mobile systems(MSWiM05)*. New York, NY, USA: ACM, 2005, pp. 234–241.

[65] L. Romdhani, Q. Ni, and T. Turletti, “Adaptive EDCF: enhanced service differentiation for IEEE 802.11 wireless ad-hoc networks,” in *Proc. of IEEE Wireless Communications and Networking (WCNC03)*, vol. 2, New Orleans, Loisiana, USA, March 2003, pp. 1373 –1378 vol.2.

[66] A. Banchs and L. Vollero, “Throughput analysis and optimal configuration of 802.11e EDCA,” *Computer Networks*, vol. 50, no. 11, pp. 1749 – 1768, 2006. [Online]. Available: http://www.sciencedirect.com/science/article/B6VRG-4GY844F-6/2/469f21335a260113a3a1462802fcf96d

[67] J. Antoniou, A. Pitsillides, G. Hadjipollas, M. Stylianou, V. Vassiliou, A. Correia, A. Soares, and E. Cabrita, “Designing a System Level simulator for E-UMTS,” in *Proc. of IST-SEACORN Project Workshop*, Cambridge, UK, Mar. 2004.

[68] S. Haemaelaeinen, H. Holma, and K. Sipilae, “ Advanced WCDMA radio network simulator,” in *Proc. of 13th IST Mobile & Wireless Communications Summit*, Lyon, France, June 2004.

[69] S. Ghorashi, E. Homayounvala, F. Said, and A. Aghvami, “ Dynamic simulator for studying WCDMA based hierarchical cell structures,” in *Proc. of IEEE International Symposium on Personal, Indoor and Mobile Radio Communications (PIMRC01)*, San Diego, CA, USA, Oct./Nov. 2001, pp. 32–37.

[70] J. Rodriguez, V. Monteiro, A. Gameiro, R. Legouable, N. Ibrahim, and M. Shateri, " 4 MORE System Level Performance," in *Proc. of 6th International Telecommunications Symposium (ITS06)*, Fortaleza-CE, Brazil, Sep. 2006.

[71] T. Rappaport, *Wireless Communications: Principles and Practice*, 2nd ed. Prentice Hall, 2002.

[72] Z. Kong, D. H. K. Tsang, B. Bensaou, and D. Gao, "Performance Analysis of IEEE 802.11e Contention-Based Channel Access," *IEEE Journal on Selected Areas in Communications*, vol. 22, no. 10, Dec. 2004.

[73] A. V. Babu and L. Jacob, "Analysis of IEEE 802.11 Multirate Wireless LANs," *IEEE Transactions on Vehicular Technology*, vol. 56, no. 5, Sep. 2007.

[74] D. Malone, K. Duffy, and D. Leith, "Modeling the 802.11 Distributed Coordination Function in Nonsaturated Heterogeneous Conditions," *IEEE Transactions on Networking*, vol. 15, no. 1, Feb. 2007.

[75] R. Jain, D. Chiu, and W. Hawe, *A quantitative measure of fairness and discrimination for resource allocation in shared computer systems*, dec-tr-301 ed., Digital Equip. Corp, Littleton, MA, USA, Sep. 1984.

[76] K. Duffy, D. Leith, T. Li, and D. Malone, "Modeling 802.11 mesh networks," *IEEE Communications Letters*, vol. 10, no. 8, pp. 635–637, Aug. 2006.

[77] K. Duffy, D. J. Leith, T. Li, and D. Malone, "Improving Fairness in Multi-Hop Mesh Networks Using 802.11e," in *Proc. of 6th International Symposium on Modeling and Optimization in Mobile, Ad Hoc, and Wireless Networks and Workshops (WiOPT 2008)*, Boston, Massachusetts, USA, April 2006, pp. 1–8.

[78] R. Oliveira, L. Bernardo, and P. Pinto, "The influence of broadcast traffic on IEEE 802.11 DCF networks," *Computer Communications*, vol. 32, no. 2, pp. 439–452, Feb. 2009.

[79] L. Wu and P. K. Varshney, "Performance analysis of CSMA and BTMA protocols in multihop networks: Part I. Single channel case," *Information Sciences*, vol. 120, no. 3, pp. 159–177, Nov. 1999.

[80] Y. Wang and J. J. Garcia-Luna-Aceves, "Modeling of collision avoidance protocols in single-channel multihop wireless networks," *Wireless Networks*, vol. 10, no. 5, pp. 495–506, 2004.

[81] *Broadband Radio Access Networks (BRAN); HIPERLAN Type 2; Requirements and Architectures for Interworking between HIPERLAN/2 and 3rd Generation Cellular Systems*, V1.1.1 (2001-08) ed., ETSI TR 101 95.

[82] Evolving systems beyond 3G, IST-2000-28584 MIND. [Online]. Available: http://www.ist-mind.org

[83] Capacity Utilizations in Cellular networks of present and Future Generation. IST project CAUTION. [Online]. Available: http://www.telecom.ntua.gr/CautionPlus/

[84] Evolutionay stategies for RRM, IST project EVEREST. [Online]. Available: www.everest-ist.upc.es

[85] Advanced Resource Management Solutions for Future All IP Heterogeneous Mobile Radio Environments. IST project AROMA. [Online]. Available: www.aroma-ist.upc.edu

[86] A. Mihovska, E. Tragos, E. Mino, J. Luo, C. Mensing, R. Fracchia, S. Horrich, L. Hui, A. Klockar, and S. Kyriazakos, "Requirements and Algorithms for Cooperation of Heterogeneous Radio Access Networks," *Wireless Personal Communications*, vol. 50, no. 2, Oct. 2008.

[87] W. Figel, N. Shepherd, and W. Trammel, "Vehicle location by a signal attenuation method," *IEEE Transactions on AES*, vol. 18, no. 3, Nov. 1969.

[88] *Revision of the Commission's Rules To Ensure Compatibility with Enhanced 911 Emergency Calling Systems*, FCC, CC Docket.

[89] J. Reed, K. Krizman, B. Woerner, and T. Rappaport, "An overview of the challenges and progress in meeting the E-911 requirement for location service," *IEEE Communications Magazine*, vol. 36, no. 4, pp. 30–37, April 1998.

[90] T. S. Rappaport, J. H. Reed, and B. Woerner, "Position location using wireless communications on highways of the future," *IEEE Communications Magazine*, vol. 34, no. 10, pp. 33–41, Oct. 1996.

[91] K. J. Krizman, T. E. Biedka, and T. S. Rappaport, "Comparison of methods of locating and tracking cellular mobiles," in *Proc. of IEE Colloquium on Novel Methods of Location and Tracking of Cellular Mobiles and Their System Applications*, London, UK, May 1999, pp. 1–6.

[92] S. Ryu, B.-H. Ryu, H. Seo, M. Shin, and S. Park, "Wireless packet scheduling algorithm for OFDMA system based on time-utility and channel state," *ETRI Journal*, vol. 27, no. 6, pp. 777–787, Dec. 2005.

[93] P. Hosein, "On the optimal scheduling of uplink resources in OFDMA-based wireless networks," in *Proc. of 12th European Wireless Conference (EW06)*, Athens, Greece, Apr. 2006.

[94] *3GPP 25.214, Physical layer procedures (FDD)*, 3rd Generation Partnership Project, Technical Specification Group, Dec. 2004-6.

[95] M. Hildebrand, G. Cristache, K. David, and F. Fechter, "Location-Based Radio Resource Management in Multi Standard Wireless Network Environments," in *Proc. of IST Mobile & Wireless Communications Summit*, Thessaloniki, Greece, June 2002.

[96] C. Mensing, E. Tragos, J. Luo, and E. Mino, "Location Determination Using In-Band Signaling For Mobility Management in Future Networks," in *Proc. of the 18th IEEE International Symposium on Personal Indoor and Mobile Radio Communications (PIMRC07)*, Athens, Greece, Sep. 2007.

[97] M. Zorzi and R. Rao, "Geographic random forwarding (GeRaF) for ad hoc and sensor networks: multihop performance," *IEEE Transactions on Mobile Computing*, vol. 2, no. 4, pp. 337–348, Dec. 2003.

[98] A. Bletsas, A. Khisti, D. Reed, and A. Lippman, "A simple Cooperative diversity method based on network path selection," *IEEE Journal on Selected Areas in Communications*, vol. 24, no. 3, pp. 659–672, Mar. 2006.

[99] *3GPP TR 25.892 v6.0.0, Feasibility Study for Orthogonal Frequency Division Multiplexing (OFDM) for UTRAN enhancement*, 3rd Generation Partnership Project, Technical Specification Group Radio Access Network, June 2004.

[100] CEA-LETI and al., "1.1.1 Definition of Cross-Layer and Cross-System Framework Scenarios," IST-4-026906 UNITE, IST Central Office, Brussels, Belgium, Deliverable D1.1.1, Sep. 2006, www.ist-unite.org.

[101] Key results of World Radiocommunication Conference (WRC-07). [Online]. Available: http://www.itu.int/dms_pub/itu-t/oth/21/04/T21040000030014PPTE.ppt

[102] *3GPP TS 36.213 v9.0.0, Evolved Universal Terrestrial Radio Access (E-UTRA); Physical layer procedures (Release 9)*, 3rd Generation Partnership Project, Technical Specification Group Radio Access Network, Dec. 2009.

[103] *3GPP TR 36.814 v1.7.0, Further Advancements for E-UTRA Physical Layer Aspects (Release 9)*, 3rd Generation Partnership Project, Technical Specification Group Radio Access Network, Feb. 2010.

[104] *3GPP TR 36.815 v9.0.0, LTE-Advanced feasibility studies in RAN WG4 (Release 9)*, 3rd Generation Partnership Project, Technical Specification Group Radio Access Network, March 2010.

[105] L. Chen, W. Chen, X. Zhang, and D. Yang, "Analysis and Simulation for Spectrum Aggregation in LTE-Advanced System," in *Proc. of IEEE 69th Vehicular Technology Conference (VTC09-Fall)*, Anchorage, Alaska, USA, Sep. 2009, pp. 1–6.

[106] G. Yuan, X. Zhang, W. Wang, and Y. Yang, "Carrier Aggregation for LTE-Advanced Mobile Communication Systems," *IEEE Communications Magazine*, vol. 48, no. 2, pp. 88–93, Feb. 2010.

[107] Y. Wang, K. Pedersen, P. Mogensen, and T. Sorensen, "Carrier load balancing methods with bursty traffic for LTE-Advanced systems," in *Proc. of IEEE International Symposium on Personal, Indoor and Mobile Radio Communications (PIMRC09)*, Tokyo, Japan, Sept. 2009.

[108] Y. Wang, K. Pedersen, T. Sorensen, and P. Mogensen, "Downlink Transmission in Multi-Carrier Systems with Reduced Feedback," in *Proc. of IEEE 70th Vehicular Technology Conference (VTC2010-Spring)*, Taipei, Taiwan, May 2010.

[109] J. Dixton, C. Politis, , and C. Wijting, "Considerations in the choice of suitable spectrum for mobile communications," in *Proc. of Wireless World Research Forum Meeting 21*, Stockholm, Sweden, Oct. 2008.

[110] F. M. O., Cabral, F. Velez, A. Mihovska, and N. Prasad, "Spectrum Aggregation with Multi-Band User Allocation over Two Frequency Bands," in *Proc. of IEEE Mobile WiMAX Symposium (MWS09)*, Napa Valley, California, USA, 2009.

[111] (2007, March) IST-4-027756 WINNERII D 5.10.2 Spectrum Requirements for System beyond IMT- 2000. [Online]. Available: http://www.ist-winner.org/deliverables.html

[112] W. C. Y. Lee, *Mobile Communications Design Fundamentals*, 2nd ed. New York, NY, USA: John Wiley and Sons, 1993.

[113] *IST MATRICE-2001-32620, D4.5 Layer 2& 3 reference simulation results dynamic resource allocation algorithms and IP transport*, Sept. 2004. [Online]. Available: http://www. ist-matrice.org/

[114] R. Skehill, M. Barry, W. Kent, M. O'Callaghan, N. Gawley, and S. Mcgrath, "The common RRM approach to admission control for converged heterogeneous wireless networks," *IEEE Wireless Communications Magazine*, vol. 14, no. 2, pp. 48–56, April 2007.

[115] *Radio Resource Management Strategies, TR 25.922*, 3GPP, Technical Specification Group RAN, Working Group 2 (WG2).

[116] *R1-03-0249, Validation of System-Level HSDPA Results for CDMA and OFDM in aFlat Fading Channel*, Nortel Networks, 3GPP TSG-RAN-1 Meeting #31, 18th 21th Feb. 2003.

[117] *3GPP2-C30-20030429-010, Effective SNR mapping for modelling frame error rates in multiple-state channels*, Ericsson.

[118] J. K. Karlof, *Integer Programming: Theory and Practice*, 1st ed. CRC, 2005.

[119] F. Meucci, A. Mihovska, B. Anggorojati, and N. R. Prasad, "Joint Resource Allocation and Admission Control Mechanism for an OFDMA-Based System," in *Proc. of the 11th International Symposium on Wireless Personal Multimedia Communications (WPMC08)*, Lapland, Finland, 2008.

[120] H. Kellerer, U. Pferschy, and D. Pisinger, *Knapsack Problems*, 1st ed. Springer Verlag, 2005.

[121] *TR25.211: Physical channels and mapping of transport channels onto physical channels (FDD)*, 5th ed., 3GPP, June 2005.

[122] K. Chen and J. R. B. de Marca, *Mobile WiMAX*, 1st ed. West Sussex, England: John-Wiley & Sons, Ltd., 2008.

[123] H. Holma and A. Toskala, *WCDMA for UMTS HSPA evolution and LTE*, 1st ed. West Sussex, England: JohnWiley & Sons, Ltd., 2007.

[124] E. Dijkstra, "A Note on Two Problems in Connexion with Graphs," *Numerische Mathematik*, vol. 1, pp. 269–271, 1959.

[125] M. Mitchell, *An Introduction to Genetic Algorithms*. Cambridge, MA, USA: The MIT Press, 1999.

[126] V. Ramasami, "BER Performance over Fading Channels and Diversity Combining," Department of Electrical Engineering and Computer Science, University of Kansas, Tech. Rep., Spring 1999, eECS 862 Project.

[127] A. Carlson, *Communication Systems*, 3rd ed. McGraw-Hill, 1986.